Research and Development Program

Conservation Division

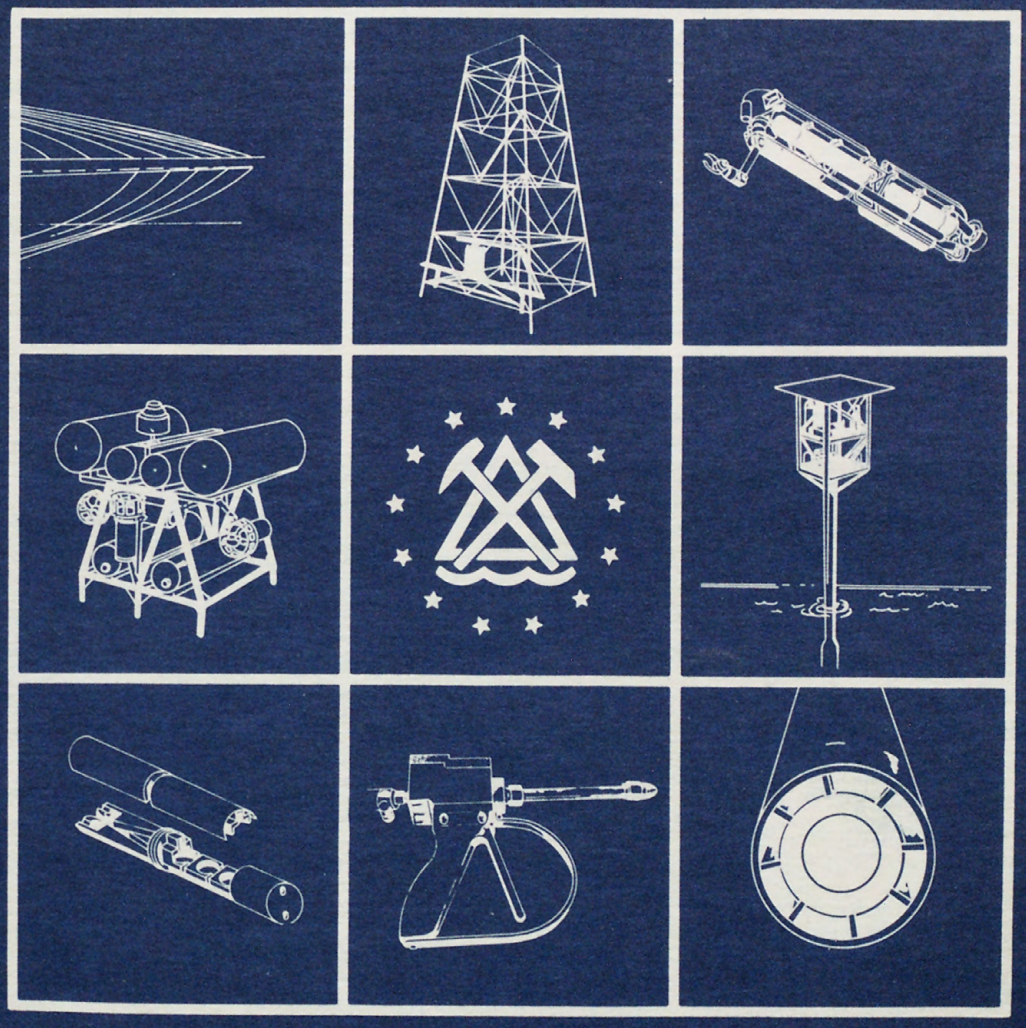

Outer Continental Shelf Oil and Gas Operations

Technical Report 1981

U.S. Geological Survey Open-File Report 81-704

The sea! the sea! the open sea!
The blue, the fresh, the ever free
Without a mark, without a bound,
It runneth the earth's wide regions round.
—*Barry Cornwall,* The Sea, *st. 1*

Never trust her at any time, when
the calm sea shows her false alluring
smile.
—*Lucretius,* De Rerum Natura, *bk. II, l. 558*

Established by an Act of Congress in 1879 and charged with responsibility for "classification of the public lands, and examination of the geological structure, mineral resources, and products of the national domain," the Geological Survey has been the principal source of information about the Nation's physical resources—the configuration and character of the land surface, the composition and structure of the underlying rocks, and the quality, extent, and distribution of water and mineral resources. Although primarily a research and fact-finding Agency, the Survey has responsibility also for the classification of Federal mineral lands and waterpower sites.

Since 1926, the Geological Survey has been responsible for the supervision of oil and gas and mining operations authorized under leases on Federal land. More recently, petroleum exploration on the Outer Continental Shelf (OCS) expanded the Survey's responsibilities. With the passage of the OCS Lands Act of 1953, the Survey was assigned the responsibility for assuring safe, pollution-free oil and gas operations on the OCS. The responsibilities are further delineated in internal guidelines that include a research program as an integral part of its marine oil and gas operations. The program is currently being expanded to address the Survey's technology needs for onshore minerals.

The Research and Development Program, Conservation Division (formerly known as the Research and Development Program for OCS Oil and Gas Operations), assesses research and development conducted by industry, the universities, and Government institutions, and contracts for studies that are considered to offer further assurances for improving safety and preventing pollution. With regard to OCS activities, these studies comprise a coordinated research effort that, for purposes of management, is divided into three sections: structures and pipelines, well control, and environmental concerns.

For onshore minerals operations, the research program is in its formative stages. The Geological Survey has asked the National Academy of Sciences for guidance in establishing a balanced program that will provide the technological insights needed for equitable development of the mineral resources.

In effect, the program is a focal point for applying science and technology to the operational needs of the Conservation Division. USGS field personnel who have firsthand experience assist the program manager in identifying research needs and in reviewing proposals and project accomplishments.

Research is conducted at universitites, private companies, and Government laboratories—wherever there are promising ideas and capabilities for advancing the "regulatory technologies."

United States Department of the Interior
Geological Survey

Research and Development Program

Conservation Division

OCS Oil and Gas Operations
Technical Report 1981
Open-File Report 81-704

Compiled and Edited by John B. Gregory and Charles E. Smith

This report has not been edited for conformity
with Geological Survey Editorial Standards

FOREWORD

The technical studies, which are being conducted to support the Geological Survey's operations on the Outer Continental Shelf, are summarized in this report. It is printed in advance of our Program seminar which occurs every 18 months, the next being mid-November 1981. Both the report and seminar are advertised in the *Federal Register*.

This year, we have opened up the printed material to make reading a bit easier, but unfortunately for some readers, we have left in a sprinkling of equations and curves. We couldn't resist this temptation, being proud of our investigatiors and their dedication to our needs and to the discovery of the natural truths. Through the enlightenment they provide to our regulatory mission, one can only expect that both industry and Government will more equitably move together into the frontier areas of the deep ocean and the ice-covered Arctic, where new technologies will be needed for proper development of the resources.

At this writing, the Research Program has been established for about 4 years, during which time it has concentrated upon generic studies in structural dynamics, blowout prevention, and operational consequences upon the environment. In the next printing, however, the special problems associated with operations in frontier areas will be more apparent to the readers as projects continue to zero in upon them. One needs to "crawl before learning to walk," especially in research. Technologies in areas such as underwater communications and inspection, drilling mud dynamics, or the recapture of oil from blowing wells need to be understood before studying the more demanding requirements of the above-mentioned frontier areas.

It's an exciting program of research and development and we welcome your comments and suggestions for improving it. Lastly, perhaps we'll meet at our next seminar.

John B. Gregory
Research Program Manager
Conservation Division
U.S. Geological Survey
620 National Center
Reston, VA 22092

Contents

Illustrations

INTRODUCTION

About the Program

As a result of recommendations several years ago from the National Academy of Sciences, the University of Oklahoma, and the National Aeronautics and Space Administration (NASA), the U.S. Geological Survey has embarked upon a program of research and development to provide the technological insights needed for its regulatory operations offshore—operations which provide assurances to the public for safety and for the prevention of pollution in oil and gas drilling and production. These clear objectives are, therefore, those of the research program, not the economics of operations, which are of concern to industry.

The Program is a contract research program and is an integral part of the Conservation Division. It is a focal point for deriving possible solutions from the university community, private industry, and the Federal laboratory system for identified offshore operational problems. This vast interdisciplinary body of science and technology provides the kind of research needed by the Division in its Outer Continental Shelf (OCS) operations which involve such problematic areas as structural dynamics, fluid flow, and geotechnology.

The Program encourages innovation and creativity which can be accomplished only by talented scientists and engineers who are dedicated to man's endeavor to make breakthroughs in science and technology.

Because the Division's mission is operational, in a sense like the U.S. Navy, the R&D Program must progress in a timely manner even though technological advances cannot really be scheduled. As the Navy's Office of Naval Research (ONR) has so successfully coped with the seeming dichotomy of anticipating the occurrence of innovations, so must the Conservation Division. Thus, USGS, like ONR, makes use of the unsolicited proposal and the best effort contract to accomplish its objectives. Good science and technology can only be accomplished when several variables converge: a talented investigator doing his own research, which happens to coincide with our needs, availability of resources, time scales, etc. Our task is to "beat the bushes" so that these people come to us with their innovative ideas and concepts. They have done so by learning of our interests through announcements of the Program in the *Federal Register*, reading reports which emanate from the Program, and by attending our seminars.

Research and Development

For purposes of management, the Program is divided into three generic categories—structures and pipelines verification; well control, or the prevention of blowouts and consequent fires; and the effects on the environment from OCS operations. The projects described herein are arranged in that order.

Structures and Pipelines

With regard to structures, in the fall of 1979 the Geological Survey established within the Conservation Division a Platform Verification Section whose task is to administer a program of offshore structures verification. This program was recommended by the Marine Board of the National Academy of Engineering in a 1977 report "Verification of Fixed Offshore Oil and Gas Platforms." Since that time, the Survey, with the Board's guidance, has been devising requirements for the design and initial inspection of new fixed and bottom-founded platforms. These structures consist of all the new OCS platforms to be erected outside the Gulf of Mexico (including gravel and ice islands), new structures within the Gulf to be located in water depths greater than 400 feet, structures whose natural fundamental periods exceeds 3 seconds, those to be located on an unstable

bottom, or those of unique design. The Survey's requirements are detailed in the publication "Requirements for Verifying the Structural Integrity of OCS Platforms," October 1979.

Though initial inspections are required after platform installations are completed, at this writing no decisions have been made by the Government on requirements for subsequent periodic inspections. North Sea experience, however, indicates that for some of the above-mentioned situations, mandatory underwater inspections of some type will be quite likely. Even if not required, the Survey needs an understanding of the latest technologies for such factors as design, inspection, remote monitoring, and the determination of failure probabilities.

With regard to pipelines, the Geological Survey is basically responsible for assuring the integrity of about 25 percent of the lines (mostly gathering lines) on the OCS. The remainder are under the jurisdiction of the Department of Transportation. Although the Federal Government does not require underwater inspection, it must keep abreast of new technologies for detecting leakage and other pipeline irregularities; the regulatory agencies need to be informed and maintain a certain level of proficiency.

Several basic technologies, involving various combinations of instruments, submersibles, technicians, and divers, are presently used to verify the integrity of offshore platforms and pipelines. When viewing advancements in technology over recent years in this field, as well as for other ocean engineering applications, no single inspection procedure has sufficed. Instead, the basic methods now in use probably will be improved and will be used for years to come. As evidenced by NASA's space ventures, both manned and unmanned systems have their places because of the complementary advantages they provide.

From accumulated experiences, however, the use of divers in relatively deep, harsh environments such as the North Sea is not only very expensive, but also quite dangerous. These factors suggest a thorough search for alternative means of inspection. Several years ago, the results of such a search may not have been encouraging, but from time to time key breakthroughs occur to cause technological advances which dramatically change the ways people do things—the jet engine and transistor, for example. At the heart of the very latest advance is the microprocessor. When combined with several other relatively new developments, such as large-scale integrated circuits, high energy-density batteries, and optical fiber signal transmission, it allows technologists to seriously explore the field of robotics. To replace man underwater by a supervised robot or an almost autonomous vehicle which could navigate, inspect, perform useful services, and communicate would be quite innovative. This technology is under development by the Research Program and is described herein.

These projects make use of testbed vehicles fabricated by the University of New Hampshire and the Naval Ocean Systems Center, but much of the technology is applicable to the methods used to obtain information and to perform useful tasks underwater. For example, cavitation erosion technology developed by the Program for cleaning structural joints prior to inspection was initially evaluated as a diver-held device, but because of its small size and low power drain, it will be adapted to a robot submersible. Other developments, such as those in optical fiber and acoustic signal transmission, can be used not only from submersibles, but also from divers or fixed instruments.

Industry and the universities are placing much emphasis on gaining a better understanding of the response of structures to the fatigue excitation of ocean waves. The importance of these investigations will become more apparent as industry moves into the deeper, more hostile waters of the Atlantic shelf. The Research Program is studying dynamic response of structures to gain an improved understanding of damping (both structural and artificial) as well as the applicability of several monitoring techniques. The monitoring effort is being coordinated with the Structural Mechanics Program of the Office of Naval Research whose interest is in the structural dynamics of ships.

As the individual investigations progress, and as their advantages and limitations are assessed, comparisons need to be drawn which are based upon typical offshore situations. Thus,

"round-robin" excerises are being conducted for each competing method of monitoring or nondestructive examination (NDE). In this respect, the Geological Survey and ONR have formed a committee of specialists who have prescribed "round robin" exercises which are being conducted using selected NDE techniques on models. Successful techniques will be investigated further for eventual evaluation offshore.

Well Control

At the heart of offshore operations is well control—the ability to drill and produce oil and gas without sustaining blowouts. If such catastrophies do occur, the situation becomes one of recontrol or even recapture of the oil before dispersal in the ocean. Both normal operations and blowout situations can be reduced to practical problems in fluid mechanics which can only be solved, first, by understanding all the variables which force the system as well as contain it, and second, by using effective equipment and enlightened personnel.

Though basically all the variables of the well-control problem have been identified and are considered during operations (drilling mud density, rock porosity, and others), uncertainties still exist which sometimes lead to blowouts and wellhead fires. If the geophysics of the rock and sediment were better known, together with the behavior of the various fluids in the well, and if the driller could see what was happening downhole in a timely manner, better decisions could be made to maintain control when potential blowout conditions arise.

Added to the problem of dynamically balancing the flow of fluids during normal drilling operations is the uncertainty that some part of the structure has failed, whether it be casing, cementing, or formation. Again, timely conveyance of these failures to the driller is most important in order for him to take effective countermeasures.

The Research Program is addressing well control in several major areas. At Louisiana State University, a research oil-well facility is being constructed to conduct studies pertaining to the dynamic behavior of drilling mud and the means for handling it during transient conditions of well kicks, shut-ins, and startups. Communications down a borehole are under investigation at Harry Diamond Laboratories. In deep ocean drilling operations, effective telemetry systems between drilling operations at the surface and conditions at the drill bit will mean the difference between control or blowout. When blowouts do occur, resulting wellhead fires can destroy a rig, prolong loss of oil, and cause considerable pollution. The National Bureau of Standards is investigating the application of advanced technology for suppressing such fires. The subsea recapture of oil from a blowout well, at this writing, has not been accomplished successfully though once attempted on a grand scale in the IXTOC 1 blowout of 1979. MIT is presently investigating a method based on an extrapolation of the "Steel Sombrero" methodology, and the outlook for successfully recapturing oil looks promising for application to future blowouts.

Environmental Concerns

The Geological Survey's major environmental responsibility on the OCS is the prevention of oil spills. In large measure, this task is accomplished by means of specific operational regulations called OCS Orders which pertain both to the drilling and to the production of oil and gas. To be in compliance with these Orders, prospective driller must submit, for the Survey's consideration, an oilspill contingency plan which specifies the organization, equipment, and procedures he will use in the event of a spill.

Liquid and solid discharges such as sewage and deck drainage are regulated by the Environmental Protection Agency. Both liquid and solid drilled material, for example, are of concern depending upon the proximity of operations to biologically important benthic communities such as coral reefs. These discharges may amount to several thousand barrels of cuttings, some of which may contain

small amounts of bacteria and heavy metals, together with drilling mud which has not been separated for reuse downhole. In ecologically sensitive areas, operators may be required either to shunt all drilling discharges through a down pipe directly to the ocean floor, thus preventing their lateral dispersion through the water column, or to barge such discharges to other areas for disposal or processing.

Areas of biological sensitivity and the restrictions imposed by the Government are generally described in "Stipulations" which are attached to OCS oil and gas leases. In consultation with the Bureau of Land Management and the Fish and Wildlife Service, the Survey enforces these restrictions. Others who use the Outer Continental Shelf, such as commercial and sport fishermen, have rights which must be protected. Little conflict exists with the latter group because offshore structures serve their interests as artificial fishing reefs, as navigational aids, and as emergency stations. Commercial fishermen, however, are likely to snag their trawls upon unmarked underwater protrusions if permitted to exist. Therefore, stipulations require that abandoned wellheads and platforms piles be removed below the mud line by offshore operations. In addition, in these commercial fishing areas, pipelines must be buried or have a smooth surface design.

The equitableness of Orders and Stipulations in preventing pollution, while allowing maximum economy of operations, necessitates that the several regulatory agencies involved not only understand but also foster improved technology to protect the environment. Environmental sciences are difficult and expensive to pursue in the ocean. The many animals and organisms which swim, drift, and otherwise live in it interact greatly with each other over markedly different life spans. Valid conclusions about the effects of offshore operations result only from rigorously planned and executed experiments; only then can the information be used as a basis for regulation.

At present, the Research Program is continuing its study of the effects of drilling muds on corals. Results from this project, being conducted by the Survey's Fisher Island Station, are intended to provide information to regulatory personnel on distances from coral reefs at which drilling operations can proceed without impairment.

Another project, which is attempting to quantify the effects of using explosive charges to remove wellheads, is being transferred from the Naval Surface Weapons Center (where blast models were tested) to Woods Hole Oceanographic Institution where the blast effects upon various fish are to be studied.

Frontier Area Emphasis

The generic studies begun several years ago are now yielding to specific frontier area applications—the Arctic and the deep ocean.

In the Arctic, leasing schedules are being advanced and the U.S. Geological Survey, very soon, will have to be in the position of assuring the public that offshore operations through the ice pack proceed safely. Production of oil and gas will occur near shore first, and then probably from ice islands, some of which may be artificially reinforced. Monopods may be deployed for operations in ice infested waters. The many operational problems in the Arctic stem from the cold weather, ice operations, and long supply lines. The most predominant engineering problem concerns the forces exerted on structures by the ice pack. Stresses build up on the ice sheet because of wind and current drag, which cause the sheet to crack and force it against islands and structures. The cracks throw up ridges and create keels, the latter of which scour the bottom when grounded, causing hazardous conditions to pipelines and cables. To engineer for these large ice forces and to cope with such problems as locating drilling and production operations on ice sheets, the mechanical properties of sea ice need to be better understood. In addition to ice, permafrost (frozen soil) is a problem which occurs not only on land but also underneath the waters of the shelf. Offshore operations have to develop methods to cope with this material when drilling, producing, or pumping oil in pipelines laid through it.

The Research Program presently is beginning studies in these areas. Also reported herein is a study concerning another cold weather problem—the fracture toughness of welded joints. As one reads this summary, he will observe the regulatory Agency's responsibilities in establishing current minimum industry requirements.

The deep ocean, too, is becoming increasingly important. Note, that to the oil industry, "deep" means depths in excess of, say, 600 feet whereas in usual parlance, the connotation is directed to operations off the continental shelf. Though industry has not produced oil in depths exceeding 1,000 feet or so, it is moving toward the Atlantic slope where prospects, based on geological extrapolations, indicate deposits of hydrocarbons. The National Science Foundation presently is embarking on a program of exploratory drilling which will deploy the huge *Glomar Explorer* to verify these anticipations. As industry moves farther outward, conventional jacket platforms seen the world over will give way to configurations which are held in place, to a large extent, by tensioned members, or rest on the sea floor without projecting upwards through the water column. This latter concept, known as a subsea production system, has been examined experimentally but not in practice except where a standard jacket platform assists in the production operation. Of most interest over the next several years are the tensioned structures; figure 1 compares the economics of their design, fabrication, and installation with those of a standard jacket platform.

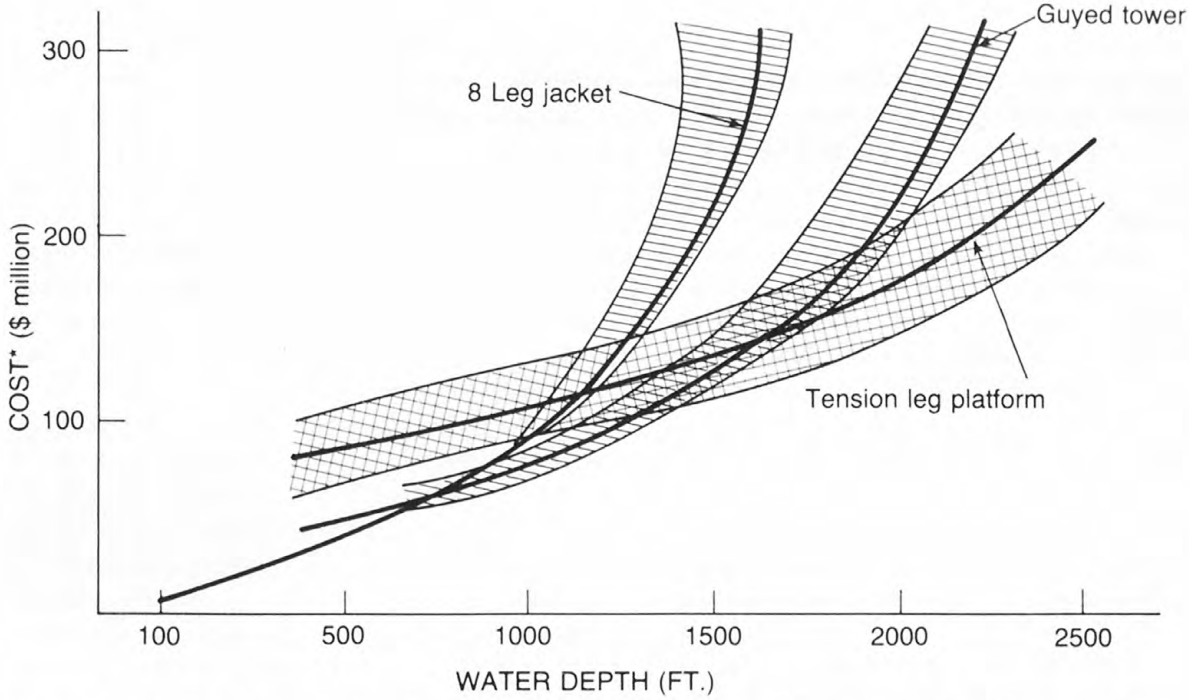

DESIGN, FABRICATION AND INSTALLATION COST, EXCLUDING TOP SIDE EQUIPMENT AND FACILITIES.

FIGURE 1.—Order of magnitude cost comparison for deepwater structures in the Gulf of Mexico (from Dunn, F. P., 1979, Outer Continental Shelf frontier technology: Marine Board, National Academy of Engineering, symposium, Proceedings, p. 27, fig. 1).

Guyed towers are shown to be economical between, say, 600 feet to 1,500 feet, and the tension leg platform is the most favored between 1,500 feet and 2,500 feet. For depth greater than 2,500 feet, the subsea system, or some other concept such as floating production operations, will be needed.

Most static structures (such as buildings, tunnels, and platforms) used by mankind are predominantly compressive structures, their major members and foundations being under compressive loading. Suspension bridges are composed of both compression and tension members, but their primary support—the piers—are in compression. Very little information is available on the behavior of tensioned ocean structures because, with special exceptions, they have not been built. These exceptions mainly concern U.S. Navy projects involving cable systems positioned in the deep ocean for long-range acoustic detection. In addition, the Navy has conducted extensive development of the explosive impedment anchor, a device which is designed to hold bottom against vertical pullout forces. These exceptions not withstanding, if tension leg platforms and guyed towers are to be successfully used, the predominant problems of holding bottom will have to be studied further. These tension loads must be considered to be high amplitude, cyclic forces. The forces acting on the structures are driven by wind, wave, ocean current, and very importantly, current-induced oscillating forces caused by vortex shedding on cables and risers, all of which are dynamic in nature. These predominant engineering problems associated with deep-water operations are now being studied by the Research Program.

Dynamic Properties of Offshore Structures

Principal Investigator:—Dr. J. Kim Vandiver
Department of Ocean Engineering
Massachusetts Institute of Technology
Cambridge, MA 02139

Objective: To determine dynamic design criteria for offshore structures.

As the offshore industry migrates from the relatively benign Gulf of Mexico into deeper waters of the open ocean, design and operational requirements will become more demanding. Traditional offshore engineering practice will yield to structures whose dynamic performance will be of much more concern, thus requiring an increased understanding of the structural dynamics. The ability to predict, measure, and interpret this performance is of much consequence in the regulatory responsibilities of the Geological Survey. The principal investigator has addressed these concerns as follows:

1. The accurate determination of natural frequencies, mode shapes, and damping ratios of offshore structures from data collected in the field, and

2. The prediction of dynamic response of offshore structures to wave excitation.

The measurement of dynamic response properties has two important applications. The first is the development of inspection techniques which minimize the use of divers. Some of these techniques are discussed elsewhere in this report. All of them require accurate measurements of natural frequencies, mode shapes, or modal damping ratios, and this project has centered on the development of new spectral analysis techniques for the determination of these quantities. The other important application of spectral analysis research is the verification of platform design. Once a platform is installed, accurate measurements need to be obtained of the actual dynamic performance of the structure for comparsion with the estimates used in the design. Feedback is essential for improving design estimates of the performance of future structures in deeper and more hostile environments. The development of the Maximum Entropy Method (MEM) has substantially improved the accuracy and confidence of determining damping from ambient response data.

Response prediction research is essentially applicable to the problem of fatigue-life prediction. Fatigue has become one of the controlling design issues for deepwater structures whether they be jacket structures, tension leg platforms, or guyed towers. Such structures may have natural periods of vibration which, unfortunately, correspond to quite energetic regions of daily occurring wave spectra. Under such circumstances, the dynamic amplification at these natural periods is critically dependent on damping, and the ability to predict it during the process of design is essential. MIT researchers have applied unique relationships between linear wave forces and wave radiation damping, which has revealed additional useful relationships between nonlinear drag forces and viscous hydrodynamic damping.

Measurement of Dynamic Response Properties

To date conventional methods of spectral analysis, including Blackman-Tukey and Fast Fourier Transforms (FFT), of ambient vibration records have proved inadequate in providing accurate estimates of modal damping ratios. For example, a commonly used technique for estimating the damping ratio of the fundamental flexural mode of an offshore platform is to compute the half-power bandwidth of that mode's peak as it appears in the spectrum of acceleration response to ambient wind and wave excitation. While working with Vandiver at MIT, Campbell showed that

half-power bandwidth estimates of damping, computed from conventional estimates of the response spectrum, are generally unreliable (Vandiver and Campbell, 1979). Long records lengths are required to obtain good estimates. Further, many such records must be averaged together to reduce the variance of the estimate. Unfortunately, the total record length required may often violate the assumption of stationary excitation. Use of nonstationary response time histories usually leads to overestimates of damping.

An alternative method has been developed at MIT—the Maximum Entropy Method (MEM). This method of spectral analysis is a high-resolution estimator, capable of providing accurate estimates of the half-power bandwidths from ususually short record lengths (Campbell and Vandiver, 1980). The damping ratios thus obtained are less likely to be invalidated by the effects of nonstationary excitation.

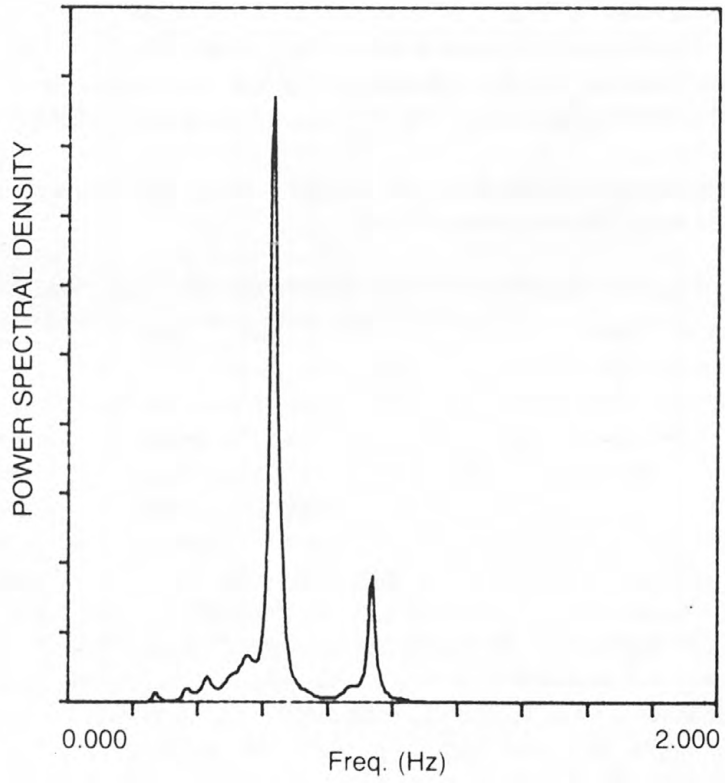

FIGURE 2.—MEM spectral estimate of broadside deck acceleration

Figure 2 shows an MEM estimate of the broadside acceleration response spectrum of the deck of Shell's South pass 62C platform. From this spectrum and a similar one for end-on response, the damping ratio was estimated. These estimates are determined by the Blackman-Tukey method of using the same data. Both of these estimates are compared below with the values published by Ruhl and Bergdahl (1979) as determined by transient decay measurements. The conventionally obtained results are far too low, whereas the MEM results compare quite favorably to Ruhl's measurements, which were taken during mild sea conditions. The MIT spectral estimates were obtained from data recorded in 2- to 3-foot seas and 10-15 knots of wind. Damping values should be expected to increase with sea state. The spectral estimates were computed from a record 30 minutes in length. Note, from the tabulation, that the MEM method also provides estimates of the 95 percent confidence bounds on the damping.

South Pass 62C Damping Estimates for First Order Modes

	MIT Spectral Analysis		Ruhl's Transient Decay Damping
	Blackman-Tukey	MEM	
Broadside	1.14	2.0 ± 0.6	1.65
End-up	0.45	2.1 ± 0.6	1.72
Torsion	0.27	1.3 ± 0.4	1.20

Single channel MEM techniques are being extended to multiple channel methods in order to allow their demonstrated advantages to be used in the calculation of cross-spectra and transfer functions between input and output variables. The new methods will first be applied to the Amoco caisson of figure 3 to identify mode shapes from the vibrational data.

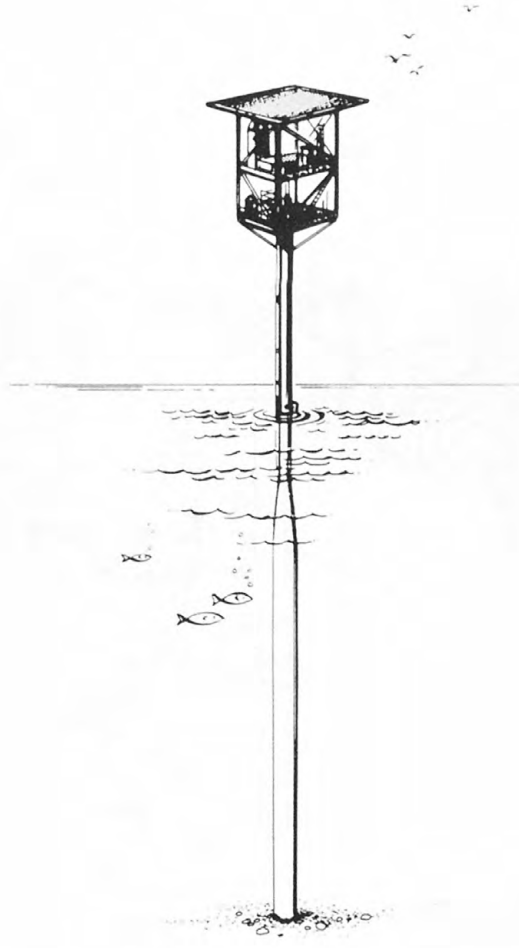

FIGURE 3.—Amoco caisson

Whereas MEM techniques can be used to determine response, accuracy depends upon the quality of data. Manuel (1981) conducted studies to investigate obstacles in detecting structural degredation by measuring changes in internal demping. Conclusions showed that both hydrodynamic viscous effects and the radiation of sound from structural members may obscure any possibility of detecting small changes in material damping of local member modes. The exact results depend strongly on local member properties and the frequency range of interest and, therefore, final conclusions on the applicability of internal damping measurements will have to be decided on a case-by-case basis.

Response Prediction Analysis

With the work on the prediction of structural response to linear wave forces completed (Vandiver, 1979), research emphasis has been directed at the more complex problem of coping with the nonlinear drag forces which excite the structures. The goal has been to develop a frequency domain response prediction technique which would include these nonlinear considerations. Results demonstrate a relationship between sea state and viscous hydrodynamic damping of dynamically active structural modes (Dunwoody, 1980). Numerical simulation and wave tank tests show that viscous damping increases with sea state, and under some conditions viscous damping results in decreased response when higher seas prevail. This anomaly is illustrated in the remaining figures.

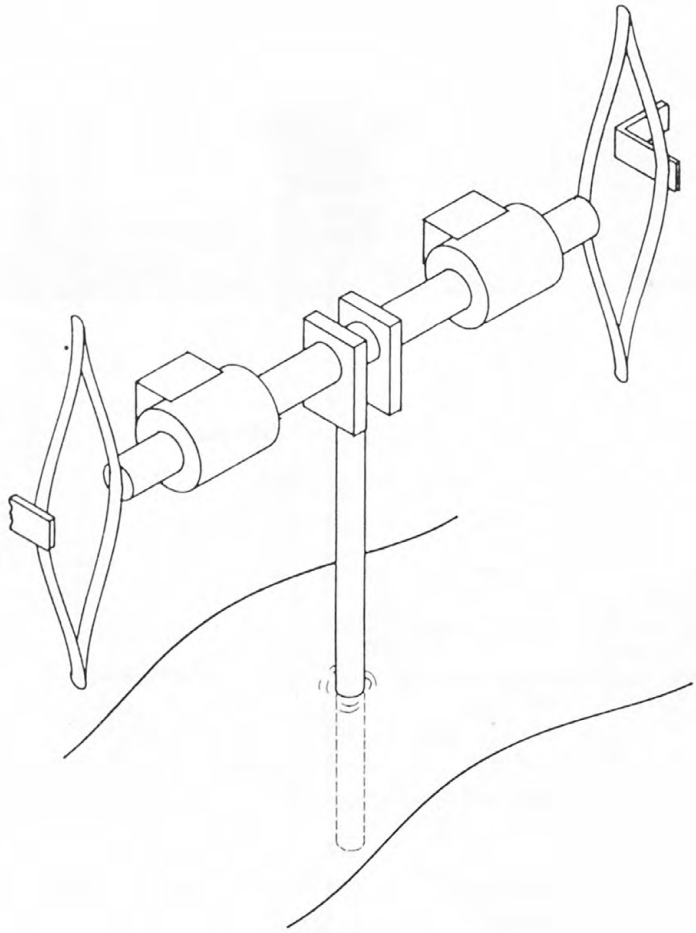

FIGURE 4.—Experimental apparatus for oscillating cylinder

Figure 4 depicts a spring mounted vertical cylinder which extends downward into the water. The cylinder is free to move horizontally on air bearings in the direction of wave travel. The damping of the air bearings is extremely small, thus accentuating the importance of hydrodynamic damping. This system was mounted in the MIT towing tank and excited by various Pierson-Moskowitz modeled sea states. The natural frequency of the cylinder was adjusted to correspond approximately to the frequency of the peak of a 20-knot sea state. The measured wave spectrum was used to predict the response spectrum of the cylinder and the hydrodynamic damping. Figure 5 is the

measured wave spectrum corresponding to a 50-knot wind-driven sea. Figure 6 shows the observed and predicted response spectrum of the cylinder. The predicted and measured root mean square (rms) displacement of the cylinder and the predicted and measured damping are shown in figure 7. As predicted, the damping increases with sea state and the rms response decreases with increasing sea state. This phenomenon was observed in the field test of the caisson structure in the Gulf of Mexico. A direct relationship exists between the drag exciting force spectrum and viscous damping. Whereas the earlier research on dynamic response to linear wave forces demonstrated that the spectrum of these forces is proportional to the radiation (wavemaking) damping of each structural mode, this latter research shows that the drag exciting force spectrum is proportional to the square of the viscous damping of each mode.

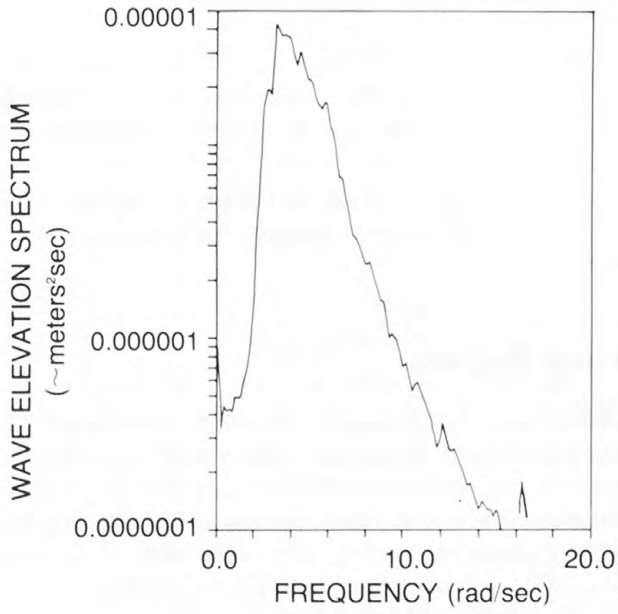

FIGURE 5.—Wave elevation spectrum for 50 knot sea state

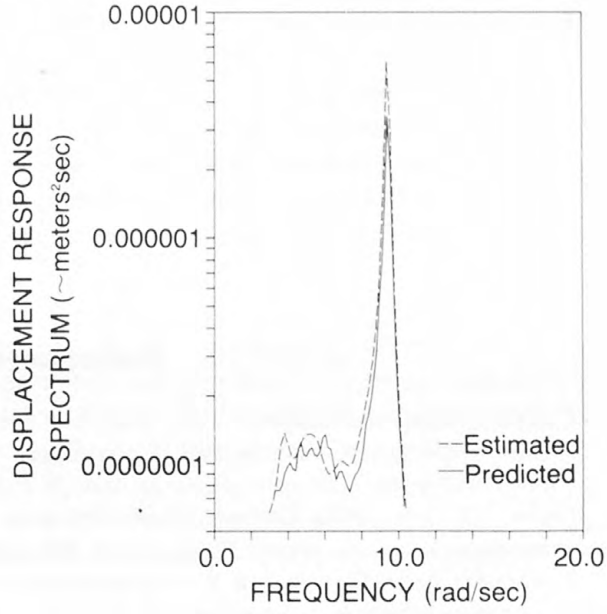

FIGURE 6.—Cylinder deflection spectrum for 50 knot sea state

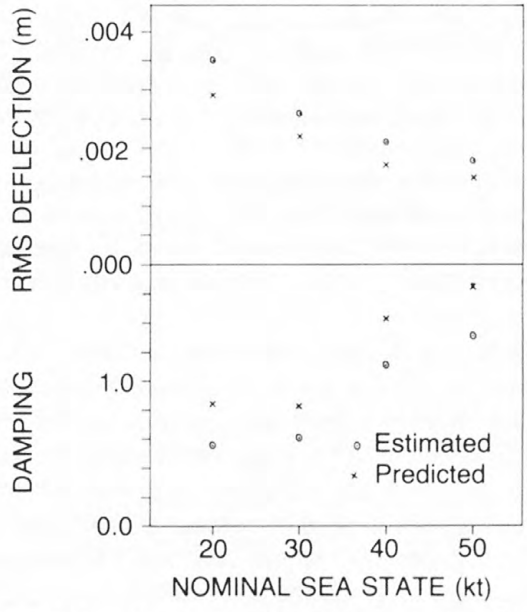

FIGURE 7.—Estimated (from data) and predicted response and damping versus sea state

One of the most important issues in the design of deepwater structures is fatigue life prediction. Professor Vandiver has been investigating the sensitivity of such predictions to variations in modal damping, structural natural frequency, and wave spreading. This research has yielded some rather surprising conclusions (Vandiver, 1980). The fatigue damage contributed by the damping controlled response of a structure at a natural frequency is extremely sensitive to errors in the predicted value of the natural frequency and moderately sensitive to the modal damping ratio and to wave spreading.

The particular example of a simple caisson structure responding principally in its fundamental flexural mode has been worked out analytically. In this case, the fatigue life has been shown to vary in proportion to the natural frequency raised to a power which may vary from 14 to 20. In other words, if the natural frequency is overestimated by 10 percent, the fatigue life is overestimated by a factor of six.

In similar calculations for a simple caisson, fatigue life has been shown to be proportional to approximately the square of the modal damping ratio. By including the influence of wave spreading, fatigue life estimates may be increased by as much as a factor of two for the simple caisson and likely more than that for larger jacket structures.

These analytical results provide considerable insight into the sensitivity of fatigue life calculations of very complex jacket structures to the influence of natural frequency, damping, and wave spreading.

References and Reports

Campbell, R.B., and Vandiver, J.K., 1980, The determination of modal damping ratios from maximum entropy spectral estimates: ASME Winter Annual meeting, Chicago, November 1980, ASME paper No. 80-WA/DSC-29.

Dunwoody, A.B., 1980, The role of separated flow in the prediction of the dynamic response of offshore structures to random waves: Ph.D. Thesis, Department of Ocean Engineering, MIT, May 1980.

Dunwoody, A.B., Campbell, R.B., and Vandiver, J.K., 1981, A mathematical basis for the random decrement vibration signature analysis technique: ASME Design Engineering Technical Conference, Hartford, Conn., September 1981.

Manuel, F., 1981, Detection of structural damage in offshore structures by vibration monitoring of their elements: unpublished thesis, Department of Ocean Engineering, MIT, January 1981.

Ruhl, J.A., and Bergdahl, R.M., 1979, Forced vibration tests of a deepwater platform: Offshore Technology Conference, Houston, Tex., May 1979, Proceedings paper no. 3514, p. 1341-1345.

Vandiver, J.K., 1979, Prediction of the damping controlled response of offshore structures to random excitation: Offshore Technology Conference, Houston, Tex., May 1979, Proceedings paper no. 3515, p. 1355-1364.

_____, 1980, The significance of dynamic response in the estimation of fatigue life: Norge Tekniske Hogskole, Trondheim, Norway, October 1980.

Vandiver, J.K., and Campbell, R.B., 1979, Estimation of natural frequencies and damping ratios of three similar offshore platforms using maximum entropy spectral analysis: ASCE Spring Convention, Boston, Mass., April 6, 1979.

Damage Detection in Offshore Structures by Vibration Measurements

Principal Investigator: Dr. Sheldon Rubin
The Aerospace Corporation
El Segundo, CA 90245

Objective: To assess and advance the utility of vibration measurements for detection of significant strength degradation in steel template structures.

As an outgrowth of vibration measurement studies conducted by the principal investigator on offshore structures and on models, a new technique was devised which may offer significant advantages over present measurement methodologies. This new detection concept promises improved sensitivity and reliability though it requires underwater sensor placement and highly accurate relative amplitude measurements. The following summary addresses the status of past work in two categories of vibration monitoring whose aim is to detect frequency shifts and vibration mode shapes to indicate damage: global mode monitoring and local mode monitoring. The new concept mentioned above will be described and needed research identified.

Global Mode Monitoring

Over the past 7 years, a number of investigators have evaluated above-water ambient vibration measurements for damage detection. The technique is based upon the detection of frequency and shifts of mode shape in lower global modes of vibration (fundamentals, second- and perhaps third-mode groups). Advantages claimed are quickness in making measurements, inexpensive manpower and equipment costs, safety, and independence of weather and sea conditions. The technique is envisioned to be complementary to visual and other nondestructive examination (NDE) methods.

The principal investigator has conducted both experimental and analytical studies on an eight-legged jacket platform in a water depth of 327 feet in the Gulf of Mexico. These investigations and sensitivity studies on generic platform models have yielded the following results in Rubin (1980) and Coppolino and Rubin (1980):

1. Accurate experimental detection of fundamental and certain higher global vibration modes was accomplished in both calm and moderately rough seas.
2. An adjusted mathematical model, satisfactory for failure sensitivity studies, was devised by adjusting interdeck and foundation stiffnesses to yield reasonable correspondence with the measured modes.
3. A 1 percent frequency threshold change of the three fundamental modes (two sways and one torsional) theoretically made possible the detection of complete severance of nearly any one of the vertical diagonal members in an outside face and of a main pile. A corner leg failure was judged detectable because of a 3 percent shift of the second torsion mode. With few exceptions, other types of severances (horizontals, interior diagonals, noncorner main legs) were not detectable. The scope of this study did not include investigation of the masking effect of such nonfailure changes as deck mass, marine growth, and foundation stiffness.
4. Sensitivity analysis of generic platform-bracing configurations produced a good correlation between the largest frequency change of a fundamental mode and a simple compliance parameter involving: (1) the effective number of bays of the platform (fig. 8). The effective number of bays is the number of diagonally braced bays required to yield an overall shear stiffness equal to that at the deck of the actual structure. Foundation flexibilities and above-water unbraced section flexibility contribute to an increase in effective number of bays

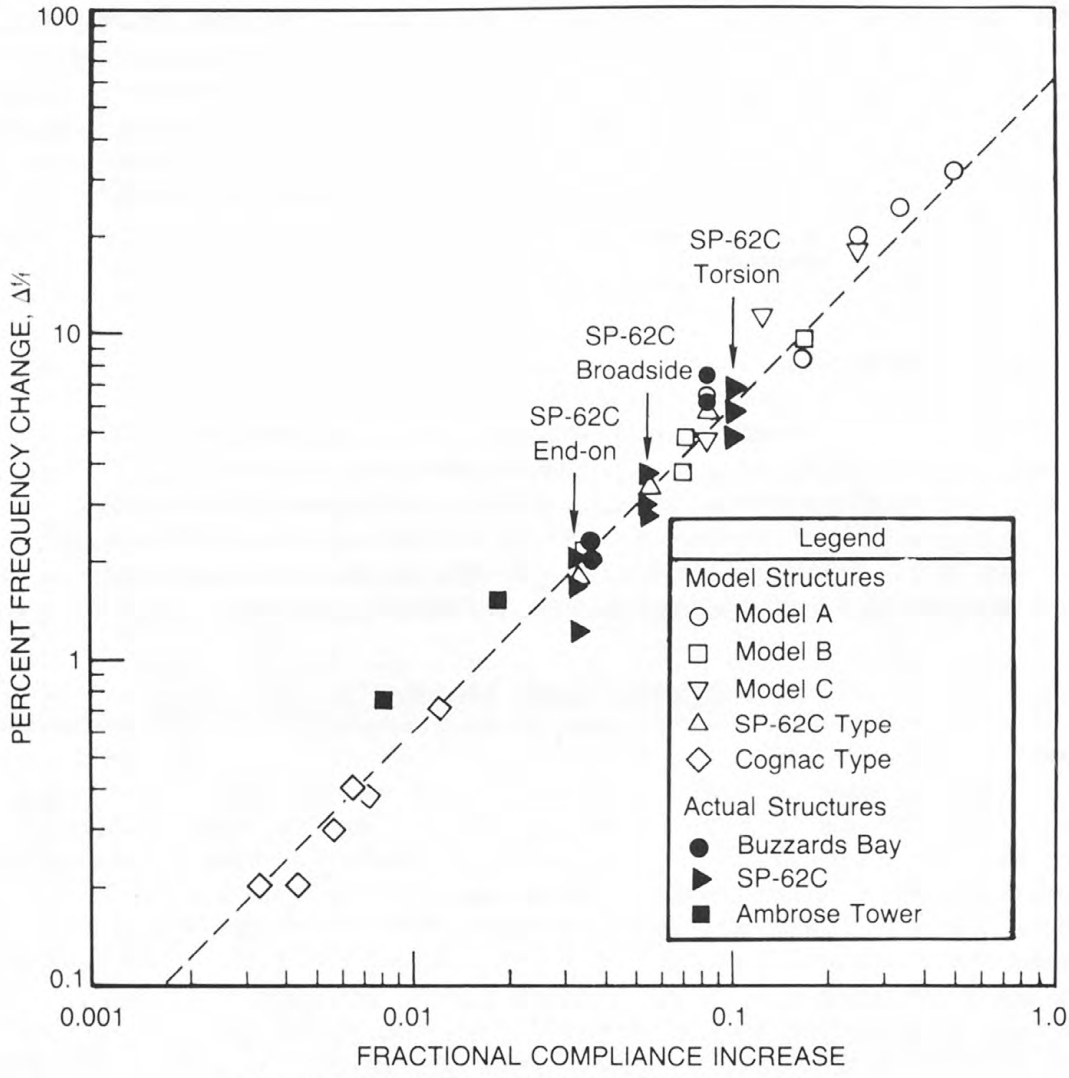

FIGURE 8.—Frequency sensitivity of fundamental modes

over the actual number. Using the method described in Coppolino and Rubin (1980), estimation of the frequency detection capability required for diagonal failure identification is simply accomplished.

5. On the basis of the worst case increase in the axial loading of diagonal members resulting from failure(s), linear analysis of generic bracing models yields a relationship of overall strength loss versus number of effective bays, with frequency detection threshold as a parameter (Coppolino and Rubin, 1980). The results to be conservative in that true strength loss is less than predicted by linear analysis because of the consequences of yielding.

The major shortcomings with the utility of this technique are (1) the uncertain variation of modal frequencies for repeat measurements, often referred to as "stability," stemming from unknown changes other than platform damage (such as changes in deck mass, in soil stiffness, in conductor/guide interaction, and in brace flooding); (2) the difficulty to unambiguously identify higher than fundamental global structural modes; (3) the requirement for substantial frequency change in a fundamental mode for unambiguous detection of damage; and (4) the conflicting desire to detect damage before an unacceptable loss of strength has occurred (fig. 9).

As a result of considerable experience with North Sea structures, estimations indicate that the technique will reliably detect an overall stiffness change in excess of 5 percent (2.5 percent frequency change) based upon an observed frequency stability of 1 to 2 percent (Kenley and Dodds,

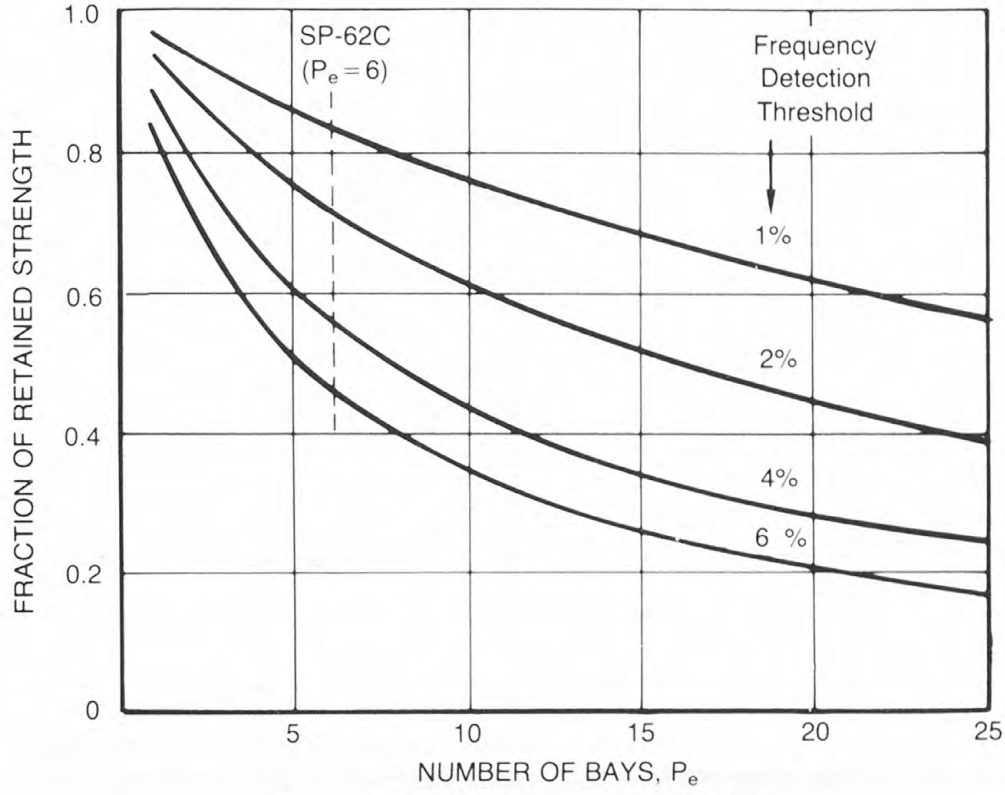

FIGURE 9.—Retained strength from linear analyses

1980). Investigators have concluded that no major developments in the technique appear likely in the near future. Using the results in figure 9, a 2.5 percent frequency change corresponds to about a 30 percent strength loss for a 5-bay structure, increasing to 60 percent for a 20-bay structure. Missing, for an overall assessment of the utility of the technique, is an industrywide definition on an acceptable threshold for strength loss.

A pessimistic appraisal of the technique was made by a joint industry project involving three Gulf of Mexico platforms (Duggan and others, 1980). Observations from one of the platforms (SS274 A) led to the conclusion that as much as a 10 percent variation in a fundamental mode could exist between repeat visits. Only a minor portion of the 10 percent shift was thought to result from a change in mass of oil in a storage tank. Unfortunately, a discussion of the various possible explanations of the shift and the degree of investigation accorded to those possibilities is lacking in the above report. Furthermore, conclusions indicated that second and higher order modes were difficult to identify experimentally and that the modes were substantially effected analytically by the true constraint of conductor tubes within guides and the extent of brace flooding, both of which are uncertain. An analysis of the mathematical model of platform SS274 A along with measurements taken on the actual structure upon removal of one or two diagonal brace members at the waterline, and again after replacement, led to the conclusion that surface vibrational monitoring could not detect with certainty the actual removal of the members. Clearly, this report has raised considerable doubt concerning the general efficacy of the technique.

Local Mode Monitoring

Another monitoring technique under development seeks to detect the vibration modes of individual or groups of brace members in order to identify partial severance caused by major cracking. Such a technique requires divers to place sensors on the brace member(s) being checked. Several variations in the technique have been investigated such as (1) reliance on ambient response

(Kenley and Dodds, 1980), and (2) utilization of forced response, either by forcing directly on the member or by forcing remotely, and measuring frequency responses to position on the brace(s) under investigation (Lepert and others, 1980). These investigations claimed to be able to detect the through cracks extending from 120° to 180° or more circumferentially and flooding of a member, possibly indicating a through crack of any size (although weld porosity could also be the cause).

Two serious concerns about the utility of this method have not been investigated and these have not been addressed in the available literature. First, so-called "local modes" are often not really isolated to a single member or close-connected group of members, such as a K-brace group. Repeated and near repeated geometries of bracing on a typical jacket tend to cause weak coupling interactions among the similar braced sections. Thus, the ability to locate a failure is fraught with danger of misinterpretation. Evidence of the reality of this concern is shown in a recent report by Kenley and Dodds (1980) where measured frequency changes show several gross inconsistencies with computed changes based upon a local structural model. Secondly, the technique does not appear to be able to distinguish between mass change resulting from an unknown degree of partial flooding (perhaps due to porosity or an insignificant through crack) and stiffness change due to major cracking. Thus, detection of mode shifts does not necessarily indicate damage of concern but only indicates that additional inspection is required.

New Concept: Flexibility Monitoring

This concept takes advantage of the basic shear beam behavior of a fixed offshore structure and that the three fundamental mode shapes closely approximate deflections caused by a static load at the deck. The goal is to approximate the shear flexibility across individual bays of the jacket as well as gross flexibilities in respect to the foundation. The term "flexibility" is used to imply deflection per unit force. The forces applied to the jacket are inferred to be proportional to the measured relative deflections of the above-water structure between the deck and jacket top. An estimate of gross shear flexibility of a bay is proportional to the corresponding relative deflection across the bay, divided by the above-water relative deflection. Similarly, by appropriate relative measurements at the foundation, normalized by the same above-water deflection, various foundation flexibilities are estimated.

The attractive characteristics of such an approach are:

1. Total reliance is placed upon detection of the fundamental modes, thus completely avoiding problems with identification of higher modes;
2. Sensitivity is relatively low to deck mass changes, to marine growth, to limited brace flooding, or to conductor/guide contact uncertainty.
3. Sensitivity to damage and the ability to locate damage is enhanced relative to global mode monitoring because flexibility changes are detected on a per structural bay basis and separately for the base/foundation portion. Thus, sensitivity is not reduced for tall structures having numerous bays, or those having a soft foundation, as is the case for global mode monitoring. For example, the model structure (fig. 16) in the Round Robin program, discussed elsewhere in this report, was analyzed to determine indicated flexibility changes for a series of damage and nondamage possibilities. The results for a series of four diagonal severance cases, in the affected first sway mode, are shown in figure 10. The percent frequency reduction in the mode for each failure case is shown by the Δ f/f values. Note that the increases in flexibility for the damaged bays vary from about 90 to 190 percent, whereas much smaller changes (from a 20 percent reduction to a 4 percent increase) are indicated for the nondamaged bays because of minor deviations from the assumed idealized behavior. The face on which the damage exists is indicated clearly by the much larger deflection across that face relative to the opposite undamaged face. Computed results for major deck mass and marine growth changes show little influence on the flexibility indications.

Two complications of the new concept are the needs for underwater placement of sensors and for highly accurate relative amplitude measurements. Underwater placement, as an operational issue, is somewhat mitigated because only sensor positions on main legs are required. Instrument chutes,

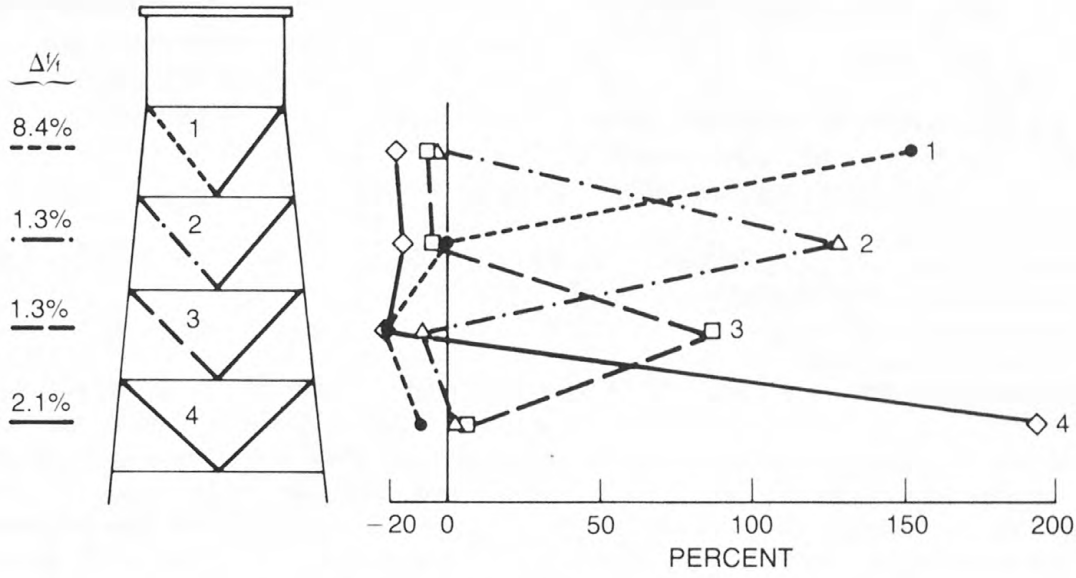

FIGURE 10.—Indicated flexibility changes in first sway mode

which have been placed on corner legs of several platforms installed in the last few years for design evaluation purposes, are ideally suited to the needs of flexibility monitoring. The key measurement issue for flexibility monitoring is the accuracy with which amplitudes can be measured. The principal investigator currently is determining those values from random data obtained by various techniques used on the Round Robin model. The next step will be an offshore investigation to determine accuracy, repeatability, and sensitivity.

Reports and References

Coppolino, R. N., and Rubin, S., 1980, Detectability of structural failures in offshore platforms by ambient vibration monitoring: 1980 Offshore Technology Conference, Houston, Tex., May 1980 Proceedings, Vol. IV, Paper 3865, p. 101-110.

Duggan, D. M., Wallace, E. R., and Caldwell, S. R., 1980, Measured and predicted vibrational behavior in Gulf of Mexico platforms: 1980 Offshore Technology Conference, Houston, Tex., May 1980, Proceedings, Vol. IV, Paper 3864, p. 91-100.

Kenley, R. M., and Dodds, C. J., 1980, West Sole WE Platform: Detection of damage by structural response measurements: 1980 Offshore Technology Conference, Houston, Tex., May 1980, Proceedings, Vol. IV, Paper 3866, p. 111-118.

Lepert, P., Chay, M., Heas, J. Y., and Narzul, P., 1980, "Vibro-detection" applied to offshore platforms: 1980 Offshore Technology Conference, Houston, Tex., May 1980, Proceedings, Vol. IV, Paper 3918, p.627-634.

Rubin, S., 1980, Ambient vibration survey of offshore platform: Journal of Engineering Division, ASCE, Vol. 106, No. EM3, Proc. Paper 15458, June 1980, p. 425-441.

Detection of Incipient Structural Failure by the Random Decrement Method

Principal Investigator: Dr. Jackson Yang
University of Maryland
College Park, MD 20742

Objective: To evaluate the applicability of the random decrement technique for determining flaws in offshore structures

The Random Decrement Method (RANDOMDEC), a relatively new procedure, has shown promise as an inspection technique for offshore structures. RANDOMDEC is a general method of analysis which is particularly suited to the class of problems in which characteristics are desired of inservice structures to unknown random excitation. The major advantage of this technique is that it requires only measurements of the dynamic response of the structure and not the input excitation causing the response. On offshore platforms, such random input forces occur from wind, waves, and currents.

The analysis of a time-history response taken at some location on a structure produces a signature which is dependent on structural properties such as natural frequencies and damping. This signature is sensitive to changes in these structural properties and thus offers a means for detecting changes. RANDOMDEC was initially developed in the late 1960's and received rather wide-spread use in the areospace industry for the determination of modal damping ratios and the detection of mechanical failures.

The method analyzes the measured output of a system subjected to some ambient random input. After analysis, a signal results which is the free vibration response or signature of the structural system. The ability to obtain unique response signatures for different modes (usually accomplished by filtering the output) enables detection of early damage before overall structural integrity is affected. Figure 11 illustrates the acquisition of RANDOMDEC signatures.

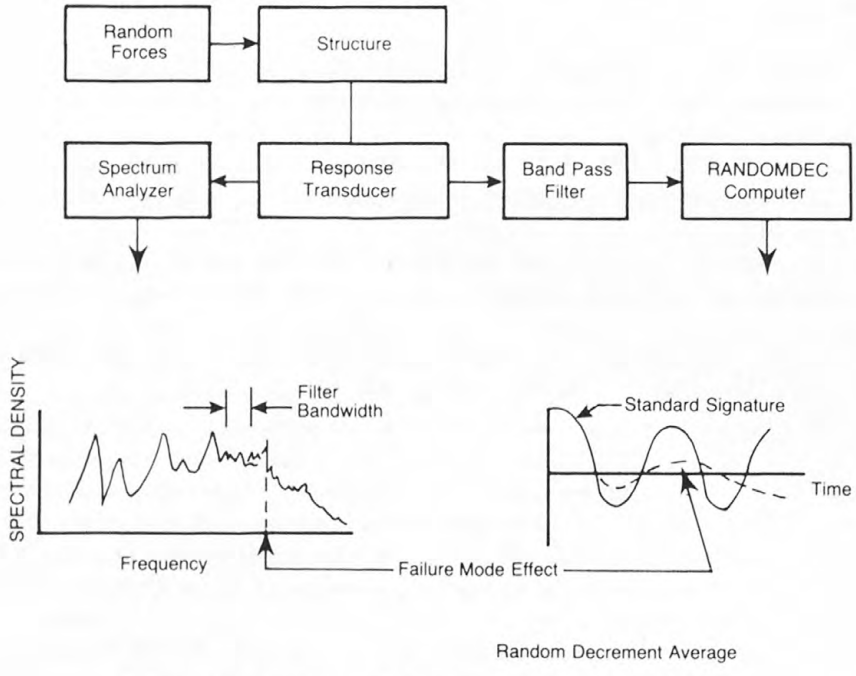

FIGURE 11.—Acquisition of Random Decrement signatures

Cracks show up as small blips in the "hashy" high modal density region of the response spectral density, and as they grow, the failure mode frequencies become lower and approach the fundamentals where failure becomes imminent. Flaws must be detected early enough—that is, at high enough frequencies—if corrective action is to be taken. Detection is accomplished by passing a random response signal through a bandpass filter which is set to screen high frequencies. If a failure develops, the signature will be affected dramatically because it will dynamically couple with structural modes within these bandpass frequencies.

The RANDOMDEC technique is applied to the filtered response data of the vibrating structure both numerically and on a special analog computer. From these signatures, the sensitivity to fatigue cracks of various lengths can be shown. Figure 12 shows four consecutive Random Decrement

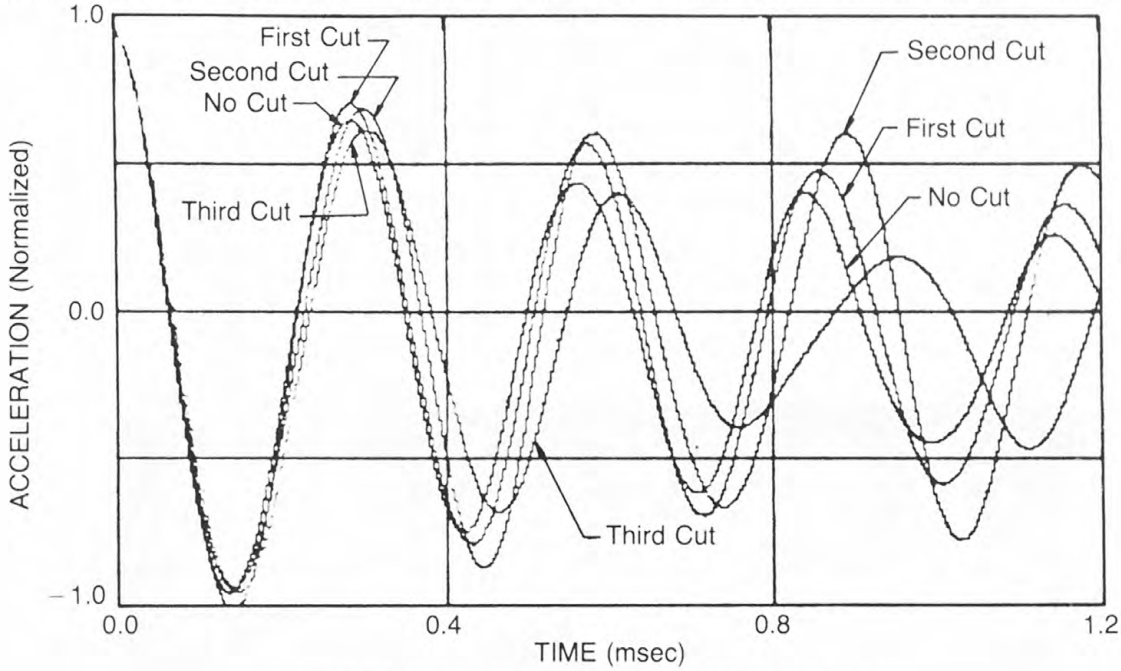

GROUND (No Cut) Test and Cuts #1, #2, #3
Band: 3000 to 4000 Hz Accelerometer #4

FIGURE 12.—RANDOMDEC signatures

signatures taken during a fatigue test of a structural member. All four signature curves were obtained from the same accelerometer sensor and location. The "no cut" curve is the signature for the undamaged condition. The "first cut" signature was obtained after 17,000 cycles of fatigue loading and was the point of crack initiation. The other signatures correspond to data obtained after additional load cycles and crack growth. An obvious decrease occurs in the signature frequency as the crack elongates.

Different correlation methods are used to identify the differences between RANDOMDEC signatures. In one case, a safety envelope is formed around the signature curve from a given sensor. If the signature response taken from a sequence analysis falls outside, it could be an indication of crack initiation or growth.

A calculation of the relative deviation from one signature to another has also been used to detect crack initiation. The equation for the deviation σ is given as

$$\sigma^2 = \frac{1}{N} \sum_{i=1}^{N} \left[f_1(t_i) - f_2(t_i) \right]^2$$

where f_1 and f_2 represent points on two different signature curves taken from the same location at the same time interval, t. The total number of points to be considered is denoted by N. In general, the deviation will increase and the modal frequency will decrease as a crack initiates and propagates.

A 1:13.8-scale offshore platform has been constructed (fig. 13). Its design was based on a dynamic similitude study (Li and others, 1979b). The model platform was fatigue loaded hydraulically and a systematic study of the effect of structural damage was conducted. Responses at various positions along the structure, subjected to random input forces, were obtained at various intervals of cyclic loading.

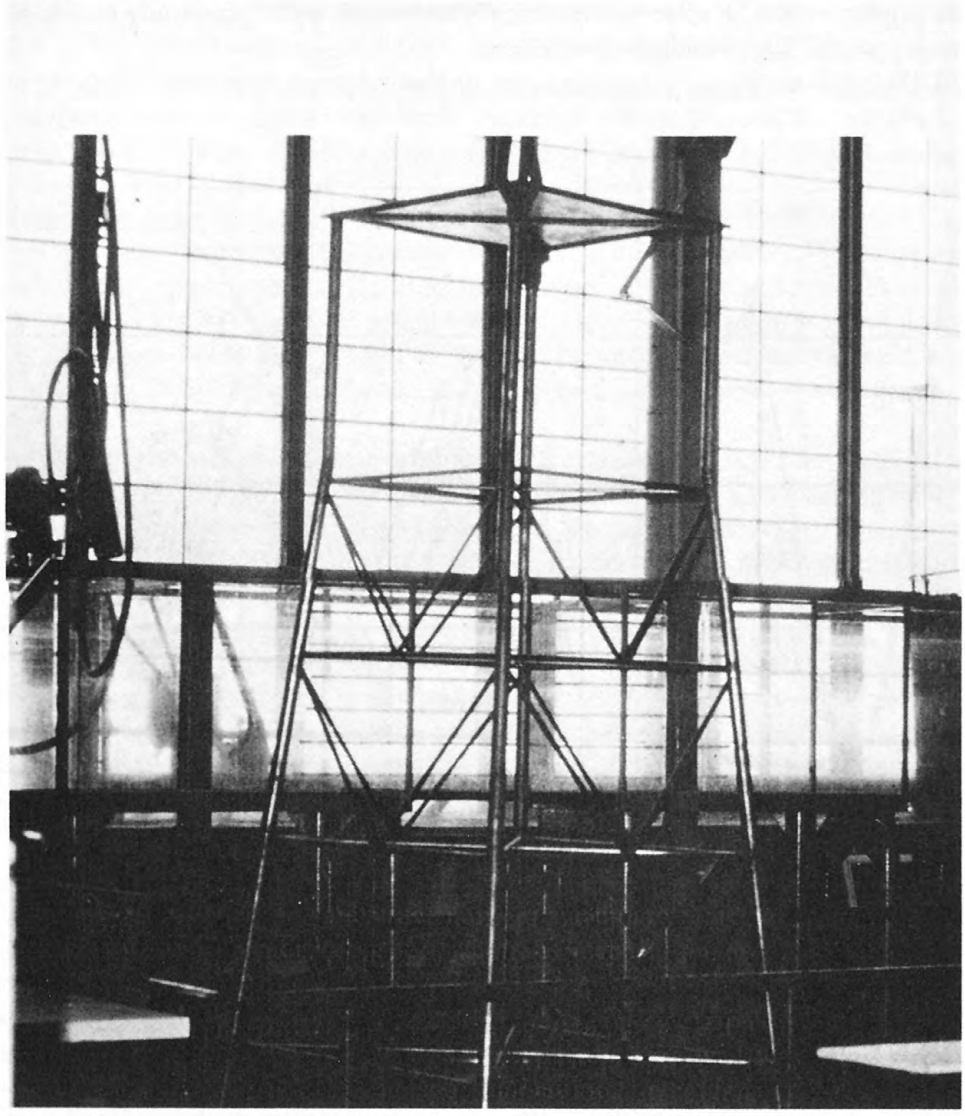

FIGURE 13.—Model offshore platform (Scale 1:13.8)

Fatigue cracks of varying lengths were measured at the welded joints of certain intersecting members. Response time histories were recorded and analyzed to obtain random decrement signatures, and from these recordings their sensitivity to fatigue crack initiation and growth were correlated.

Finite element modeling and analysis of the modeled offshore platform, using the NASTRAN computer program, were performed to determine structural natural frequencies, mode shapes, and transient responses for purposes of instrumentation selection, scaling verification, and dynamic behavior of the structure. Homogenized finite element beam models were developed for the full and the 1:13.8 scale model. The models yield gross structural frequencies, mode shapes, and transient responses which provide a verification of the scaling. This modeling aided the assessment of probable locations of cracks and the estimation of fatigue life. Effects of simulated structural

damage on natural frequency and mode shapes were studied. Results demonstrated the ability of the random decrement technique to measure progressive failure of the models in air.

As more sophisticated analytical techniques for predicting response to dynamic loading and soil-structure interaction are developed and refined, more accurate input parameters must likewise be obtained. One of the most important is the knowledge of the dynamic characteristics of the structure in a soil foundation. The damping properties for this situation are presently lacking. There is very little laboratory data and almost no usable in-situ information. Present research has shown that this difficulty may be overcome by the use of the Random Decrement technique.

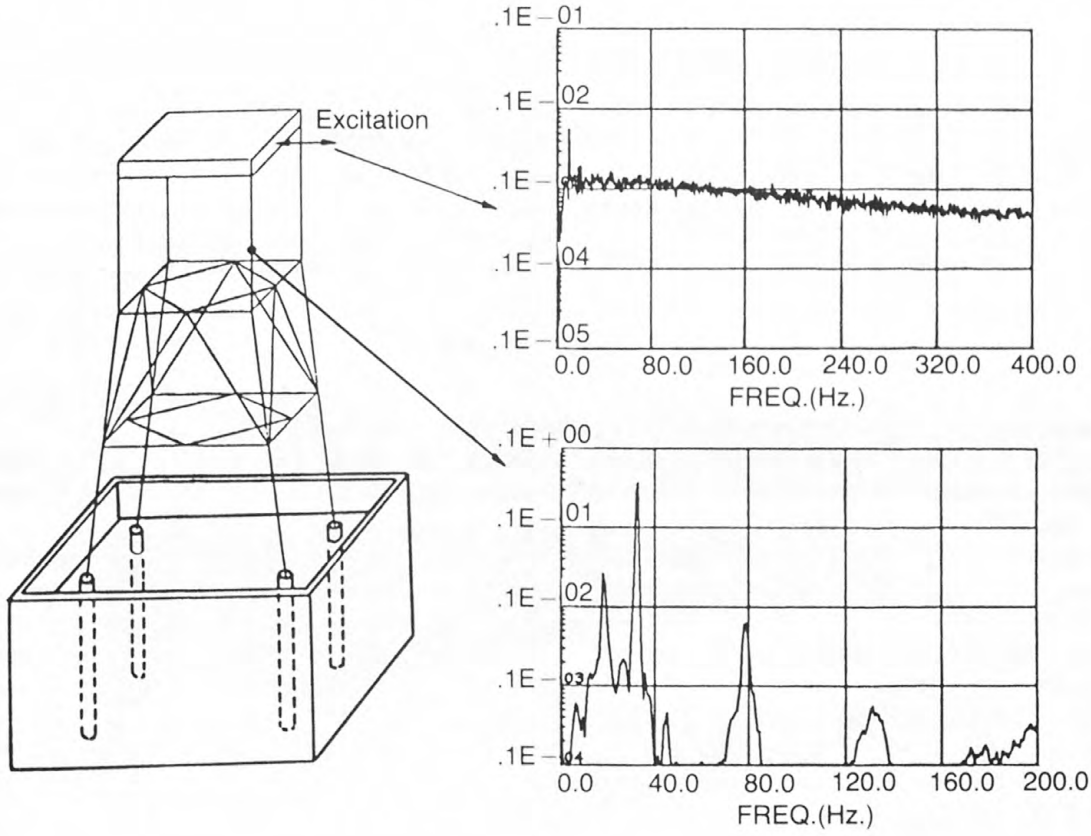

FIGURE 14.—Power spectral density—4-foot-high model on soil foundation

Test Condition	Conventional Techniques				Random Decrement	
	Sine Sweep		Free Response			
	Freq.	Damping	Freq.	Damping	Freq.	Damping
Fixed	15.1	.045-.060	15.1	.024	14.2	.015
	66.0	.0025-.0045	66.0	.0046	63.8	.0030
Free	64.9	.004-.006	64.9	.0045	62.8	.0030
Platform embedded 2 inches in sand	6.9	.065 -.085	6.9	.070	8.1	.065
	59.5	.02 - .04	59.5	.029	60.5	.017

FIGURE 15.—Summary of results

Figure 14 represents a structural model about 4 feet high which is affixed to piles imbedded in sand. A dynamic analysis was performed on the model using the RANDOMDEC technique. Damping ratios and resonant frequencies were obtained by classical methods and compared with RANDOMDEC results (fig. 15).

The RANDOMDEC technique is also being evaluated under the NDE Round Robin Program discussed elsewhere in this report. Future investigations will be made for soil-structure interaction conditions and the model structure will be tested in water.

This project is jointly sponsored by the Geological Survey and the Structural Mechanics Program of the Office of Naval Research.

Reports and References

Kummer, E., Yang, Jackson C. S., and Dagalakis, Nicholas G., 1981, Detection of fatigue cracks in structural members: 2d American Society of Civil Engineering/EMD Specialty Conference, Atlanta, Ga., Jan. 15-16, 1981, Proceedings, p. 445-460.

Li, C. S., Yang, Jackson, C. S., Dagalakis, Nicholas G., 1979a, Dynamic analysis of prototype and 1:13.8 scale model of an offshore platform: ONR-USGS Report No. NO-78-C-0642-3.

_____, 1979b, Similitude analysis of an offshore platform structure: ONR-USGS Report No. NO-78-C-0642-2.

_____, 1980, Similitude analysis and testing of prototype and 1:13.8 scale model of an offshore platform: Shock and Vibration Bulletin (in press).

Miller, M. W., Spiegelthal, D. Yang, Dagalakis, Nicholas G., 1979, Application of the random decrement technique for detection of structural cracks: ONR-USGS Report No. NO-78-C-0632-4.

Yang, Jackson C. S., Aggour, M. S., Dagalakis, Nicholas G., and Miller, F., 1981, Damping of an offshore platform model by Random Dec Method: American Society of Civil Engineers/EMD Specialty Conference, Atlanta, Ga., Jan. 15-16, 1981, Proceedings, p. 819-832.

Yang, Jackson C. S., and Caldwell, Donald W., 1976, The measurement of damping and the detection of damages in structures by the random decrement technique: 46th Shock and Vibration Bulletin, Aug., p. 29-36.

Yang, Jackson C. S., and Dagalakis, Nicholas G., 1980, Detection of incipient failure in structure using Random Decrement Technique: Fall meeting of Society of Experimental Stress Analysis, Ft. Lauderdale, Fla., Oct. 12-15, 1980, Proceedings, p. 43.

_____, 1980, Novel technique is being explored to warn of impending failure of operating systems: Journal of the Acoustic Society of American Supplement 1, Los Angeles, Calif., Nov. 1980, Proceedings, vol. 68.

Yang, Jackson C. S., Dagalakis, Nicholas G., and Hirt, Manfred, 1980, Application of the random decrement technique in the detection of induced cracks on an offshore platform model *in* Computational Methods for Offshore Structgures: Amer. Soc. of Mech. Eng., AMD, vol. 37.

NDE Round Robin

Principal Investigator: Dr. Richard Dame
Mega Engineering
10800 Lockwood Drive
Silver Spring, MD 20901

Objective: To determine the applicability of several nondestructive evaluation (NDE) techniques for determining the structural integrity of fixed offshore platforms

Since the Research and Development Program was established, it has collaborated with the Structural Mechanics Program of the Office of Naval Research (ONR) on NDE technology development. During the past several years, research and development projects have been initiated in NDE methods based on frequency response monitoring, Random Decrement monitoring, internal friction monitoring, and ultrasonics. Research scientists who develop particular techniques often proclaim certain advantages as to their capability as inspection methods, and some techniques have shown certain promise as in situ inspection tools for offshore structures. In order to compare the applicability of these specific techniques for structural monitoring and inspection and to assist in planning future NDE research, USGS, in a joint effort with ONR, has established a round robin testing program.

The principal investigator, Dr. Richard Dame, is serving as a neutral agent for the ONR-USGS program to independently evaluate the several NDE techniques for detecting offshore structural failures. Dr. Dame devised several damage and nondamage situations for a model of an offshore

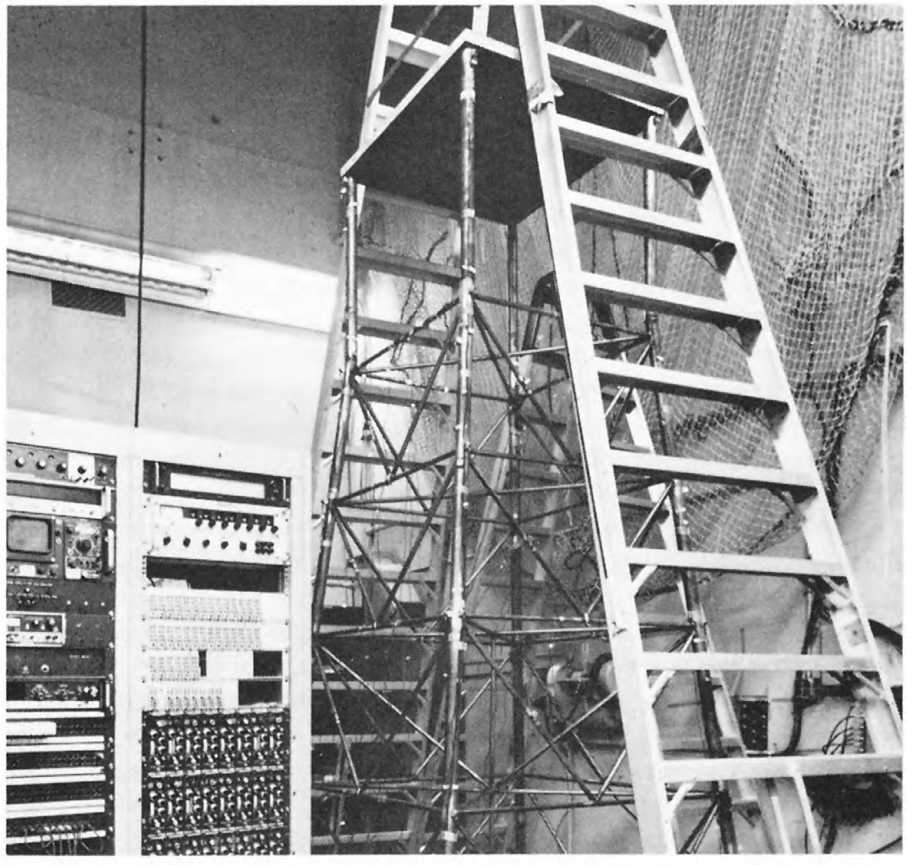

FIGURE 16.—Four legged jacket platform model on test at Goddard Space Flight Center (Scale 1:13.8)

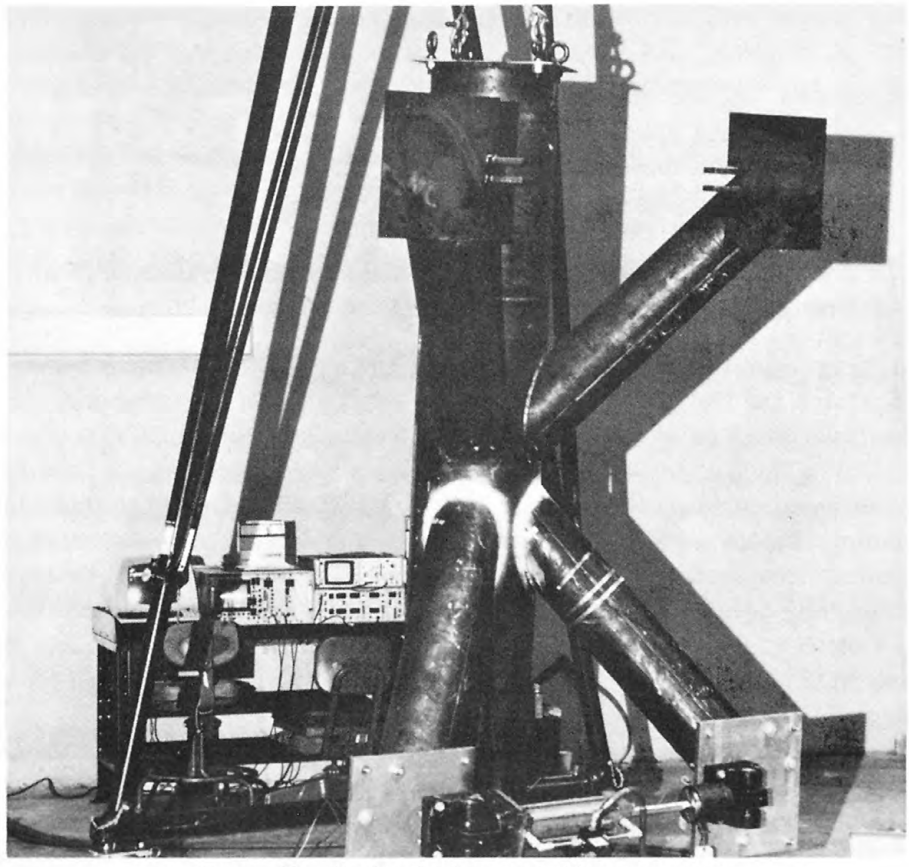

FIGURE 17.—Double K-joint model (40 percent scale)

structure. For each situation, the NDE techniques have been applied to determine if damage has occurred and, if so, the location and extent of the damage.

The actual models used in the validation test are shown in figures 16 and 17. Figure 16 is a photograph of 1:13.8-scale model of a four-legged offshore platform which was built by the University of Maryland. This model is a welded tubular steel structure with a honeycomb sandwich reinforced deck structure. The deck was reinforced to more closely model the stiffness of an actual structure and to avoid any vibration coupling between the deck and the jacket. During testing, the four legs of the platform were rigidly mounted to the test facility floor. The second structure shown in figure 17 is a 40 percent-scale model of a typical offshore tower double K joint and was used only for verification of damage by the ultrasonic method.

The initial series of tests was conducted to establish baseline data for each NDE method. The researchers, or advocates, were permitted to see the models and to adjust their particular instrumentation only for purposes of obtaining this baseline data. The intent of the baseline data is to provide each advocate with a physical description of the tower's performance prior to any damage and against which the data from the damaged mode could be compared. Subsequent monitoring is being performed as a series of blind-mode tests where the testing operations are being accomplished by personnel of the NASA Goddard Space Flight Center, Greenbelt, Md.

Using a series of damage scenarios, data are being taken for each of the NDE methods and are given to the corresponding advocates to be analyzed and interpreted. Based on this information, the advocates will attempt to predict the type of damage and its location within the structural model. The results of each advocate's evaluation will be reviewed, and each technique will then be ranked as to its ability to predict and locate damage.

At this writing, test results have been obtained for four failure scenarios. This information has been given to the advocates who are now in the process of analyzing the data. The nature and extent of further testing within the program will depend upon their findings.

Fracture Toughness of Steel Weldments for Arctic Structures

Principal Investigator: Dr. Harry I. McHenry
Fracture and Deformation Division
National Bureau of Standards
Boulder, CO 80303

Objective: To develop a fracture mechanics rationale for the establishment of toughness requirements on steel weldments of Arctic structures.

The development of oil and gas resources in the Arctic will require the construction of fixed offshore platforms capable of operating safely at temperatures of −40°F and possibly lower. Some of these platforms are likely to be of welded steel construction because of ease of fabrication, high strength, and the availability of grades that are highly fracture resistant at low temperatures. The Arctic environment is potentially hazardous from a structural integrity standpoint because steel weldments have increased susceptibility to brittle fracture at low temperatures. Given this concern, determining the degree of fracture resistance needed for optimum structural integrity is necessary. Following is a summary of the current status of fracture criteria for Arctic structures, the need for further work, and the research plans to develop a technical basis for fracture toughness requirements.

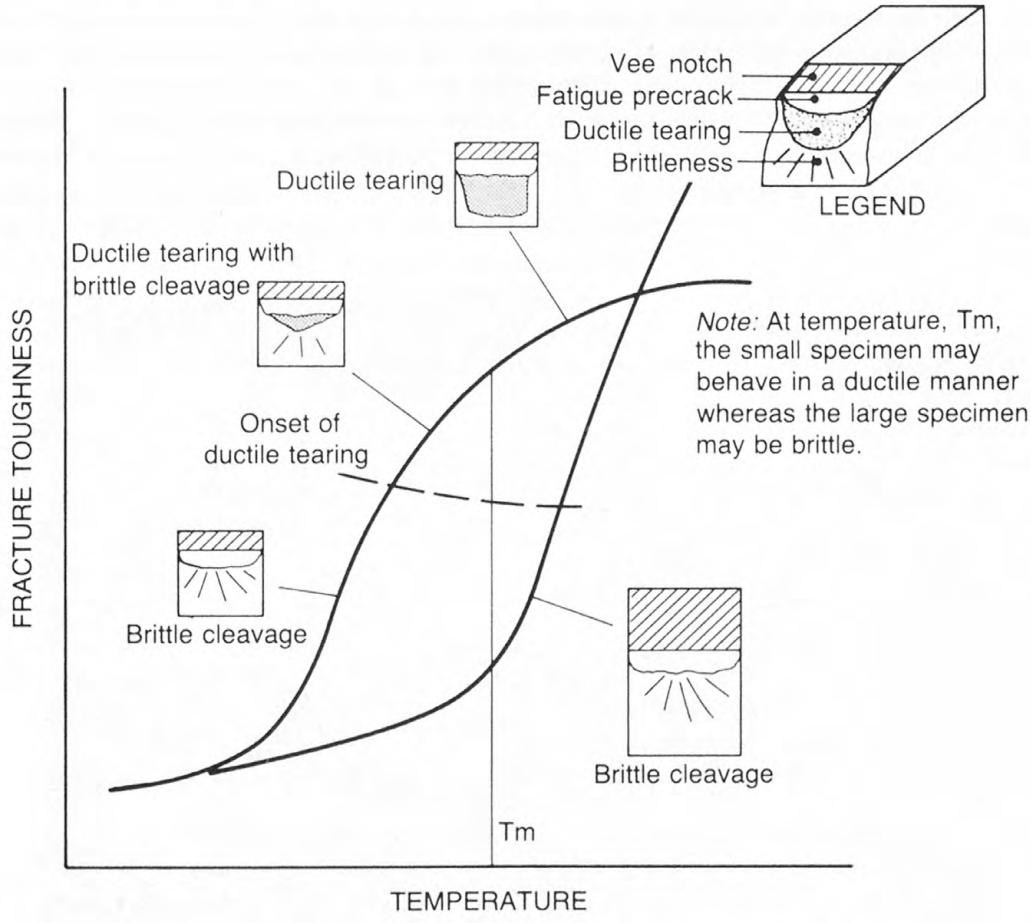

FIGURE 18.—Ductile to brittle transition in small and large specimen steel weldments

In 1979, the U.G. Geological Survey published "The Requirements for Verifying the Structural Integrity of OCS Platforms." These requirements include state-of-the-art performance standards which must be met in designing, fabricating, and installing OCS structures, including those on ice or gravel islands.

To assure satisfactory fracture resistance, guidelines are provided for specifying minimum levels of Charpy V-notch (CVN) impact toughness for low and intermediate strength steels. The CVN toughness guidelines for intermediate strength (45-60 ksi yield strength) steel plates is 25 foot pounds in the longitudinal orientation. The test temperature for steels in the most severe applications is 54°F below the service temperature. Testing at these low temperatures (-104°F), however, is not practical for Arctic structures because economical steels with sufficient toughness are simply not available. Thus, the requirements state: "For service temperatures less than -22°F, test temperatures (for CVN testing) should be specially considered." Selection of the test temperature is not clear. For example, steels used for fracture critical applications such as bridges located in Arctic regions, where the minimum service temperature is -60°F, are CVN tested at 10°F, which is 70°F above the service temperature. Thus, CVN test temperatures may range from 54° below to 72°F above the minimum service temperature, depending on the severity of the application and the applicable guidelines. Clearly, improved test temperature criteria are necessary.

Test temperature is not the only uncertainty in developing fracture criteria. Ductile-to-brittle transition in steels, shown schematically in figure 18, is affected by many factors, primarily temperature, strain rate, and notch geometry. The micromode of fracture changes from ductile tearing, called microvoid coalescence, to brittle cleavage as temperature is reduced; both strain rate and notch-tip constraint are increased. The variations in fracture criteria are due to the qualitative nature of the criteria and the efforts to trade-off test temperature and strain rate. For example, the rationale used for fracture criteria in bridge steels is that a high strain rate test at temperatures above the service temperature is equivalent to a slow strain rate test at lower temperatures; the magnitude of the strain-rate shift is 72°F for intermediate strength steels.

The present investigation is using a quantitative approach for developing fracture criteria based on elastic-plastic fracture mechanics (EPFM). The fracture toughness necessary to avoid brittle fracture at representative service temperatures and strain rates is being determined. The main test variable is notch tip constraint, which is the variable least understood. Ductile-to-brittle transition is being determined as a function of constraint for a 1-inch thick plate of ABS grade EH 36 steel, a 51 ksi yield strength C-Mn steel. The steel is in the normalized condition and has very uniform properties because of sulfide shape control. Thus, material variability is not likely to have much influence on test results. Notch constraint is varied by changing crack length-to-width ratio and specimen thickness. Single-edge-notch bend specimens are used. For each notch configuration, test temperatures cover the complete fracture mode transition, that is, cleavage-to-ductile tearing. In each test, fracture toughness is measured by the two principal EPFM parameters, the J-integral and the crack tip opening displacement. The temperatures at which the various Charpy criteria are met (including the strain rate shift criteria) will be compared with the fracture toughness values measured at that temperature for each of the specimen configurations. The implications of the results with respect to brittle fracture prevention will be assessed using EPFM concepts. Upon completion of the base metal assessment, the same approach will be used to evaluate weld metal and heat-affected zone-toughness criteria. Test welds will be in the same base plate and will be prepared using a single setup process, procedures, and consumables that are representative of practices for welding Arctic platforms.

Unmanned, Free-Swimming Undersea Inspection Technology

Principal Investigators: Paul Heckman
Naval Ocean Systems Center
San Diego, CA 92152

Dr. Robert Corell
University of New Hampshire
Durham, NH 03824

Objective: To develop the technology for underwater inspections of pipelines and structures by unmanned, free-swimming vehicles.

The technology for building small submersibles which can swim underwater, and which can observe and perform useful work as well, had its beginnings about 2 decades ago. Since then, developments have progressed along two basic lines: manned vehicles which are self controlled, and unmanned mechines which are controlled from the ocean surface by an electromechanical umbilical cable. These vehicles, no matter how configured, require online control whether the control is onboard or operated from the surface,

Within the past few years, however, new technologies have appeared which offer much promise for greatly reducing the need for online control. This technology—robotics—someday will allow machines to be programmed in advance to perform specified tasks, to reason, and to communicate with man.

At the root of this technology are microprocessors or chip-sized computers which can be arranged in large-scale integrated circuits to perform the various necessary computations and decisions. Together with other new developments, such as high energy-density batteries, optical fiber and acoustic communication links, and strong lightweight materials, robot submersible development can begin in earnest. The successful development of such vehicles (variously referred to as unmanned-untethered vehicles, unmanned free swimmers, supervisory controlled vehicles, or even

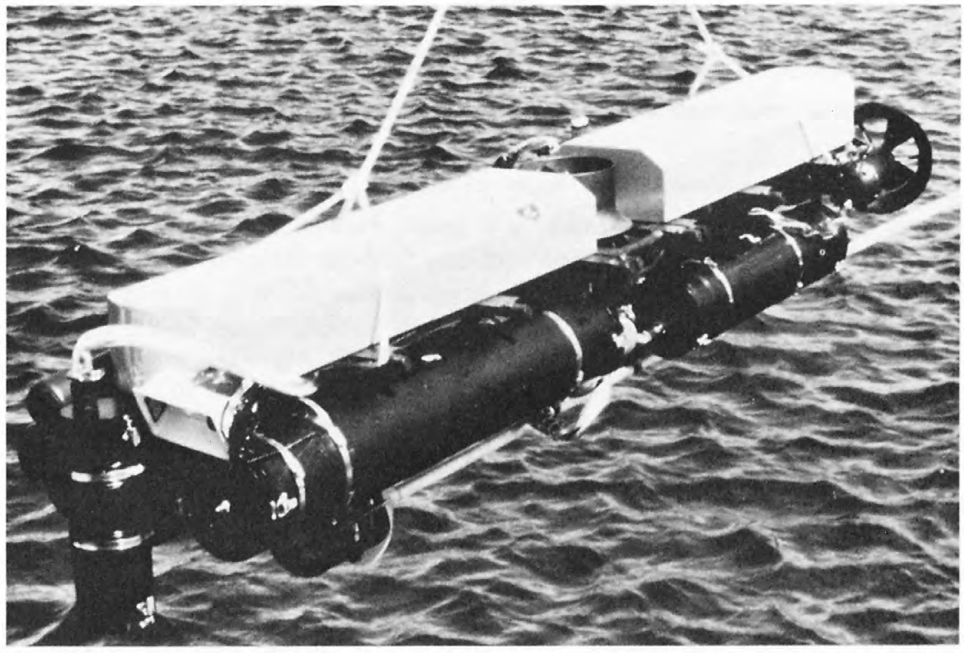

FIGURE 19.—Naval Ocean Systems Center free-swimming testbed vehicle—EAVE-West

autonomous vehicles) will provide alternative solutions to the increasingly perplexing problems regarding the economics of underwater inspection and work.

Of direct interest to the Geological Survey are two underwater situations—inspection of pipelines, and the inspection of structures. These two situations form the bases of scenarios which are being used by USGS investigators in the development of robot vehicle technology.

The program is a collaborative effort between the Naval Ocean Systems Center (NOSC) and the University of New Hampshire (UNH). At NOSC, an open-frame torpedolike submersible, figure 19, has been constructed as a test bed to study magnetic navigation and optical fiber communications. This vehicle is powered by lead-acid batteries which, together with electronics, are located in the four canisters within the vertical frame. Twin propellers are located aft, and a vertical propeller amidships, between syntactic foam buoyancy blocks, provide propulsion for the vehicle. A second

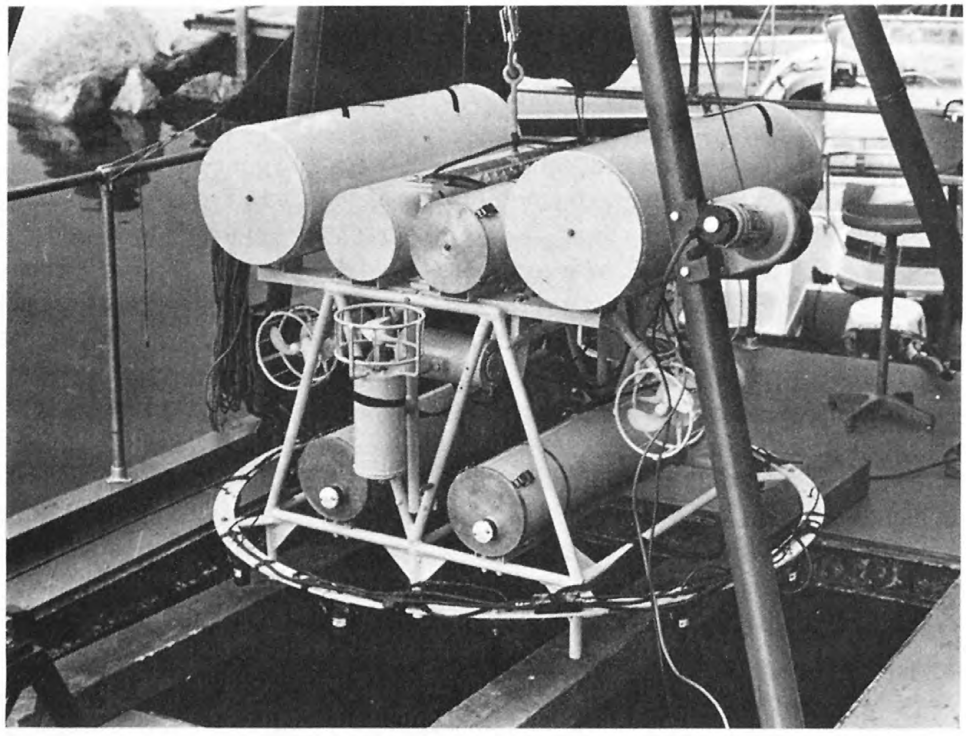

FIGURE 20.—University of New Hampshire free-swimming test-bed vehicle—EAVE-East

test bed, figure 20, this one roundish and able to propel itself in any direction, is being developed by UNH where work is being conducted on acoustics for both navigation and communications. This test bed has twin electrical thrusters on three orthogonal axes and is controlled by electronic equipment located in boxes which are mounted upon the bottom frame. Just below that frame is a ring upon which, for purposes of navigation, 12 equally spaced acoustic sensors are mounted. At the very top are two syntactic foam buoyancy cylinders.

Because future inspection tasks will require more than a stop-and-look capability, man-machine relationship studies are being carried out so that a submersible will be able to perform certain manual tasks such as structural joint cleaning and instrument placement. These studies are being sponsored by the Engineering Psychology Program of the Office of Naval Research.

This technology development program, called the Experimental Autonomous Vehicle (EAVE) Program, has progressed to a point where both the NOSC and the UNH test beds have been tested in water to perform certain fundamental maneuvers.

NOSC Test Bed (EAVE-West)

In developing EAVE-West free-swimming technology, using fiber optics for communications and magnetics for navigation, NOSC has adopted the philosophy of an expansible open frame containing modular subsystems which affords the utmost in development flexibility. In addition, the test bed is designed so that the structure for supervisory controlled hardware and software provides for realtime remote control or autonomous operation. This concept is shown in figure 21. Using the topside computer and CRT console, the operator observes displays, plans, and monitors operations, and issues intermittent commands in the form of program updates. The vehicle computer receives a synopsis of these instructions and executes them through relatively short feedback control loops.

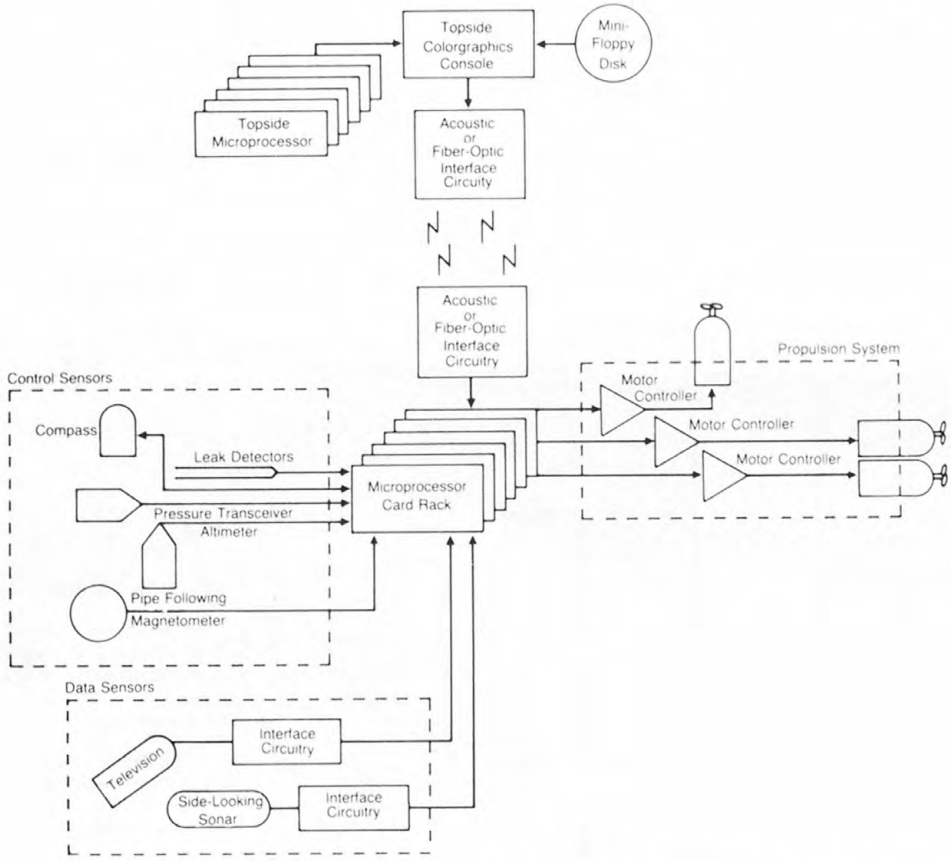

FIGURE 21.—Supervisory control concept of the NOSC free-swimming vehicle

The result is quick man-machine interaction and low bandwidth communication requirements for vehicle operation. To handle the man-machine interface, topside computer software contains 14 kilobytes of executive and utility program in PROM firmware, 24 kilobytes of real-time control routine, and 24 kilobytes of autonomous planning and control routines in random access memory (RAM).

These latter two program modules are loaded from a floppy disk and virtually share memory. The software structure for the topside console is diagrammed in figure 22.

The detailed software structure of the vehicle routines, which actually operate the vehicle after the umbilical cable is disconnected, is shown in the Warnier-Orr Diagram of figure 23. The microprocessor first compares programmed values for heading and depth with actual sensor readings and sends error signals to the thrusters through the appropriate digital-to-analog converter. It then checks a series of emergency conditions such as leaks, overpressure, or low battery voltage. If there

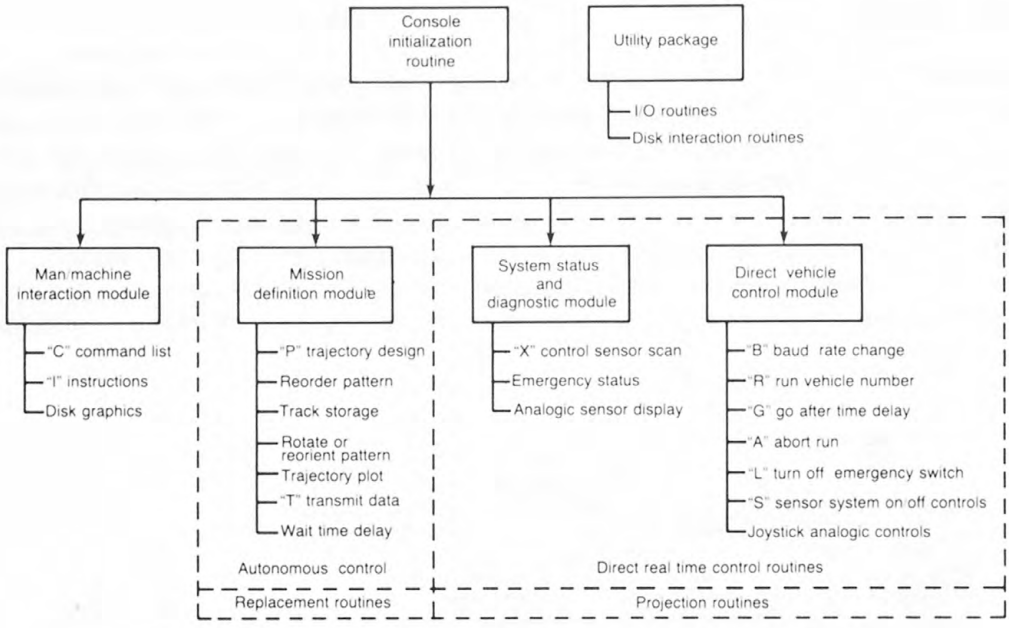

FIGURE 22.—Two processor software architecture for the topside console

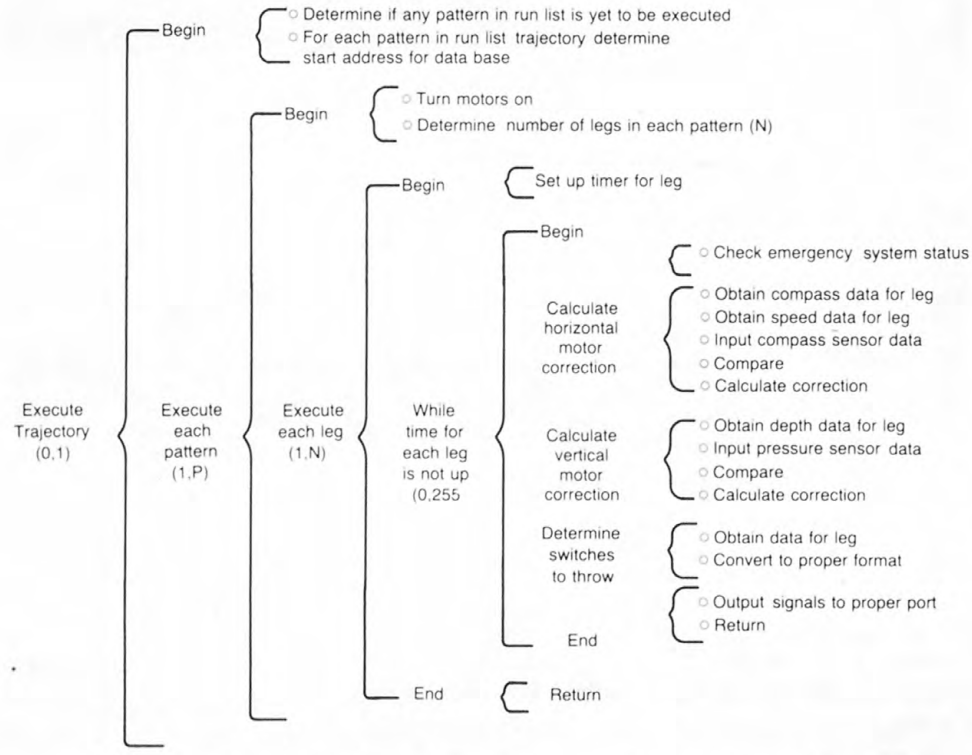

FIGURE 23.—Warnier-ORR diagram for preprogrammed trajectory execution routines

is an emergency, the processor orders the mission aborted by turning on an emergency beacon and returning the vehicle to the surface. If no emergency is evident, it checks the console for a possible abort word which might arrive through the fiber-optic communication link. If all is satisfactory, the vehicle will check a clock chip to determine if it is time to start a new leg. If not, the program will continue to cycle as before; otherwise, it will input the next leg of data and begin its implementation. Details of the EAVE-West modular free-swimming submersible test bed and

description of the supervisory control software are included in Heckman and McAshen (1979) and Heckman (1980).

A fiber optics link for an unmanned submersible offers greater real-time high-bandwidth communication than is possible with electrical communications cables with tethered submersibles, and it allows the vehicle to have the same performance advantages as untethered submersibles having no physical connection (faster speed, higher maneuverability, and relaxed support ship station keeping).

The optical fiber cable is deployed from a spool mounted in the after end of the vehicle. As the vehicle moves through the water, it literally lays the cable astern. Except for a very small drag force on the cable, which is preset to prevent excessive unspooling, the vehicle is not aware of the presence of the linkage. Thus, the vehicle is truly a free swimmer. A development program on fiber

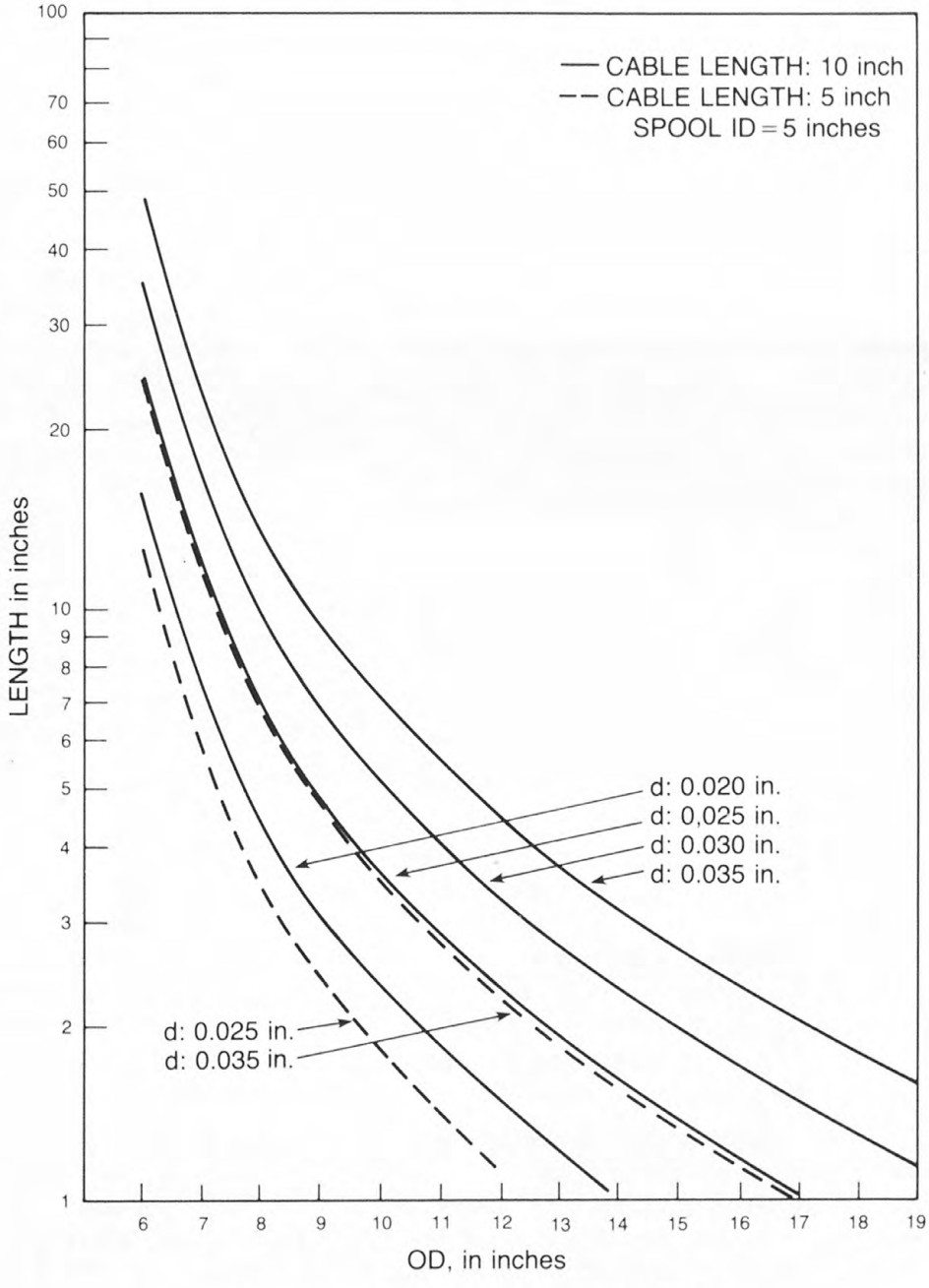

FIGURE 24.—Spool length as a function of OD

optics communications cables, partially in support of the EAVE West Program, has been conducted by NOSC (Cowen, 1979, and Cowen and others, 1980); in addition to cable deployment technology, the factors important to the usage of optical fiber cables have been studied. For example, cost studies have shown that optical fiber costs are lowering quite rapidly and that in the near future, cables probably will be an expendable item.

In addition, studies have been made of the winding of cable on spools for long-range operations, such as in pipe following, and on armoring the cable to strengthen it against abrasion or breakage from snagging of objects. Cable capacity is dependent upon cable length and diameter. Figure 24 plots length as a function of spool OD, given an ID of 5 inches and cable lengths of 5 km and 10 km. These plots are made for cables of different diameters and indicate capacities for slight diameter changes.

Several important electrical measurements for optical fiber cable have been made. An 8 km length of ruggedized (armored) simulated optical fiber cable was wound, payed out, and filmed with high-speed photography which permitted visual verification of the winding/frabrication technique and payout procedures. Tests demonstrated the bonding adhesive used to hold the stiff cable in place on the spool was of sufficient strength and produced 0.5 lbs. of tension at payout speeds of 10-65 knots, which appears optimum. In parallel with the payout work, two 1-km lengths of ITT optical fiber were ruggedized. Electrical measurements before and after ruggedizing indicated no measurable change in attenuation. One of the 1-km lengths was then precision wound and the attenuation was measured up to 7,000 psi hydrostatic pressure. The other spool was subjected to payout tests where both attenuation and tension were measured. At a 1,000 psi pressure, excess attenuation of 0.1 and 0.6 dB/km at 0.83 micrometers wavelength was detected. The spool and cable remained structurally intact being subjected to as much as 7,000 psi, and attenuation measurements conducted many days after pressurization showed no significant change from baseline loss characteristics. Payout tests, too, indicated no detectable increase in attenuation. Attenuation measurements on the cable before and after ruggedizing and winding showed no adverse attenuation effects from either process.

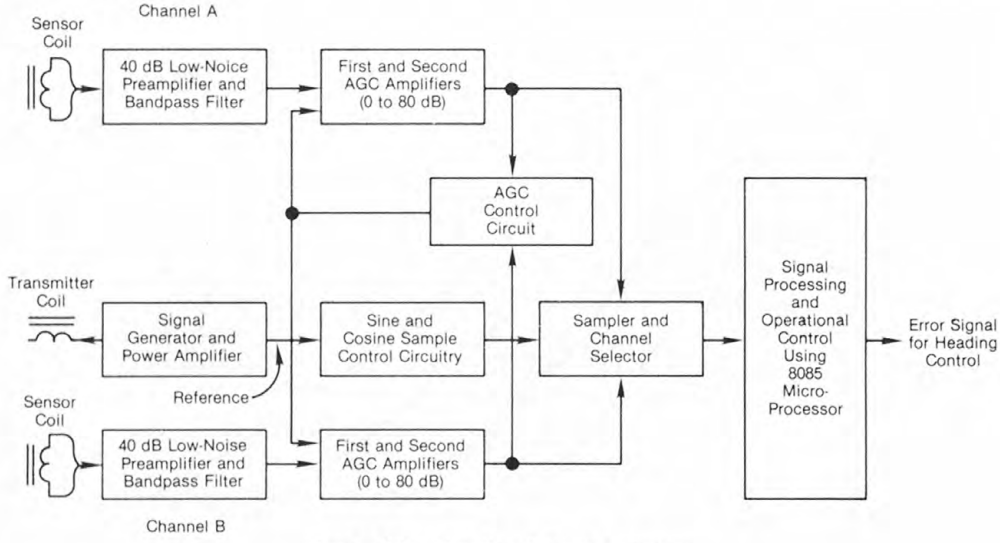

FIGURE 25.—Pipeline following system

Both active and passive magnetic techniques have been investigated for providing control information for pipeline navigation of the free swimmer. Magnetic sensors were chosen for study because of their promising prospects for detecting and following buried pipelines. Results indicate that active magnetic systems should be pursued, primarily because of their inherently cleaner control signals. Transmitter-receiver systems operating at frequencies near either 40 Hz or 4 kHz are recommended. Intermediate frequencies should be avoided because of possible cancellation of

magnetic and eddy current effects. As a result of laboratory testing, detection ranges of about 15 feet are estimated for 2-foot diameter pipelines.

An electronics system for automatically following the pipeline has been designed, fabricated, and tested in the laboratory. This system consists of two receiver coils and one transmitter coil positioned beneath the submersible and held by a fiberglass frame. The electronics, block diagrammed in figure 25, is composed of two receiver cards and one transmitter card. The transmitter sends out a CW signal at 800 Hz which induces a signal in the pipeline. The receiver coils then pick up, filter, and amplify the signal with automatic gain control circuitry. The signal is sampled in a manner to produce sine and cosine functions which can then be squared and added to eliminate any phase dependency of the received signal. The second receiver card, consisting of a dedicated 8085 microprocessor, actually performs the squaring and addition functions as well as providing a time average of up to 200 samples. The vehicle uses this information to automatically acquire and follow a pipeline even when the pipeline is buried.

The manipulator arm, shown in figure 26, has been designed and fabricated for the vehicle (Bosse and Heckman, 1980), and man-machine studies for its use are being conducted in conjunction with the Engineering Psychology Program of the Office of Naval Research, as previously mentioned.

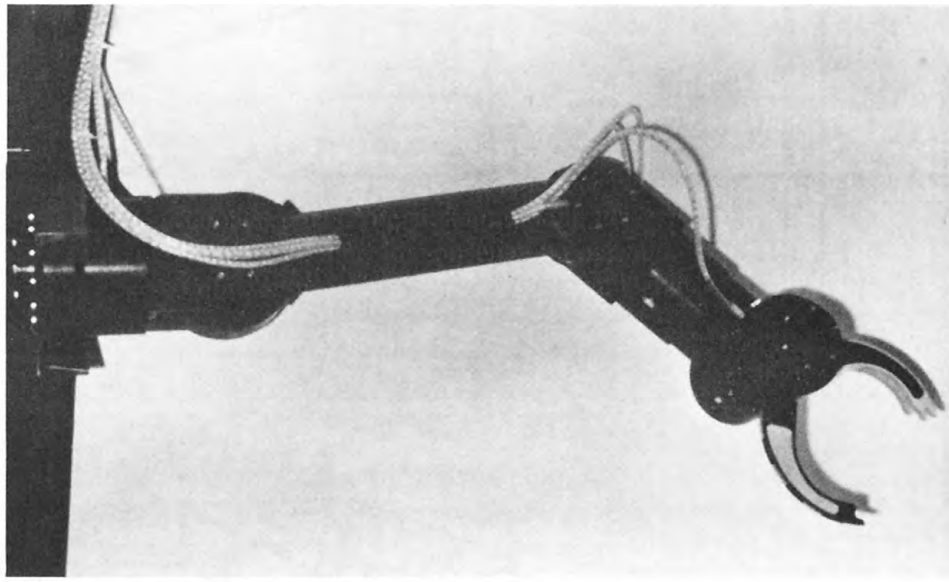

FIGURE 26.—Manipulator arm for EAVE-West

UNH Test Bed (EAVE-East)

During the past year, development efforts have been redirected from pipeline following to three-dimensional navigation, that is, to the inspection of underwater structures. This added complexity over navigating along a pipeline was deemed necessary so that decisions made on the acquisition of electronics hardware would be made in a timely manner.

For purposes of development, a test structure (fig. 27) has been designed which will ultimately be placed on the bottom of the University's test facility at Lake Winnipesaukee, N.H. The task under study is to navigate the vehicle toward the structure and then to proceed through it to a specific point. Once having arrived, the vehicle will photograph a predefined marking on the structure, return to its starting location, and then surface.

In order to implement the proposed mission, the test structure has to be defined in terms which are recognized and understood by the onboard computer system. A program has been developed

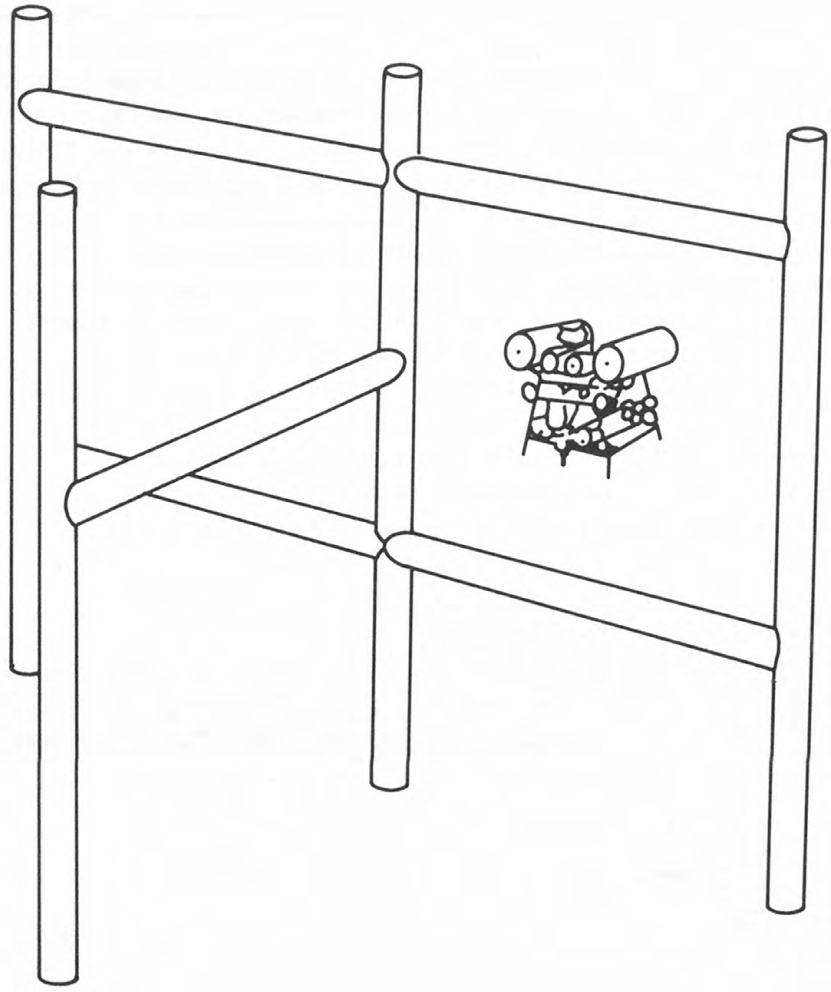

FIGURE 27.—Test structure

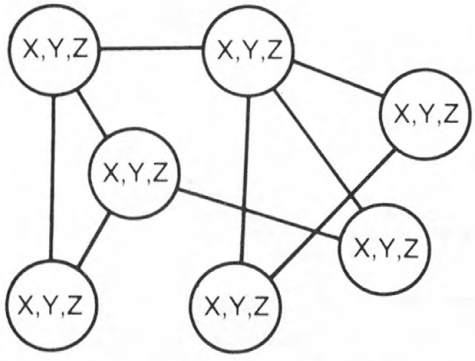

FIGURE 28.—Structure mode network

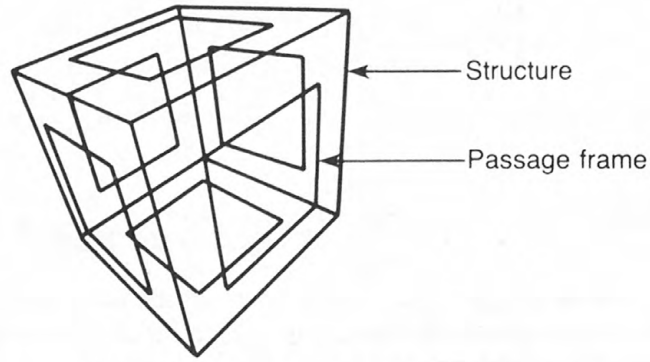

FIGURE 29.—Passage frames for a cubical structure

which defines the platform's structure, and the resulting information has been placed in the vehicle's computer memory. This definition consists of lists of vertices, structural members, and planar polygons that comprise the structure. In the case of more complex structures, the input of this information would be graphically assisted. Once provided with a description, the analysis program produces a map or node network (fig. 28) that defines all safe paths through the structure (fig. 29). The techniques used are general enough to be applicable to nearly all underwater structures.

The onboard computer for EAVE East is a multiprocessor system (fig. 30) consisting of one primary mission controlling computer (MC 68000 based) and three secondary computers (Intersil 6100 based) used for special functions. The mission controlling computer (command computer) communicates with the three secondary computers, receiving information and distributing commands and data. The three secondary computers are for control, navigation, and communications. The control computer controls the vehicle's thrusters. The navigation computer receives data from both the command computer and the onboard acoustic transponder system to calculate position and heading. The communication computer receives data from the command computer and transmits the data to the surface over an acoustic link. Information and commands sent to the vehicle from the surface are interpreted by the communication computer and relayed to the command computer.

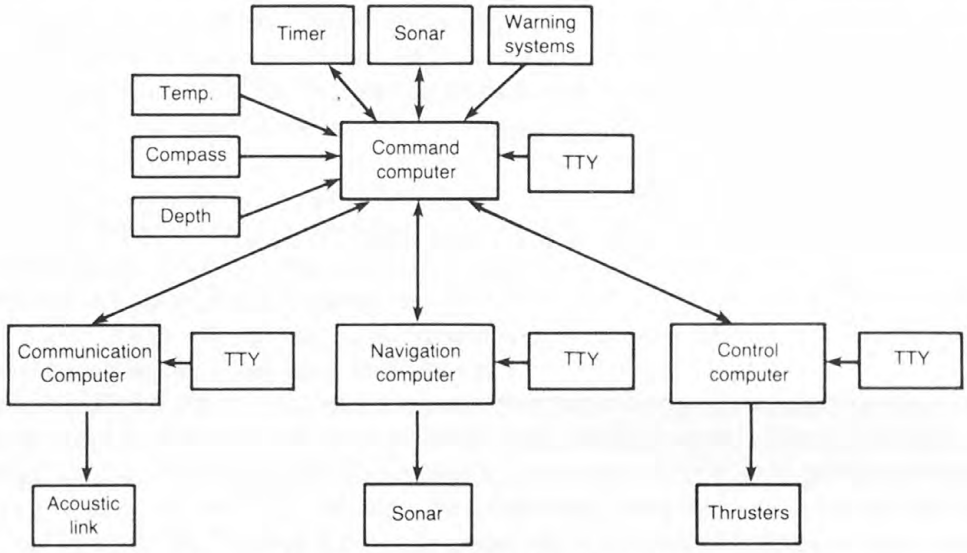

FIGURE 30.—Computer diagram of multiprocessor system

Each processor in the system has an associated body of software used to accomplish its assigned mission tasks. In addition to this task-oriented software, a standardized method of communications between processors is needed. Interprocessor communications occur as follows:

1. *Commands:* Each processor may receive a single command having several parameters. This information is decoded and immediate action is taken by the receiving processor. For example, the control computer accepts thruster speed commands in this manner.
2. *Requests for Data:* A computer accomplishes a task by requesting a block transfer of data from another computer. A coded word sent to the targeted processor contains the identification of the requesting processor and the identification of the task in the targeted processor. These are in the form of channel identification and the number of words requested.
3. *Data Transfer:* Data transferred from each task in a processor is included in the task itself. Upon receipt of a request for data, a header word is sent which contains channel identification and number of words to be transferred and is followed by the appropriate number of data bytes.

The navigation system on the vehicle triangulates on a computer-controlled, high-frequency acoustic transponder navigation range. The vehicle is equipped with three equilaterally positioned transducers, each connected to one transmitter and one receiver. Using one of the three transmitters, a sonar pulse of 95 kHz is transmitted to the three range transponders, called object transponders, each of which senses the transmitted frequency. After a fixed delay, pulses are returned and detected by the vehicle receiver. The object transponders transmit acoustic pulses at frequencies between 110 and 130 kHz. Each receiver has three detectors (one at each of the transponder frequencies) which sense the arrival of a specific pulsed frequency. When the signal is detected, the corresponding counter (started at the initial transmission) is stopped. From one 95 kHz interrogation

pulse, nine two-way travel times may be obtained. From these numbers, the navigation computer provides the necessary navigation information.

Using the coordinates of the object transponders and the respective distances from them, a position in an x-y plane can be computed as well as an absolute heading (angle in x-y plane between the vehicle longitudinal axis and a line connecting the vehicle with one of the object transponders). When the vehicle is outside a 200 foot range, the navigation computer provides a relative heading, range (from one of the object transponders), and their derivatives (relative heading dot and range dot). When the vehicle is within the 200 foot range, the navigation computer is responsible for vehicle x-y coordinates, absolute heading and their derivatives (x velocity, y velocity, heading dot).

Problems such as multipath and shadowing, as well as sound velocity errors and errors in placement of the object transponders, occur. Therefore, before any navigation calculations are performed, raw data must be checked for validity. This check is accomplished by comparing the raw data with a "window," which is a predicted value based on archived information called "history." By adjusting the width or size (tolerance) of the window, variance can be provided which permits small errors and displacement from real time.

Initialization (as it is called) of the window at the beginning of an operation is accomplished by obtaining a number of returns and checking them for uniformity. When enough data are consistent, a window is formed using the most recent sample. At long range, all transponders may not be heard and, in such a case, only windows for received data are initially set. Windows not set are initialized directly "on the fly" as the returns begin to be received.

Because the windows change as the vehicle moves, they must be continually updated. Also, since windows are based primarily upon the previously received sample, a way must be made to determine if a setting has been made correctly. In order to detect a faulty window, a coded matrix has been devised (fig. 31), which is based upon element by element comparison in matrix from between the raw data, its corresponding elements of windows, and window sizes in matrix form. If a raw-data term is within window size it is termed as a "good return," but if the return is outside of the window and window size, it is termed a "bad return." An element for which no return is obtained is termed a "no return."

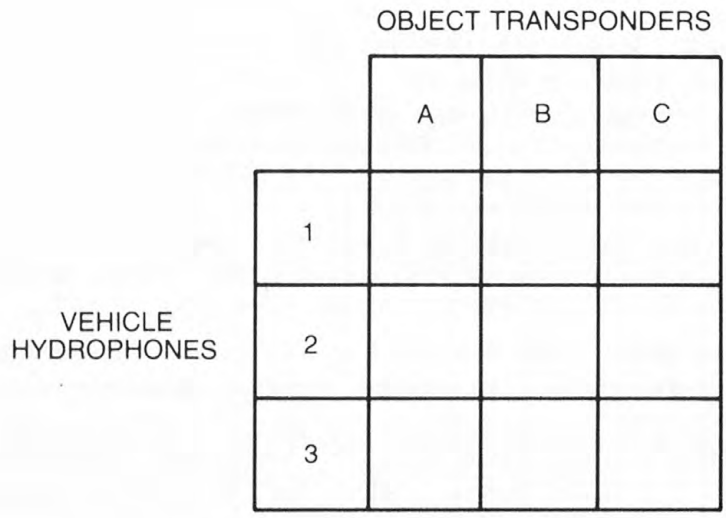

FIGURE 31.—Coded matrix

Beyond the use for window adjustment, the coded matrix is able to determine what position information can be computed. The mathematics used to compute position uses horizontal distance from two object transponders, which yields two solutions mirrored about a line drawn through the two transponders. To avoid ambiguity, either history (previous samples) or the distance to the third transponder must be used. If the distance to the third (unused) transponder is available, by computing that distance twice and using the two solutions, the closest can be determined. If history is available, by comparing the two solutions with previous samples, the closest one can be determined. In addition, upon examination of the coded matrix, if at least two returns are "good," a position can be calculated. But, if no history is available, three good returns must be received. A relative heading is computed using the distance from one object transponder to each of the three hydrophones. By examining the coded matrix, a decision can be made if sufficient good returns have been received to compute the relative heading.

When all returns in a column are consistently bad or if there is a no return status even after window correction, failure of either the counters or transponder is indicated. If the same conditions exist consecutively, a failure of the hydrophone is indicated. Each time one of these conditions occurs in the coded matrix, a hardware error is recorded. A running count of hardware errors is maintained and, if the number of errors over the number of samples is large enough, a malfunction condition is denoted. When the vehicle is within a 100 foot range of the structure in question, the probability of shadowing increases and error analysis becomes invalid. Outside the 200 foot range, one or more of the object transponders may be out of range of reception, and error analysis is again invalid. The coded matrix allows window correction, "one-look" information availability, pinger decision, and elementary error analysis.

Differential calculations are made using the difference between present (last sample) information and information stored in history over one cycle time. Because of memory limitations only one set of samples (group information generated by one pass of the algorithm) can be stored in history.

References and Reports

Blidberg, D. R., Allmendinger, E. E., Sideris, N., 1978, The development of an unmanned, self-controlled, free swimming vehicle: Offshore Technology Conference.

Blidberg, D. R., Westneat, A. S., 1978, An unmanned, untethered inspection vehicle: Marine Technology Society.

Bosse, P., Heckman, P. J., 1980, Development of an underwater manipulator for use on a free-swimming unmanned submersible: Naval Ocean Systems Center Technical Report TR 532.

Cowen, S. J., 1979, Fiber optic video transmission system employing pulse frequency modulation: Proceedings, "Oceans 79," Institute of Electrical and Electronic Engineers, September 1979.

Cowen, S. J., Heckman, P. J., Kono, M., 1980, Fiber-optic communication links for unmanned inspection submersibles: Naval Ocean Systems Center Technical Report TR 652.

Heckman, P. J., 1980, Free swimming submersible testbed (EAVE WEST): Naval Ocean Systems Center Technical Report TR 622.

_____, 1981, Undersea free-swimming testbed vehicle: Association for unmanned vehicle systems 2nd Annual Symposium on Guidance, Navigation and Flight Control of UVS, Stanford University, 18 February 1981.

Heckman, P. J., McCracken, H. B., 1979, An untethered, unmanned submersible: Proceedings, "Oceans '79," Institute of Electrical and Electronic Engineers, September 1979.

Heckman, P. J., Yoerger, D., Sheridan, T. B., 1980, The NOSC/MIT submersible manipulator: An experiment in remote supervisory control of a microprocessor based robot: International Conference on Cybernetics and Society, Session F10P on Robotics, Cambridge, MA, 10 October 1980.

Acoustic Transmission of Digital Data From Underwater Sensors

Principal Investigator: Dr. Eric J. Softley
Ocean Electronic Applications, Inc.
50 West Mashta Drive
Key Biscayne, FL 33149

Objective: To develop an environmentally adaptive acoustic link for underwater transmission of digital data.

As the offshore industry continues to move into deeper and more hazardous ocean frontiers, the need for underwater information increases. Cable systems, currently used almost exclusively from underwater data sources, are cumbersome to handle and control as well as being expensive. In addition, becuase they reach upwards through the water column and are therefore subject to the rigors of the sea, they are a major source of system failure.

Recent advances in electronics technology and power supplies, such as Complimentary Metal Oxide Semiconductors—Large-Scale Integrated (CMOSLSI) electronics, and lithium batteries, now encourage the acoustic transmission of preprocessed underwater data, thus eliminating the need for cable telemetry in many situations.

Several of these situations are being addressed in a parametric development study which employs an acoustic system that can automatically adapt to various environmental conditions. Adaptation is highly desirable because, although acoustic signals travel well underwater, such factors as depth and temperature profile have great effects on their attenuation and reverberation. The adaptive system addresses this environmental problem by using transceivers at both the data source and receiver which, in essence, "talk" to each other to decide upon acoustic frequency, bit rate, and power.

The underwater data retrieval situations being considered are:

(1) Structural monitoring of ocean platforms;
(2) Operational support of unmanned untethered vehicles; and
(3) Interrogation of underwater instruments by means of air launched transceivers.

These situations require a wide range of data transmission rates and path lengths. An example of long-range, slow-data rate transmission is the control of an unmanned, untethered vehicle wherein a simple update of the onboard computer is needed. High-data transfer would be necessary for the telemetry of video information from an underwater camera carried on such a vehicle.

The principal investigator has defined a system for adaptive acoustic data telemetry. Development of the system can be envisioned to have three phases. The first is system hardware which permits

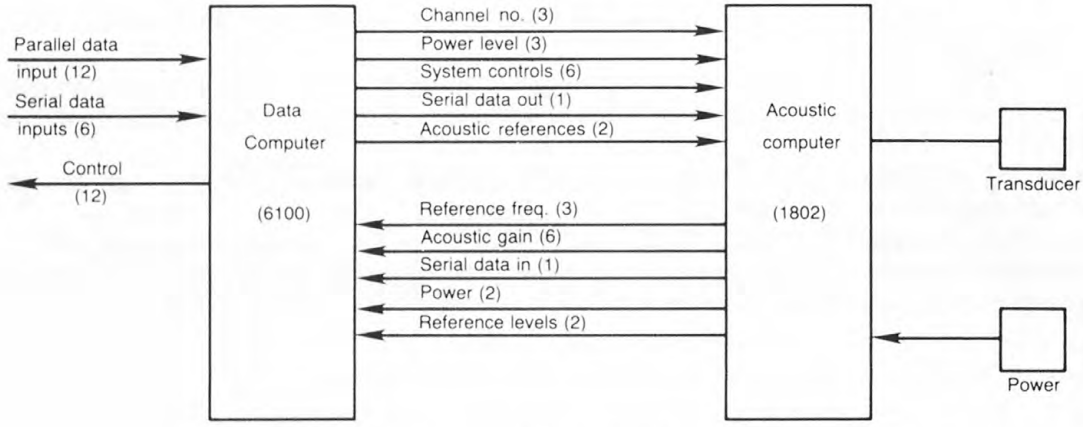

FIGURE 32.—System layout for each transceiver

acoustic communications to take place. The second is software which allows the system to analyze the acoustics and determine the adequacy of the link. The third is additional software which enables the system to use intelligence to adapt to environmental conditions. The three are interrelated and, as development has continued into the second phase, lessons learned there have caused changes in hardware design.

The hardware consists of two units: an underwater telemetry unit at the source of interest and a surface unit, which is suspended from a platform or a vessel. Each unit has a transmitter and receiver designed around a dual microprocessor system (fig. 32). The first microcomputer acts as a data source which determines the nature of the data to be transmitted, formats the data, selects the acoustic channel, and analyzes the received bit stream. The second microprocessor operates the acoustic system, synthesizes the necessary frequencies, and controls digital automatic gain. Eight acoustic channels are used over a frequency range of 12 to 90 kHz. A single transducer is to minimize the complexity of the system, but for a more optimum system, a set of transducers would be needed. Frequency modulation of the acoustic carrier is used and pulse-width coding is employed to allow recovery of the bit clock and to optimize the data rate in the presence of environmentally induced bit jitter. For each acoustic channel, a set of bit rates is used which is proportional to acoustic frequency. The lower acoustic frequencies attenuate less and have the potential for being transmitted over longer ranges, though at correspondingly lower data rates. The table below shows bit rates that can be generated. The dotted line shows the highest data rates that can be achieved at short acoustic ranges and demonstrates the upper limit of the system. Under less ideal conditions, temperature fluctuations cause bit jitter and, therefore, lower bit rates must be employed.

Bit Rate Number	0	1	2	3	4	5	6	7
Channel Number				Bit Rate				
0	151	207	284	379	455	569	759	1139
1	202	276	379	506	607	759	1013	1519
2	260	355	488	651	781	976	1302	1953
3	340	463	637	850	1020	1275	1700	2550
4	448	611	841	1121	1345	1681	2242	3363
5	578	789	1085	1446	1736	2170	2893	4340
6	752	1025	1410	1880	2256	2821	3761	5642
7	976	1331	1831	2441	2929	3662	4882	7324

For the system to analyze an acoustic channel, four important parameters must be measured. These are receiver signal strength, level of multipath signal, level of ambient noise, and unsteadiness or data bit jitter. The first three parameters are important in determining the acoustic frequency to be used, and the last parameter determines the maximum bit rate obtainable at the time.

Figure 33 is a schematic representation of the transceiver. An important element is a digital AGC (Automatic Gain Control) which controls the signal entering the digital filter array. This AGC has 64 steps, each corresponding to one decibel (dB) change. Therefore, by simply reading the AGC word, the strength of the signal entering the digital filter array is known. If no signal is present, this number corresponds to ambient noise. Multipath signals also fall within digital filter range and are not coherent with data. The presence detector is essentially a floating comparator which can isolate signals within channel range as being primary or other (multipath) signals. This determination requires that one acoustic path be three dB above the others. If this situation is not achieved, the system merely determines that no primary path is usable at that acoustic freqency.

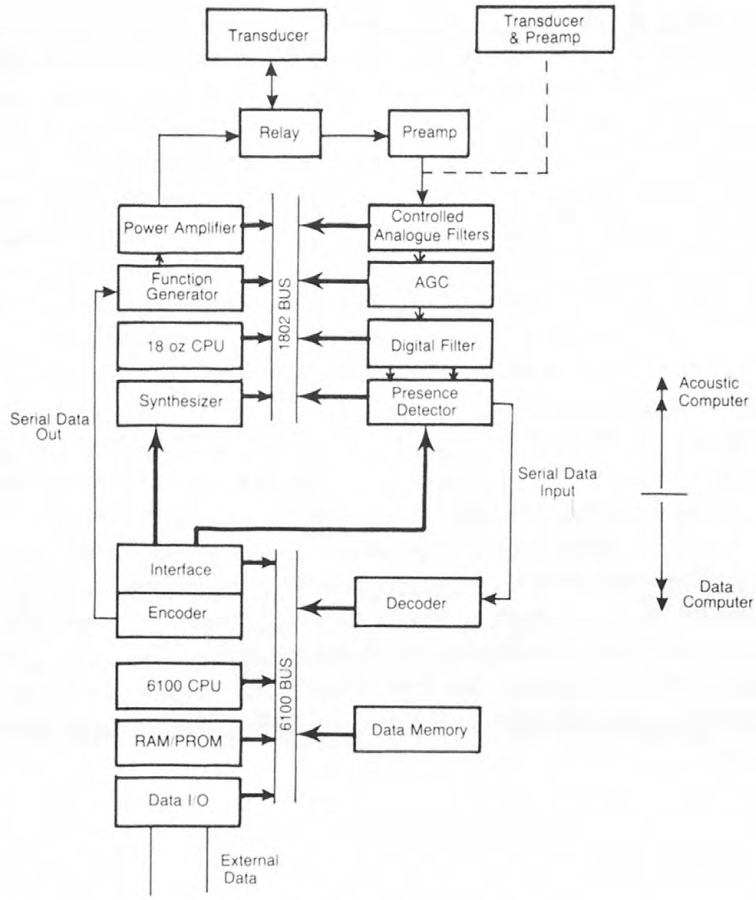

FIGURE 33.—Transceiver block diagram

Input serial data coming from the presence detector enter specially designed decoder which does not need to know, in advance, the bit rate used. It is, in essence, a counter which counts the duration of one and zero bits and determines criteria necessary to discriminate between them. It also determines jitter in bit duration. Since pulse-width modulated data can be severely distorted by both the acoustic path through the water and the electronic system, the criterion to identify bits is based on an initial bit stream of alternate ones and zeros. Coherence of bits is defined as having a bit stream whose individual bit durations are within a certain tolerance level.

Software has been developed which allows the system to analyze data. Complexity occurs within the receive operation. Because the receiver does not know which acoustic channel will be used, it must scan all channels to determine when and where a signal occurs. The following outline is the operational sequence:

- PRESCAN—Record background for each channel.
- FAST SCAN—Any signal 4 dB over noise?
  —If not, record new background and continue fast scan.
- SLOW SCAN—Which signal is highest (any dB over noise)?
  —Determine probable channel.
- SET CHANNEL—Are bits coherent? (three tries)
  —If not, record new background and continue fast scan.
- DETERMINE—Bit duration (One)
  —Bit duration (Zero)
- SET BIT DISCRIMINATOR.
- GET SYNC WORD.
- TAKE DATA.

The system first scans and records background noise; it then rapidly scans the channels (20 milliseconds per channel) to determine whether any signal is 4 dB above the ambient noise. If there is no signal, the data are considered to be new background data and the fast scan repeats. Thus, in normal receiver operation, ambient background noise is upgraded approximately six times a second. If a signal is detected, then a slow scan (50 milliseconds per channel) enables an accurate determination of the channel which has the highest level signal. The channel is then selected in the digital filter array and the three attempts are made to determine whether four consecutive bits are considered coherent. If no coherent bits are received, the system assumes that the 'signal' consisted of transient noise and returns to the scanning mode. If the bits are determined to be coherent, the system sets the bit discriminator, proceeds to look for sync word and input frames of data. This operation continues until the calibration frame (channel) is obtained. The receiver can use this information to determine bit error rate.

The following outline shows the consequences of reaching various levels of the analysis. One sees that the determination of bit coherence is a critical second step, and the receipt of the sync word initiates the remainder of the necessary information.

If bit coherence is achieved then know:

Message was attempted	
Channel	(SCAN)
Signal	(SCAN)
Background level	(SCAN)
Bit rate	(BIT COHERENCE)
Bit jitter	(BIT COHERENCE)
Noise/multipath level	(PRESENCE DETECTOR)

If sync is achieved then also know:

Transmitter
Message status
Bit error rates

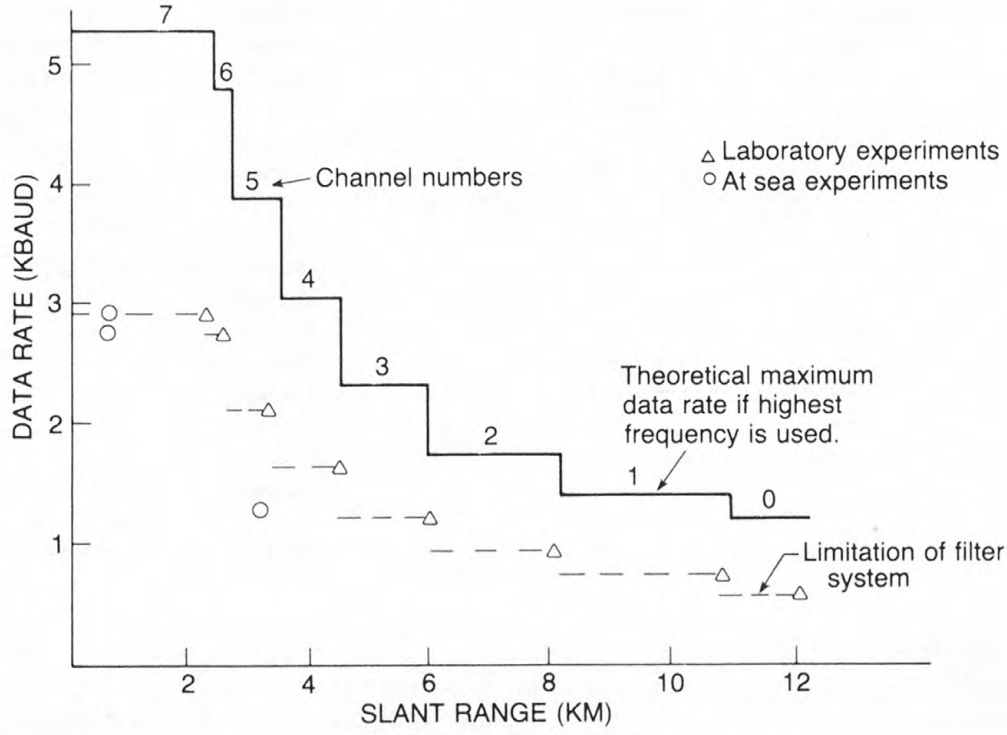

FIGURE 34.—Typical data rates for the different channels

Ocean experiments have been conducted wherein the underwater unit was programmed to transmit periodic data. The lower or sound unit was suspended from a surface float. The receiver was able to achieve zero error data over ranges up to 3 and 4 kilometers, but with only a 10 percent probability of receiving a signal. Analysis of results indicates that transient noises in the ocean caused the system to look for bit coherence and that, because of the transient nature of the noise and the open ended ability of the system to determine bit durations, extensive time was taken to determine that bit coherence did not exist. The system was often not in the scan mode when transmission occurred. These problems have been eliminated by identifying a minimum data rate and by using this information in the receiver to quickly reject transient noise.

Figure 34 is a plot of data rate as a function of slant range. Assuming a shallow water ambient noise level from archive data, the highest acoustic frequency can be estimated for any range. From theoretical considerations, a maximum bit rate can be calculated as shown. Limitations within the filter system reduce this by almost a factor of two. Experiments conducted in the laboratory and for short range, nearly ideal sea conditions support these numbers. Experiments at sea have been very limited but have achieved reasonable data rates. These experiments, however, have not yet reached the longer transmission ranges.

Adaptive software has not yet been developed. Clearly, the outputs of the acoustic analysis are the inputs to the adaptive adjustment of parameters. A conversation between the two transceivers will be used to establish optimum parameters. An example of the process follows.

	Transceiver (Ship)			Transceiver (Sub)		
Steps	Operation	Parameters	Message Status	Operation	Parameters	Message Status
0	Manual input	C1, R1, P1				
1	Transmits Calib. F	C1, R1, P1	MS = 1	Listens	C1, R1, P1	
2	Listens	———		Evaluates		
3	Listens	———		Computes	C2, R2, P2	
4	Listens	C2, R2, P2		Transmits Calib. F	C2, R2, P2	MS = 2
5	Evaluates			Listens	———	
6	Computes	C3, P3, R3		Listens	———	
7	Transmits	C3, P3, R3	MS = 1	Listens	C3, P3, R3	
8	Listens	———		Evaluates		
9	Listens	———		Computes	C3, R3, P3	
10	Listens	C3, R3, P3		Transmits	C3, R3, P3	MS = 3
11	Evaluates			Listens	———	
12	Computes	C3, R3, P3		Listens	———	
13	Transmits Calib. F	C3, R3, P3	MS = 3	Listens	C3, R3, P3	
14	Listens	———		Evaluates		
15	Listens	———		Computes	None (Data Confirmed)	
16	Listens	———		Listens	———	

In the example, the ship transceiver requests data from the source transceiver. The calibration frame only is transmitted back and forth while the parameters are adjusted until the fourth transmission includes the data and the fifth confirms data reception. C, R, and P indicate channel number, bit rate, and power level, respectively. The numbers indicate the sequential values.

Self-Contained Cavitation Erosion Cleaning Technology for Use on an Unmanned, Untethered Vehicle

Principal Investigators: William Barber
Naval Surface Weapons Center
White Oak
Silver Spring, MD 20910

William Bohli
Daedalean Associates
15110 Frederick Road
Woodbine, MD 21791

Objective: To develop the technology for operating a cavitation erosion cleaning system aboard an unmanned, untethered free-swimming vehicle.

Not to be confused with jet velocity impact, cavitation erosion is a fluid flow phenomenon in which evacuated bubbles are formed, break against a surface, and yield destructive results. Designers of ship propellers and hydrofoil struts attempt to avoid conditions which foster cavitation, but in this project the feasibility has been studied of using the phenomenon to do useful work.

Nozzles which induce cavitation are configured to reduce fluid pressure to a vacuum, thus inducing many minute vapor bubbles to form rapidly and grow as they leave the nozzle. When outside the nozzle, bubbles collapse at a distance which is dependent upon exit velocity and ambient pressure. The nuclei around which the vapor bubbles form is thought to be ordinary impurities; but other means, such as flow separation around buttons or from swirl plates within nozzles, can stimulate nucleation. To operate efficiently, however, overall nozzle design must be considered, especially because of power limitations of field operations. Test results have indicated that simple orifice plates are optimum for structural joint cleaning purposes offshore. These plates may be designed to produce a symmetrical or fan-shaped plume of bubbles, which exits from a nozzle, to

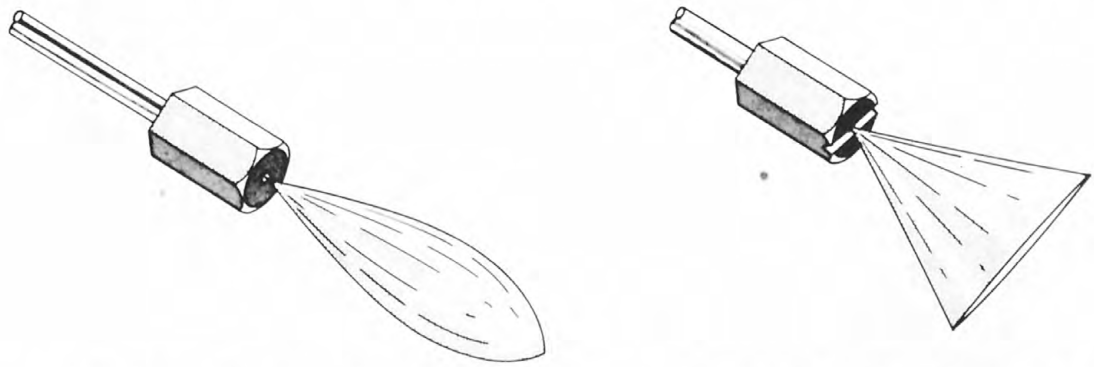

Cavitation Envelope Created by the Standard Orifice Nozzle

Cavitation Envelope Created by the Fan Jet Nozzle

FIGURE 35.—Cavitation envelopes formed by standard orifice nozzle and notched face (fan jet) nozzle

facilitate cleaning ability. Figure 35 illustrates the formations of such plumes; note the notch milled across the end of the nozzle at the right to send out the vapor bubbles. As the plume of bubbles breaks, a fairly loud sound similar to escaping steam is heard. The magnitude of the hissing of bubbles and the size of the plume are a measure of the intensity of cavitation erosion because nozzle effectiveness is determined by the number of bubbles which form and collapse. By

increasing flow through a nozzle, bubble nucleation rate has been found to vary as high as the 12th power of velocity, thus causing velocity considerations to dominate nozzle design. One can see the efficiency gained over waterjet blasting techniques, the most effective of which (pulse-jets) theoretically produces intensities of velocity squared.

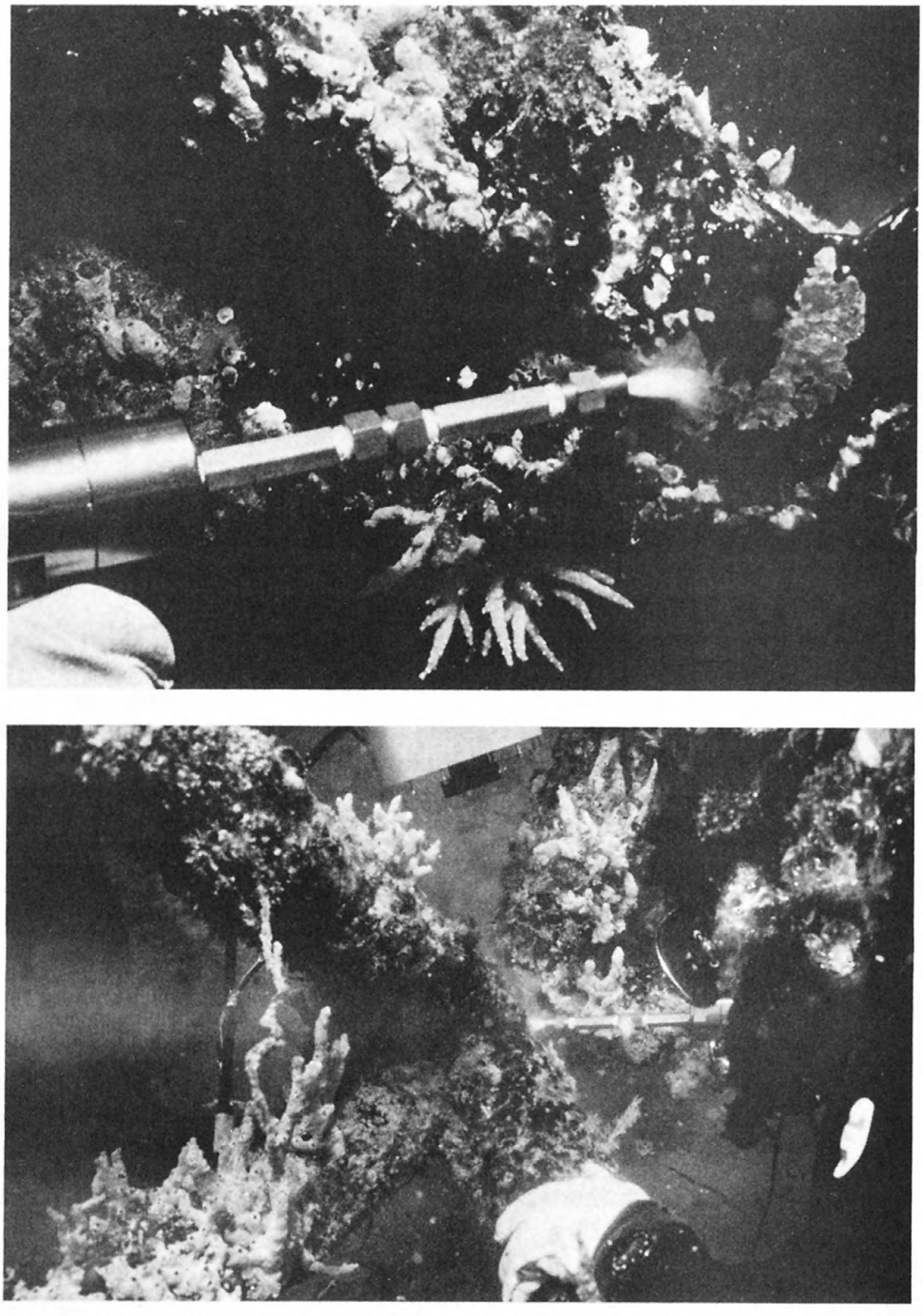

FIGURE 36.—Two views of cavitation erosion gun in use

Daedalean Associates, Inc., has completed development of cavitation erosion cleaning technology and, as a result of the many tests run to optimize nozzle design and flow conditions, the following parameters were selected for use in a hand-held device, figure 36, for diver-evaluation:

	Symmetrical plume nozzle	Fan-shaped plume
Orifice diameter	0.031 in.	0.031 in.
Orifice velocity	1100 ft./sec.	1200 ft./sec.
Optimum nozzle standoff distance from work	¾ in.	½ in.
Flow rate	2.3 GPM	2.3 GPM
Calculated power at nozzle	13.7 HP	13.7 HP
Device Weight (Gun) in air	5 lbs.	5 lbs.
Nozzle back thrust (estimated in air)	7 lbs.	7 lbs.

Results of diver-evaluation indicated the fan-shaped plume to clean the bare metal at a rate of 1 square foot a minute. The symmetrical plume was significantly less efficient because of its smaller coverage. The tests were run on the structure shown in figure 36 which was incrusted with 5 years' growth of coral like marine growth. The reaction forces generated by the cleaning device, with either nozzle, were reported by the divers to be inconsequential.

Upon determining the feasibility of using cavitation erosion for cleaning underwater structural joints (Bohli and others, 1979) research is now being directed at the efficacy of operating such a system aboard an unmanned, untethered submersible. Because of relatively low power requirements, high cleaning rate, and small size, such an undertaking appears quite promising if pressure energy to power the jet can be generated directly from chemical energy, thus circumventing the need for electrical power and an attendant pumping system. Such a direct conversion system is intended for use on the EAVE East testbed inspection vehicle, described elsewhere in this report.

Gas generator technology for the device is being developed by the Naval Surface Weapons Center (NSWC) and is an adaptation of standard military practice. Both fuel and oxidizer are combined in a metal cannister and reacted, creating high temperatures and pressures, thus producing the necessary gas flow conditions. Specifically, lithium pellets are reacted with seawater as follows:

$$2Li + 2H_2O \longrightarrow 2Li(OH) + H_2$$

To attain the operating parameters listed above for the fan-shaped plume, operating for 30 minutes, approximately 800 grams of lithium would be required. This amount could be contained in a cylindrical charge 3.75 inches in diameter by 7.50 inches long.

Daedalean Associates, Inc., is collaborating with NSWC to optimize hardware for evaluation on the EAVE East testbed vehicle.

Several substantial questions need to be resolved which relate to optimum duty cycle, the effects on cavitation erosion from mixing H_2 with water, and the methodology for on/off operations of the cleaning device. An on/off (clean/recharge) duty cycle appears inevitable, and first calculations show an optimum arrangement to be about 1 minute for each. In order to control the charge period in a simple yet efficient manner, the lithium could be pelletized to allow only a given amount to react to completion.

Standard safety tests on lithium have been completed and the use of the gas generator is considered entirely safe for cleaning operations.

Report

Parker, J. T., Bohli, W. H., Thiruvengadam, A. P., 1979, Cavitating water jet cleaning for removing marine growth from offshore structures: Daedalean Associates, Inc.

Development of Improved Blowout Prevention Procedures for Deepwater Drilling Operations

Principal Investigator: Dr. A.T. Bourgoyne, Jr.
Petroleum Engineering Department
Louisiana State University
Baton Rouge, LA 70803

Objective: To develop improved well-controlled procedures for deepwater floating drilling operations.

One of the more expensive and potentially dangerous problems faced by the oil-producing industry is the control of high-pressure formation fluids encountered while drilling for hydrocarbon reservoirs. When control is lost a blowout may occur. Uncontrolled flow discharge to the atmosphere or seafloor is called a surface blowout and uncontrolled flow from one subsurface formation, through the wellbore, to a second more shallow subsurface formation is called an underground blowout.

Surface blowouts are extremely dangerous, frequently injuring drilling personnel, and almost always damaging drilling equipment and the environment. In some extreme cases, additional wells must be drilled in order to flood the high-pressure formation which causes the flow. Underground blowouts are not usually as dangerous as surface blowouts but are more common because the flow cannot be controlled by surface blowout-prevention equipment. Usually, subsurface control can be reestablished only by sealing the lower portion of the well. Many expensive wells have had to be redrilled because of this phenomenon.

A threatened blowout or kick (as it is called) in a well occurs when the pressure exerted by a column of drilling fluid or mud decreases below the fluid pressure in a permeable formation which has been penetrated by the drilling bit. Thereupon, formation fluid enters the well and displaces or kicks the drilling mud up the well-bore annulus until the flow at the surface is stopped by closing the blowout preventers (BOP's). Before normal drilling operations can be resumed, formation fluids must be removed from the well, and the density of the drilling mud in the well increased sufficiently to prevent the fluids' further influx. This procedure is accomplished by "circulating the well" against a back pressure provided by an emergency high-pressure flowline and an adjustable choke; one of serveral established operational procedures may be used.

As the search for petroleum reserves moves offshore, blowout control continues to increase in complexity. In addition, difficulties in confining an offshore oil spill cause much environmental concern. Most modern blowout prevention equipment was developed largely for land-based drilling operations. With only minor modifications, this equipment has been applied to bottom-supported exploratory drilling rigs such as jack ups and development rigs operating on an offshore platform. More significant modifications in blowout prevention equipment and procedures are required for floating vessels used almost exclusively for deepwater operations. The first major modification for operation in deepwater was the location of the BOP stack at the seafloor rather than the surface. The current trend of the oil industry toward much greater water depths (fig. 37) emphasizes the importance of blowout control in floating drilling vessels. Future plans by the Ocean Margin Drilling Program of the National Science Foundation (NSF, 1980) call for scientific ocean drilling in water depths to 13,000 feet during the next decade.

When compared to land-based drilling operations, floating drilling operations incur more severe well-control problems. A major problem illustrated in figure 38 is the maximum drilling fluid density which can be used without hydrofracture. Note, the maximum mud density that can be used with casing penetration into 3500 feet of sediments decreases from about 13.9 lb/gal on land to 9.8 lb/gal in 13,000 feet of water. A second major problem is the rapid increase in well pressure which

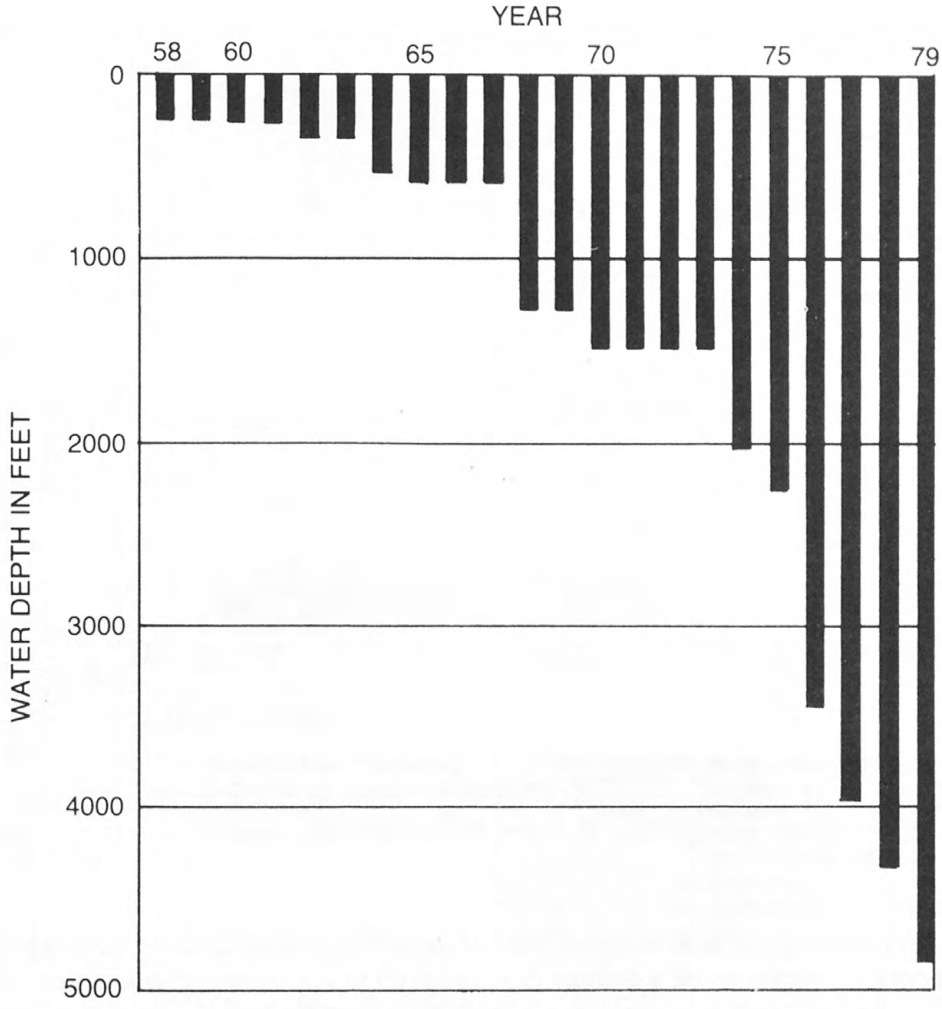

FIGURE 37.—Water depths records for floating drilling vessels (Harris, 1979)

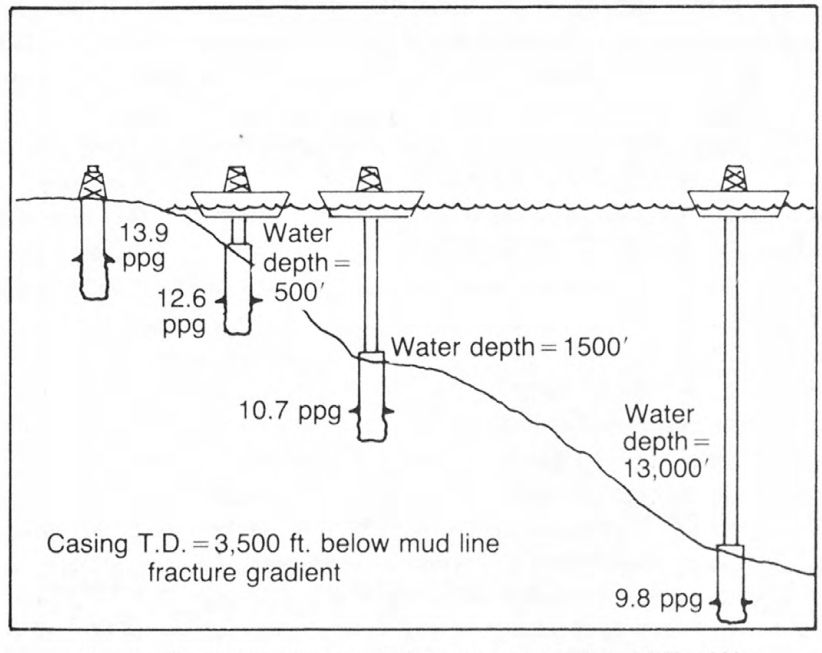

FIGURE 38.—Effect of water depth on fracture gradient (NSF, 1980)

must be held by the adjustable choke when formation gas being circulated from a well reaches the well-control equipment at the seafloor. This problem is illustrated in figure 39 for a hypothetical well-control example which is based upon well-planning information from the above-mentioned Ocean Margin Drilling Program for an offshore New Jersey location to be drilled by the *Glomar Explorer* drillship in 7,875 feet of water. Note the rapid change in required choke pressure calculated when the top of the gaseous fluid reaches the seafloor.

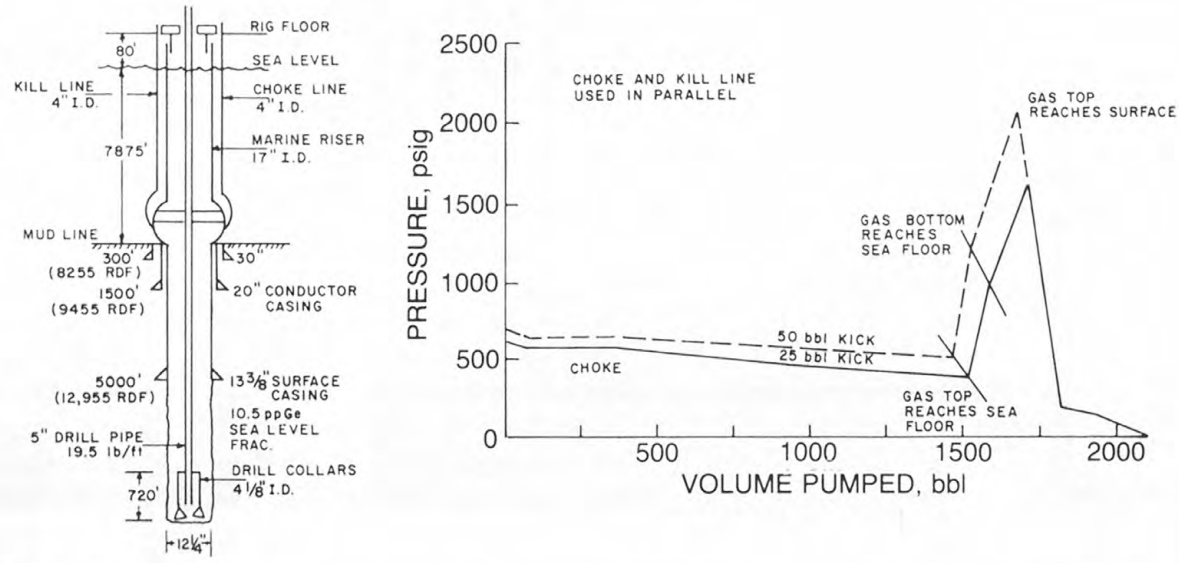

FIGURE 39.—Well-control computer simulation for *Glomar Explorer* drillship on proposed offshore New Jersey upperrise location

A well-research facility has been designed and constructed at Louisiana State University (LSU) to simulate well-control operations on a floating drilling vessel in deep water. Construction of the facility was accomplished under funding from both industry and the U.S. Geological Survey. This new facility complements an older well facility constructed in 1971 which is capable of modeling well-control operations for land rigs and bottom-supported marine rigs. A photograph of the new well facility under construction is shown in figure 40. The main features of this facility include: (1) a 6,000-foot well, (2) a choke manifold containing four 15,000 psi adjustable drilling chokes of varying design, (3) a Halliburton triplex pump, (4) mud tanks, (5) a mud/gas separator, (6) three mud degassers of varying designs, (7) a mud mixing system, and (8) an instrumentation and control house. The subsurface configuration of tubular members in the well was chosen so that the well would exhibit the same hydraulic behavior as a well being drilled in 3,000 feet of water.

The effect of the BOP located on the seafloor is modeled in the well using a packer and triple parallel flow tube as shown in figure 41. Subsea choke and kill lines connecting the simulated BOP to the surface are modeled using 2.375 inch tubing. The subsea kill line valve at 3,000 feet is modeled by using a surface-controlled subsurface safety valve. This control allows experiments to be conducted using only the choke line, the kill line being isolated from the system as is often the case in well-control operations on floating drilling vessels. The drill string is simulated using 6,000 feet of 2.875 inch tubing. Nitrogen gas is injected into the bottom of the well at 6,000 feet to simulate a gas kick. The nitrogen is injected into the well through 6,100 feet of 1.315 inch tubing inserted into the drill string. A pressure sensor is located at the bottom of the nitrogen injection line to allow continuous surface monitoring of bottom-hole pressure during simulated well-control operations. The pressure signal is transmitted to the surface through 0.094 inch capillary tubing which is strapped to the 1.315 inch tubing. A check valve, located at the bottom of the nitrogen injection line, allows the line to be isolated from the system after inducing the gas kick in the well.

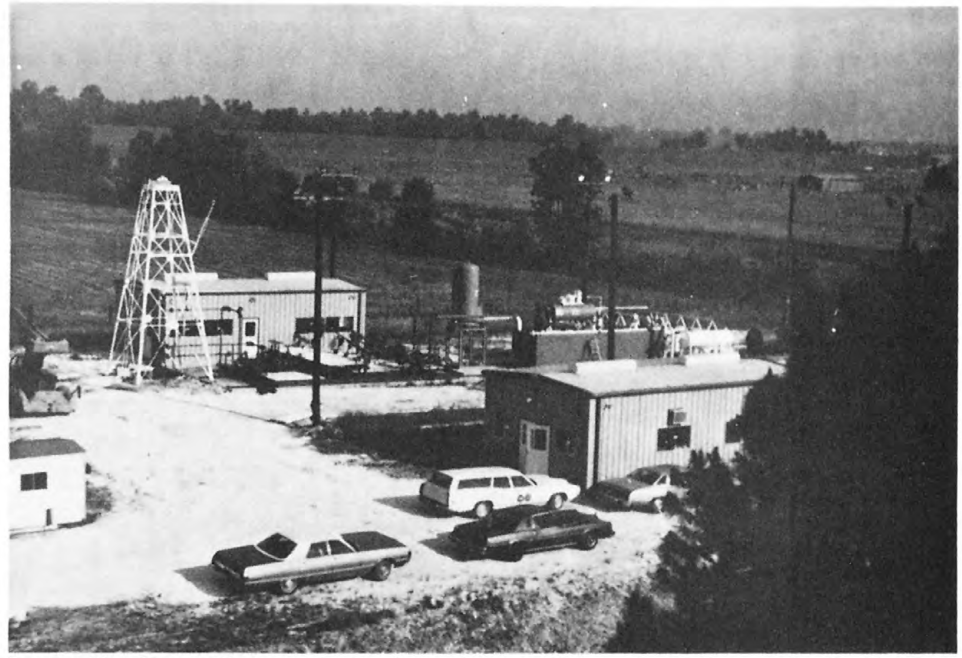

FIGURE 40.—New well-control facility for modeling well-control operations on floating drilling vessels

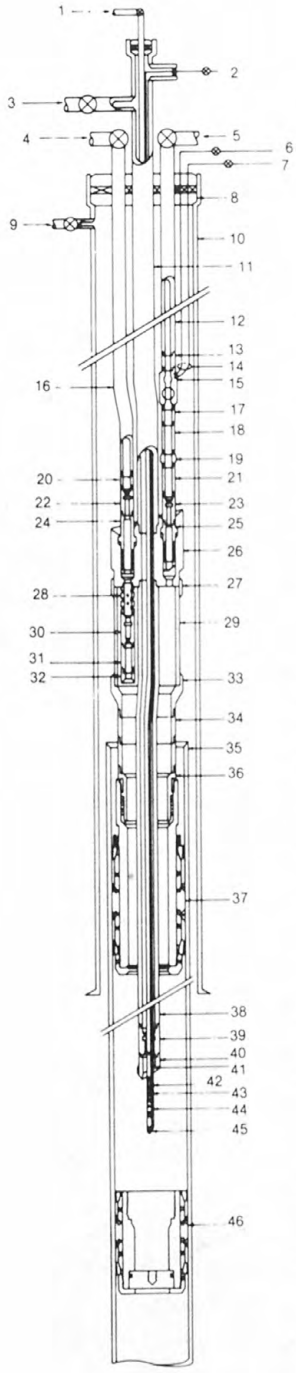

LEGEND

1. Nitrogen injection tubing
2. Bottom-hole pressure monitor line
3. Drill string
4. Choke line
5. Kill line
6. Control line
7. Balance line
8. Gray tool wellhead and triple string tubing hanger
9. Casing valve
10. Casing 10¾" OD 40.5 lbs/ft
11. Tubing 2⅞" OD 6,5 lbs/ft EUE 8rd
12. Tubing 2⅜" OD 4.7 lbs/ft EUE 8rd
13. Flow coupling size: 2⅜" EUE 8rd × 6' long
14. Hydril dual control line bundle
15. Hydril tubing mounted surface controlled subsurface safety valve Size: 2⅜" Min: ID 1.875"
16. Tubing 2⅜" OD 4.7 lbs/ft EUE 8rd
17. Flow coupling Size: 2⅜" EUE 8rd × 6' long
18. Tubing 2⅜" OD 4.7 lbs/ft EUE 8rd (one joint)
19. Baker guide collar size: 4.9 × 2⅜"
20. Pup joint 2⅜" OD 4.7 lbs/ft EUE 8rd × Pin 4' long
21. Tubing 2⅜" OD 4.7 lbs/ft EUE 8rd (one joint)
22. Baker model "F" seating nipple size 1.31 with 2⅜ EUE 8rd box × Pin min. ID 1.81"
23. Baker model "F" seating nipple Size: 1.81 with 2⅜" 4.7 lbs/ft EUE 8rd Pup joint 2' long
24. Baker "J-Lock" seal nipple Size: 40-26 min. ID 1.968" with 2⅜" EUE 8rd box × blank and chamfered bottom
25. Baker "J-Lock" seal nipple Size: 21-19 min. ID 1.323" with 2⅜" EUE 8rd box by half muleshoe bottom
26. Baker triple string parallel flow tube head Size: 9⅛ × 2⅞ × 2.688 × 1.968
27. Baker casing coupling Size: 8⅝" OD—36 lbs/ft with national buttress box × box 25' long
28. Baker perforated spacer tube Size: 2⅜" NU IO RD pin × Pin 10' long min. ID 1.995"
29. Baker casing nipple Size: 8⅝" OD—36 lbs/ft national buttress pin × Pin 25' long
30. Baker model "R" seating nipple Size: 1.81" with 2⅜ NU 10 RD box × Pin with special clearance OD min. ID (thru NOGO) 1.760"
31. Baker spacer tube Size: 2⅜ NU 10 RD box × Pin with special clearance connections min. ID 1.995"
32. Baker wireline entry guide Size: 2⅜" NU 10 RD with special clearance OD min. ID 1.995"
33. Baker casing crossover sub Size: 8⅝" OD 36 lbs/ft national buttress box by 6⅝" OD 24 lbs/ft hydril "FJ" pin
34. Baker casing nipple Size: 6⅝" OD 24 lbs/ft by 40' long with hydril "FJ" box by pin connections
35. Liner 7⅝" OD 26.4 lbs/ft
36. Baker model "K-22" anchor tubing seal nipple Size: 80FA52 min. ID 4.400"
37. Baker model "FA-1" production packer Size: 91FA52 min. ID 4.400' set at 3,034'
38. Tubing 2⅞" OD 6.5 lbs/ft EUE 8rd
39. Baker model "F" seating nipple Size 2.31
40. Baker wireline entry guide Size: 2⅞"
41. Nitrogen injection tubing Size: 1.315"-1.72 lbs/ft integral joint
42. Pressure monitor line to surface
43. Check valve
44. Ported sub
45. Sperry-Sun bottom-hole pressure sensor
46. Baker model "N-1" bridge plug (set at 6200 ft.)

FIGURE 41.—Schematic of new research well

At this writing the new well facility is nearing completion and actual pressure profiles, obtained during simulated well-control operations, should be available in the near future. Anticipated surface-pressure profiles for two sets of kick conditions are shown in figure 42. These pressure profiles were obtained using a "state-of-the-art" computer simulation of the well-control process. Note the similarity between the theoretical behavior of the new well facility and the theoretical behavior of the deepwater well-control example from the NSF Ocean Margin Drilling Programs shown in figure 39.

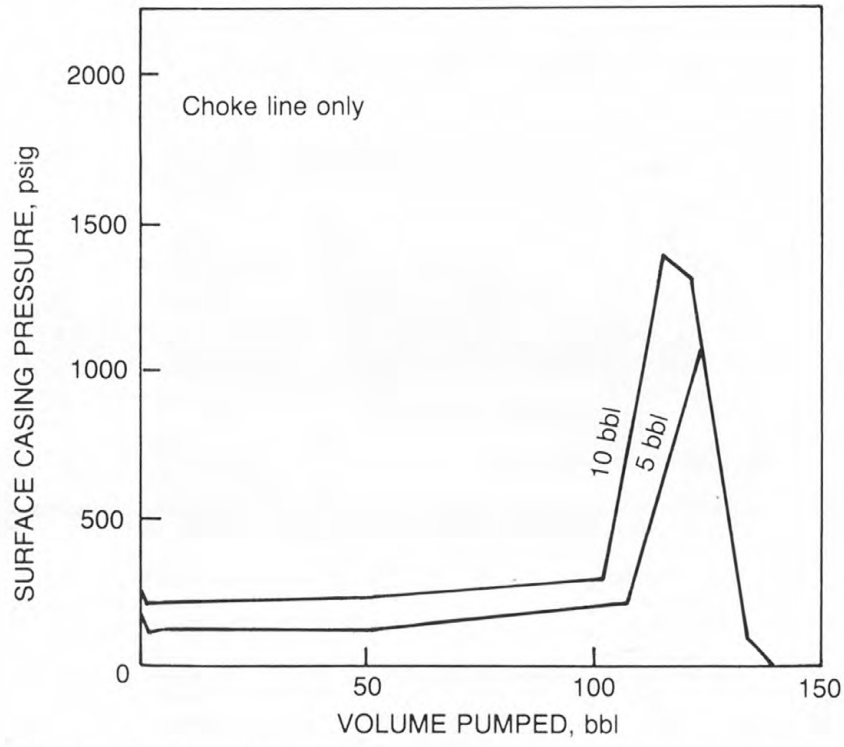

FIGURE 42.—Theoretical choke pressure profiles computer for research well

An ultimate goal of experimental well-control research at LSU is the development of more accurate algorithms for use in computer simulations of well-control operations. Computer simulators can provide an effective means of evaluating alternative well-control procedures as well as effective well-control training exercises. An accurate computer simulation of pressure-control operations requires accurate knowledge of fluid behavior in the well. LSU research has already shown that the assumptions used at present in well-control simulations do not always realistically model actual well behavior when gas is present. Two common assumptions at fault are (1) that gas influx enters the wellbore as a continuous plug which occupies the entire annular cross section of the well and remains in this configuration during subsequent well-control operations and (2) that the gas zone does not migrate upward through the column of drilling fluid but moves instead at the same velocity as the circulating drilling fluid.

Laboratory experiments are being conducted in a three-story wellbore model, figure 43, to learn more about the actual flow patterns present in well-control operations. To date, flow patterns and gas concentrations resulting from various gas feed rates have been studied in Newtonian fluids over a wide range of fluid viscosities. Shown in figure 44 are photographs obtained of flow patterns occurring in the laboratory model. These experiments indicate that bubble flow is the predominant flow pattern present as a gas kick enters a well. Very high gas feed rates are required to generate a slug flow pattern.

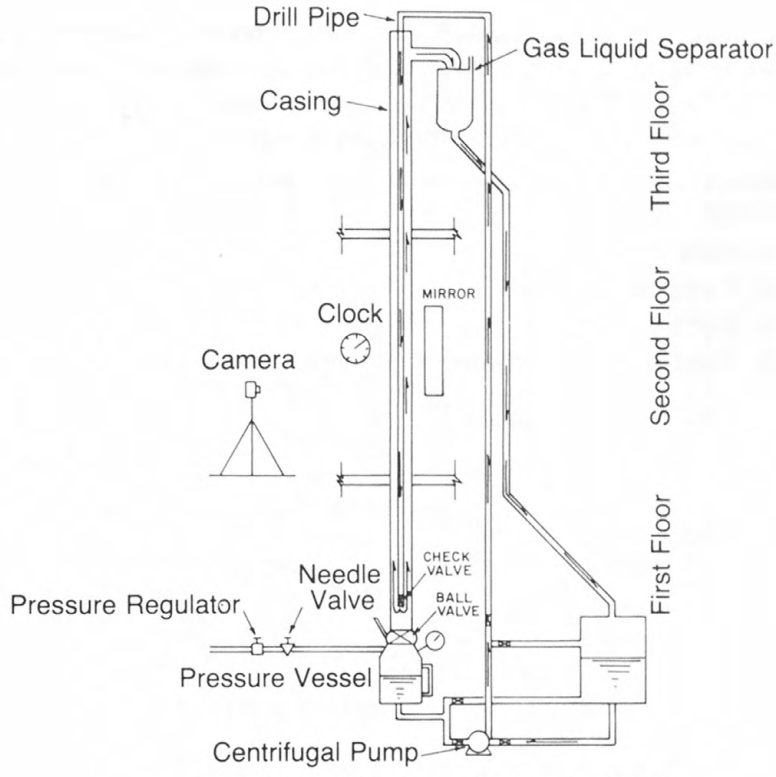

FIGURE 43.—Three story well bore visual model

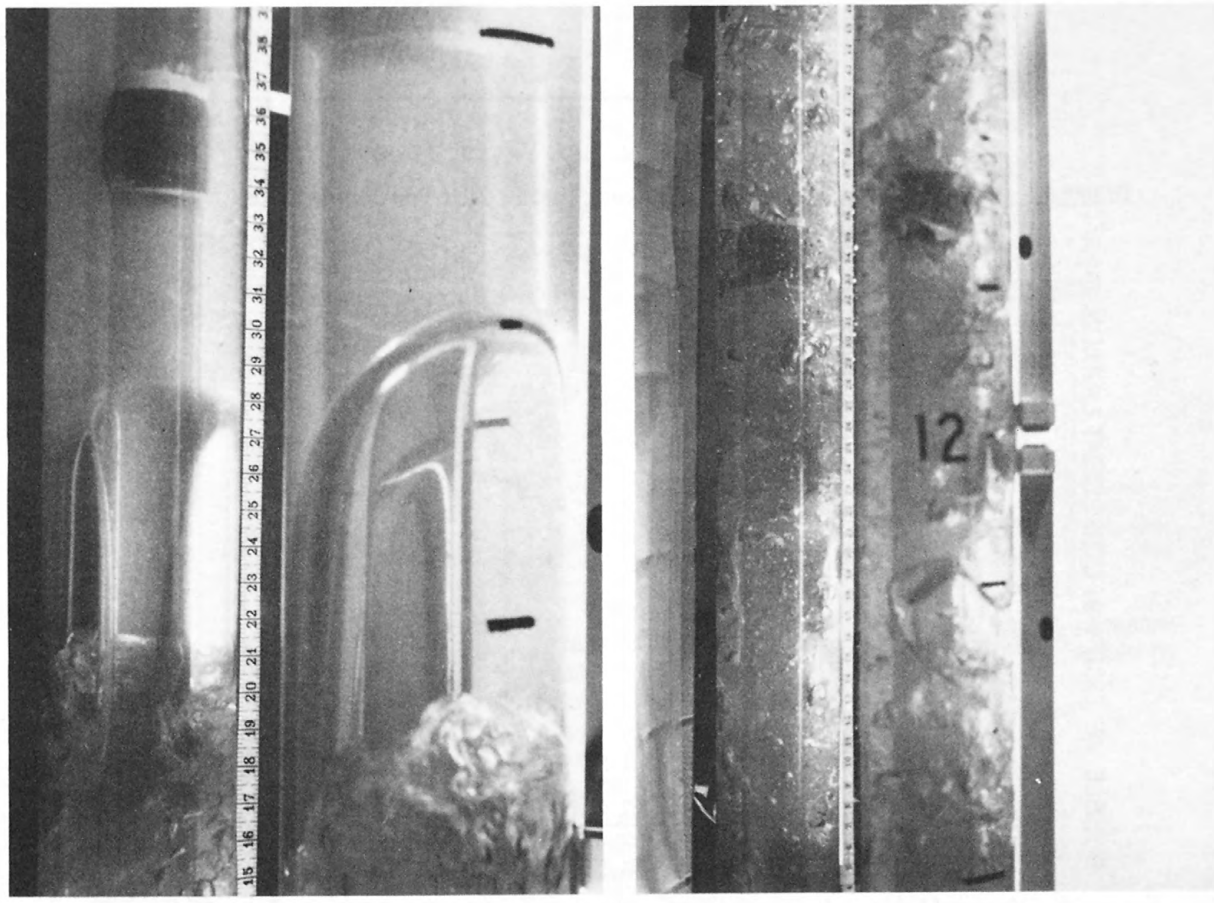

FIGURE 44.—Two phase flow patterns observed in visual laboratory model

Average gas concentration from experimental data obtained in the kick region, as a function of gas feed rate, is shown in figure 45. Gas feed rate is expressed as superficial gas velocity, that is, the gas flow rate divided by the annular cross sectional area of the well. The upper limit of the experimental data, which is about 0.8 ft/sec, corresponds to a kick rate of about 1.9 bbl/min.

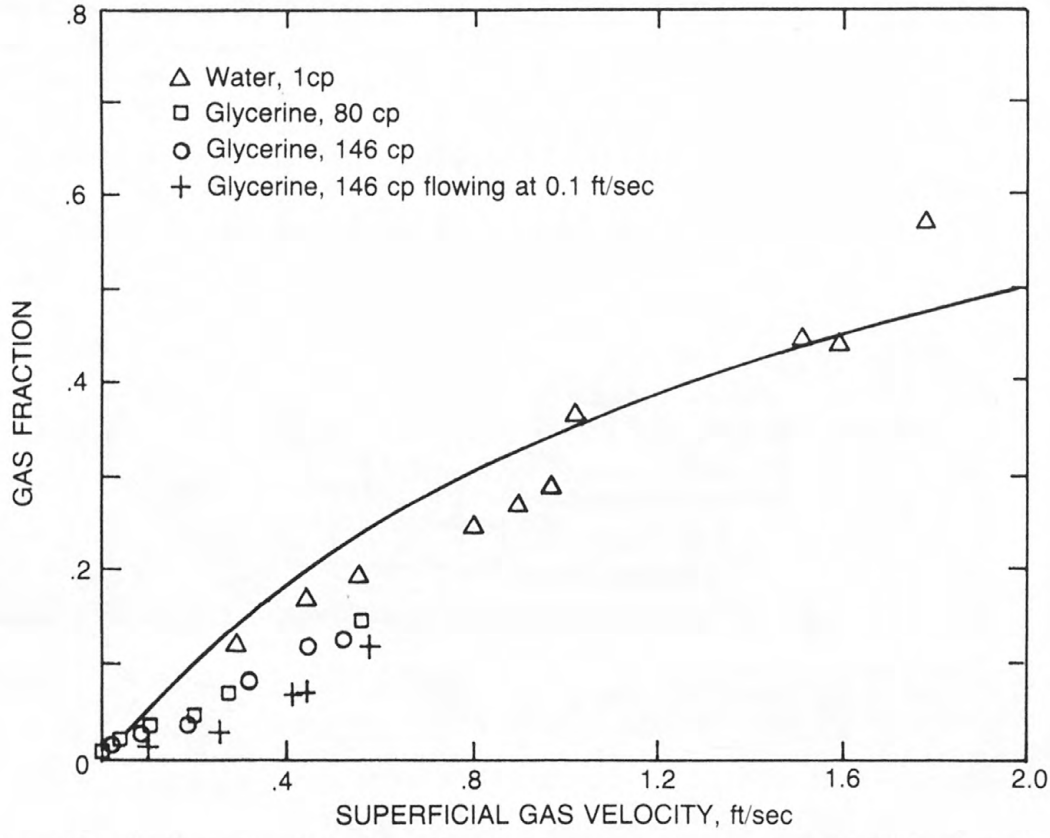

FIGURE 45.—Gas fraction in a kick zone as a function of gas feed rate expressed as superficial gas velocity.

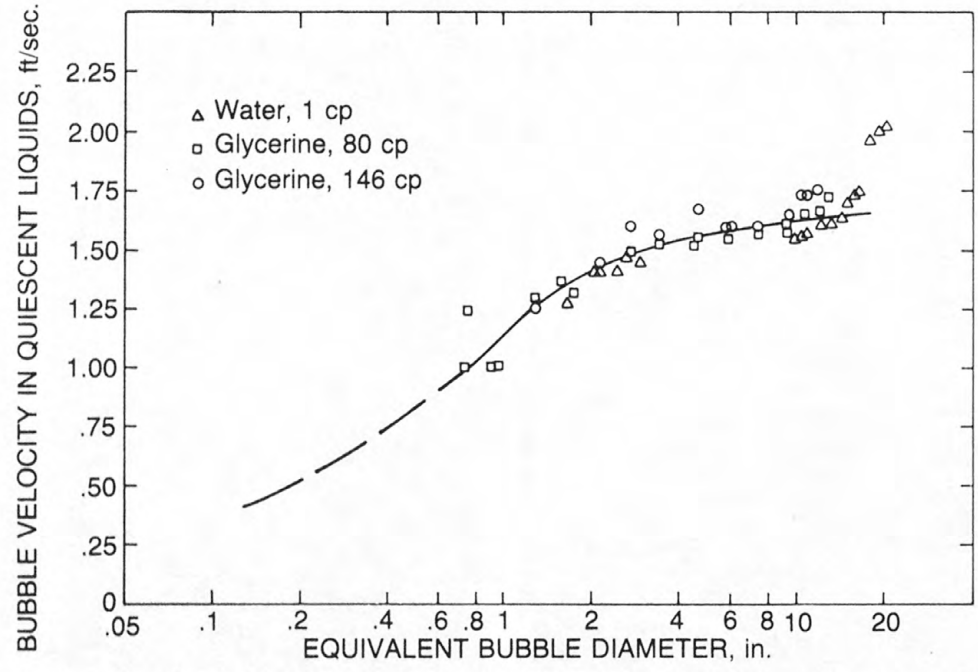

FIGURE 46.—Measured bubble velocity versus equivalent diameter of bubbles through static liquids in a 6.375 in. diameter × 2.375 in. diameter annulus

In addition to the data collected on flow pattern and gas concentration in the kick zone, data on gas bubble rise velocity was also collected for various size bubbles and slugs. Shown in figure 46 is bubble rise velocity relative to an observer at the surface for various bubble volumes (expressed as an equivalent spherical bubble diameter) and liquid viscosities. Note that for the 6.375 inch ID by 2.375 inch OD annulus, bubble rise velocity is not greatly affected by liquid viscosity. Figure 47 shows gas slug slip velocity relative to average liquid velocity above the gas slug for various slug lengths and liquid viscosities. Note, for the annular geometry studied, the gas slug slip velocity is essentially constant, having a value of about 1.5 ft/sec.

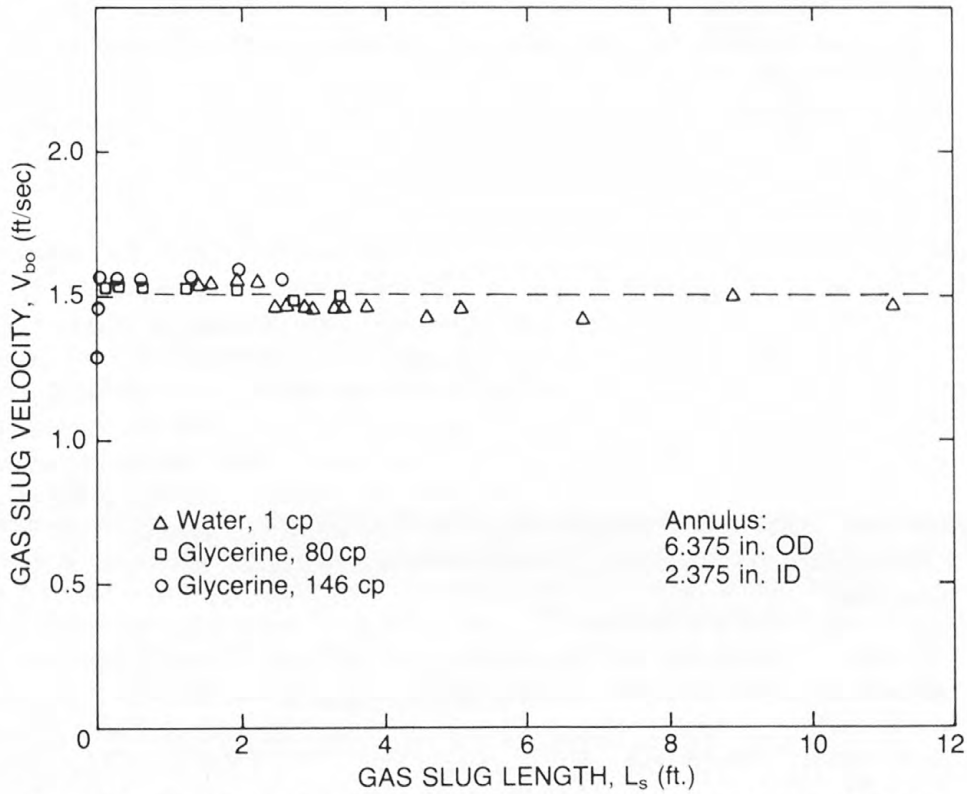

FIGURE 47.—Slip velocity of gas slugs relative to average liquid velocity above gaseous region

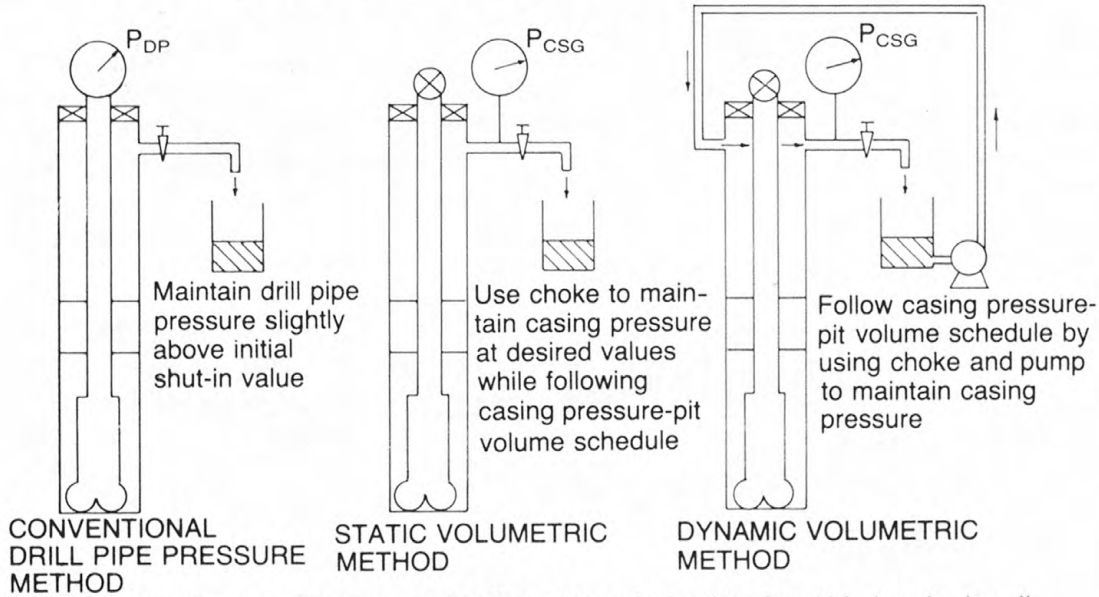

FIGURE 48.—Proposed methods for safe handling of upward migration of gas kicks in a shut-in well

Gas migration experiments have also been conducted in a 6,000-feet well. These experiments evaluated the volumetric method of handling gas migration in a shut-in well. The volumetric method of handling gas migration has been proposed as a technique which can be applied when meaningful drill pipe pressure is not available because of mechanical difficulties such as a plugged, leaking, or off-bottom drill string. The volumetric method, illustrated in figure 48, uses observed changes in pit level and casing pressure to maintain a nearly constant bottom-hole pressure. This is accomplished by:

1. Allowing casing pressure to rise (due to upward gas migration) slightly above the initial shut-in pressure to provide a margin of safety. About 100 psi is usually considered an appropriate margin.
2. Allowing casing pressure to rise (due to upward gas migration) by an additional pressure increment. About 50 psi is usually considered appropriate.
3. Bleed well fluid through adjustable drilling choke until a volume of mud has been released which would generate in the well a hydrostatic pressure equal to the selected pressure increment. Adjust choke to release well fluid at a nearly constant casing pressure.
4. Repeat steps 2 and 3 until gas reaches the surface.

A schematic diagram, showing the experimental flow loop used to evaluate the volumetric method of handing gas migration, is shown in figure 49. Typical results obtained using this experimental flow loop are shown in figure 50. Contrary to expectation and conventional calculations, surface pressure buildup did not stop after gas reached the surface. A considerable amount of gas was still rising through the drilling fluid after the leading edge of the gaseous zone reached the surface. Subsequent bleeding operations using the adjustable choke produced only gas. Again, contrary to conventional calculations, a considerable volume of gas could be bled without loss of bottom-hole pressure. As a result of experimental work performed, the volumetric method of handling upward gas migration was found to be a viable technique for the simple well geometries studied. Using the new well facility, additional data will be taken for the more complex geometries used in floating drilling operations.

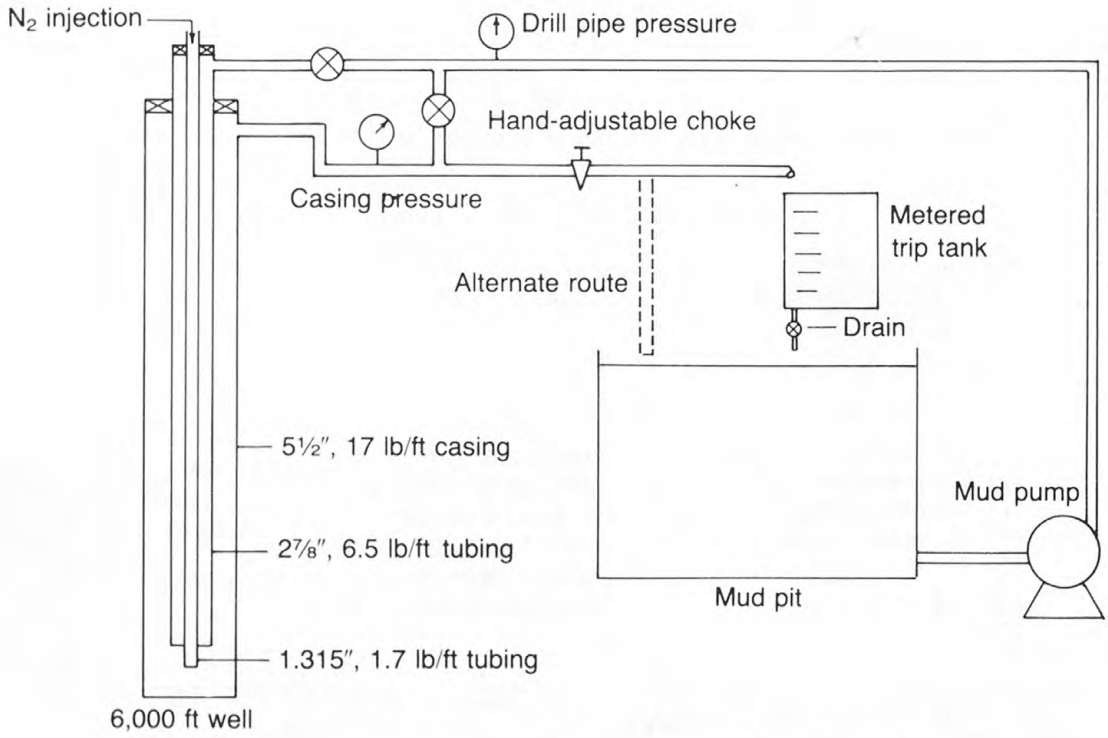

FIGURE 49.—Simplified well layout for evaluation of proposed methods

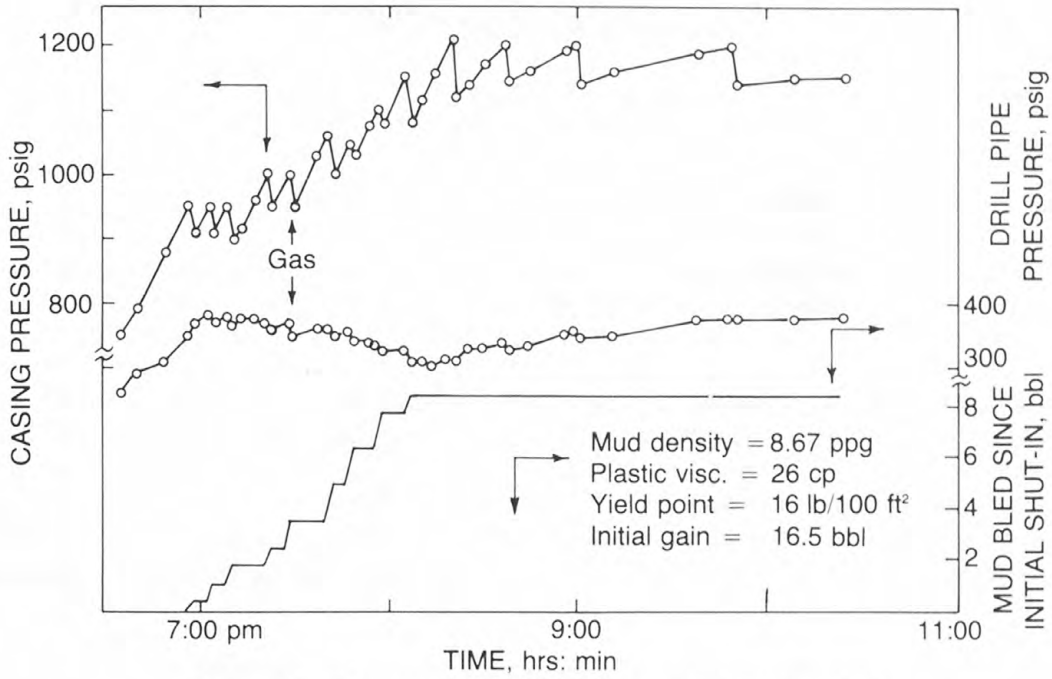

FIGURE 50.—Pressure-volume-time data for static volumetric method

The development of improved algorithms for computer simulations of well-control operations requires an understanding of well-control equipment response as well as knowledge of two-phase annular flow behavior in a well. Experimental studies at LSU are determining the flow characteristics of commercially available drilling chokes. These flow coefficient data may lead to greatly improved algorithms for computing well pressure and flow rate changes (caused by incremental changes in choke position by the choke operator) with time. Similarly, flow coefficient data collected on an annular blowout preventer for various stages of closure likely will lead to more accurate algorithms for predicting initial pressure surges during well closure. Ultimately these experiments may lead to improved shut-in procedures.

Research at LSU is evaluating alternative well-control procedures and, to keep abreast of current practice, a study is being conducted to document existing equipment and procedures. In this study, equipment currently being manufactured has been catalogued and a survey of deepwater rigs was conducted to identify the ways the equipment was used in actual practice. Subsea well-control manuals approved by the USGS have been reviewed to catalog the various recommended procedures for using existing equipment. Some limitations of existing equipment and procedures will be explored experimentally using the new research well facility.

Reports and References

Holden, W. R., Bourgoyne, A. T., Hisl, E. R., 1981, Development of improved blowout prevention procedures for deep water drilling operations: Petroleum Engineering Dept., Louisiana St. Univ.

Harris, L. M., 1979, Design for reliability in deepwater floating drilling operations: The Petroleum Publishing Co., Tulsa, Okla.

National Science Foundation, 1980, Ocean margin drilling program: Final Report, vol. III.

Fluidic Mud Pulse Telemetry

Principal Investigator: Allen B. Holmes
U.S. Army
Harry Diamond Laboratories
Adelphi, MD 20783

Objective: To investigate the feasibility of applying fluidics technology to down-hole data telemetry without interruption of drilling operations.

In a mud pulse telemetry system (fig. 51), a valve located near the drill bit responds to electrical commands from borehole instruments and produces coded pressure pulses in the circulating fluid. These pulses travel at the speed of sound through the fluid to the surface where they are detected by a pressure transducer, decoded, and displayed as information for the driller. Although mud pulsing originally was conceived as a tool for increasing the overall safety and efficiency of hazardous drilling operations, most of the mud pulsing systems in use today are for transmitting directional data only.

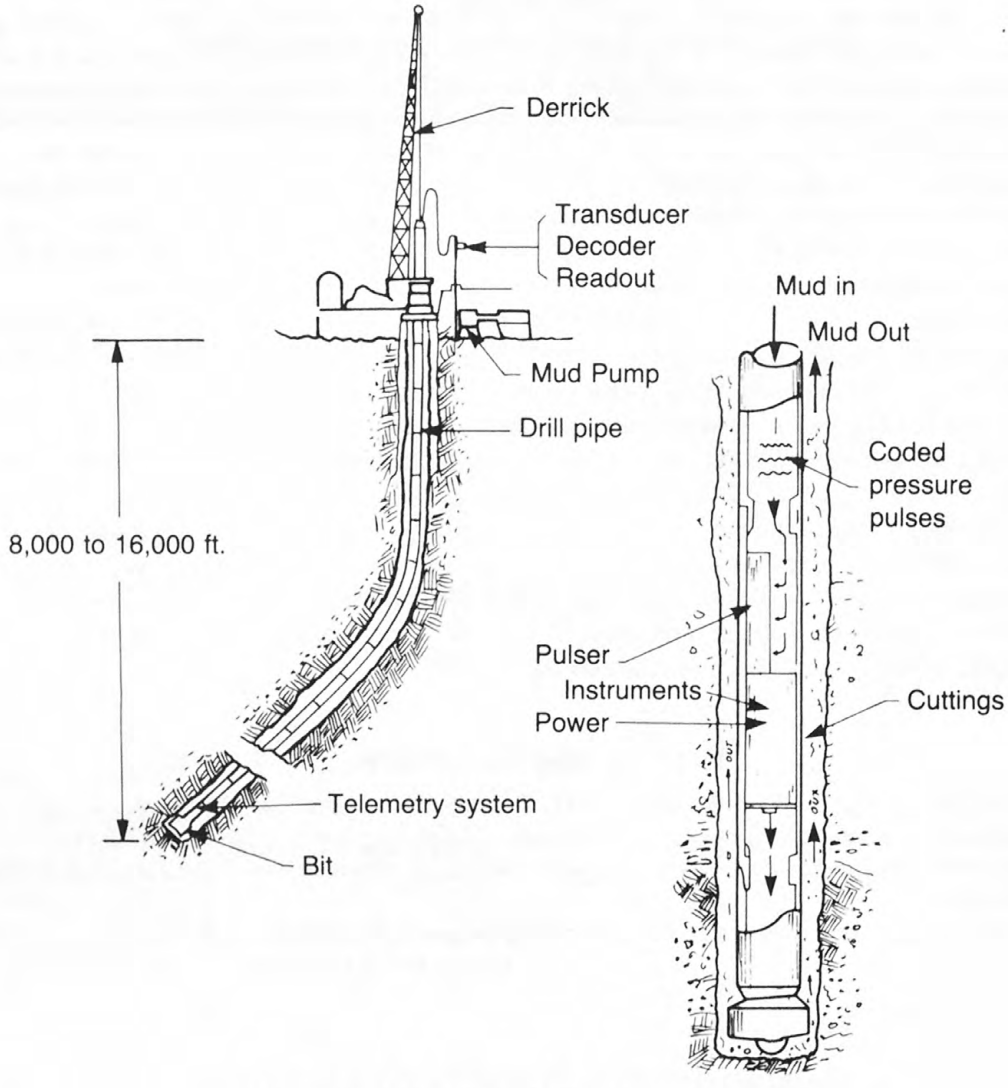

FIGURE 51.—Mud pulse telemetry in a circulating system

The major problem which has limited the application of mud pulsing techniques to directional drilling is the relatively slow pulse rates (typically less than one pulse per second) which can be produced with present mud pulsing valves. Although rates of this level are sufficient to transmit intermittent directional measurements when the drill reaches specific depths, the rate is not considered fast enough to handle the quantity of information necessary for continuous measurements of parameters related to drilling safety and efficiency.

Research at the Harry Diamond Laboratories (HDL) on the application of fluidic control techniques to mud pulser valve design is intended to improve valve dynamics to the point where safety oriented measurement data can become a reality. Specifically, the objectives are to demonstrate a valve design which has a pulsing capability above 10 pulses per second and to assess the operating characteristics of a full-size valve in a down-hole circulating system.

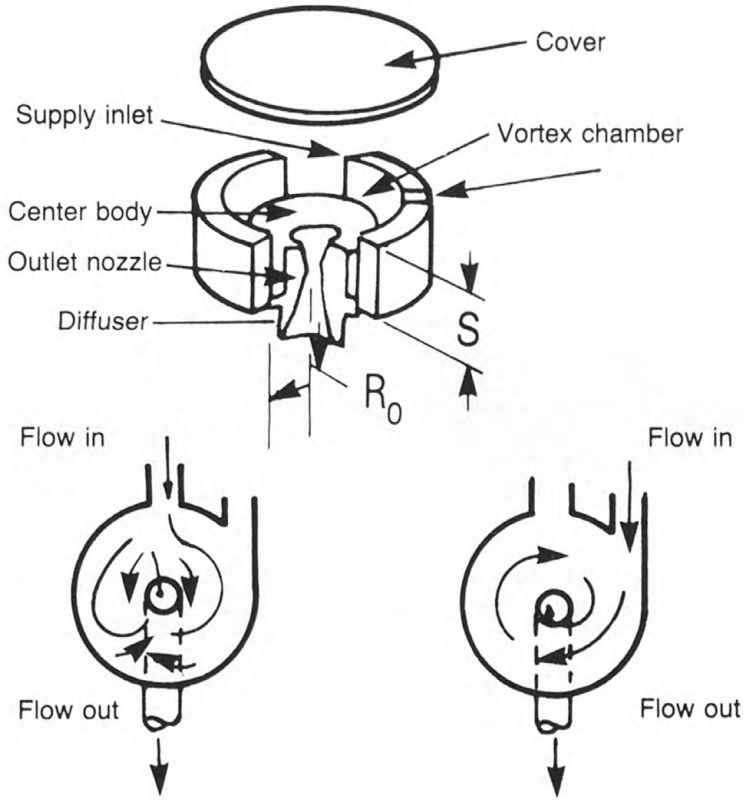

FIGURE 52.—Vortex valve design and theory of operation

Fluidic valving principles differ from those more commonly employed in mechanical valves in that a vortex flow field is used in place of a moving gate or seat to produce a change in area. The vortex flow field is generated in a cylindrical chamber which forms the body of the valve (fig. 52). When a vortex is produced, angular momentum is preserved while angular velocity increases toward the center of the vortex. Centrifugal pressure reaction forces are produced which are simply the force per unit area. Integration between the inner and outer radius of the chamber gives the total pressure differential across the vortex.

When no vortex is produced in the chamber, the fluid passes easily in a radial direction through the vortex chamber. Because centrifugal pressure reaction forces are not developed, the pressure

differential across the chamber is reduced. The differential pressure and/or flow rate through the chamber in each operating mode is equated to an effective discharge port area by

$$A = K_o Q / \sqrt{P/\sigma} \qquad (1)$$

where A = effective port area, Q = flow rate, σ = the density of working fluid, K_o = dimensional constant, and P = the differential pressure across the valve. The ratio of the calculated areas (A_E/A_H) both without and with a vortex, respectively, is defined as turn down.

Several methods have been investigated for producing vortex valving action. These methods differ mainly in procedures used to produce and dissipate vortices. Two of the more common methods are illustrated in figure 53.

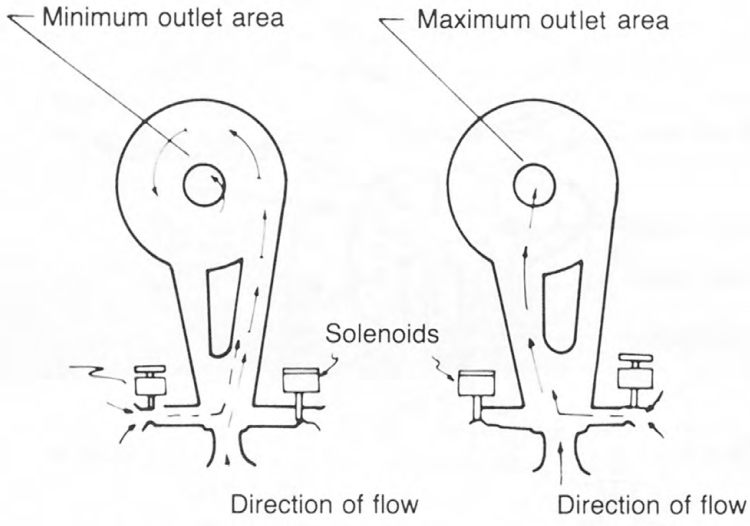

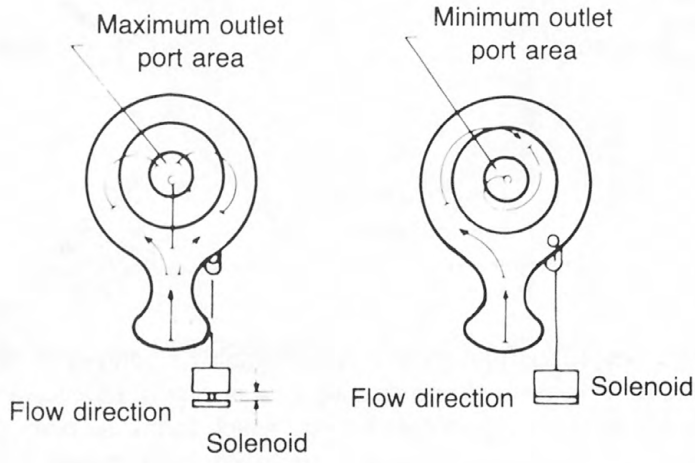

FIGURE 53.—Plan views describing operation of (a) G-type circuit stages, (b) B-type circuit stages

In flow diagram (a) in figure 53, a fluid amplifier directs flow alternately between two channels leading to the vortex chamber. When fluid is directed to the central inlet, fluid passes radially through the chamber and easily through the outlet. Because centrifugal pressure forces are not developed, the valve is considered open. When fluid is directed to the tangential inlet, a trangential velocity component is imparted to the fluid by the chamber walls. The centrifugal reaction forces produce an increased pressure differential across the chamber, and the valve is considered to be shut. The change in pressure differential and/or flow rate produced by the vortex is equated to a reduction in area.

In diagram (b) of figure 53, the amplifier has been eliminated and replaced by a divergent inlet. When fluid passes radially through the chamber, the valve is considered open; but when directed into a curved path upon entering the inlet, a vortex flow field is generated, and the passage of fluid is restricted. In this circuit, the stream is deflected by a tab which is moved into the chamber by action of a solenoid. The tab destroys the natural symmetry of the inlet stream, which returns to its undisturbed state when the tab is retracted and symmetry is reestablished.

The effective port area produced by a particular valve configuration is a function of geometric parameters such as chamber diameter, chamber height, nozzle diameter, and inlet width. Because of the number of variables involved, the effective areas produced in the vortex mode (A_E) and non-vortex mode (A_H) are generally determined experimentally from measurements of pressure flow rate and density.

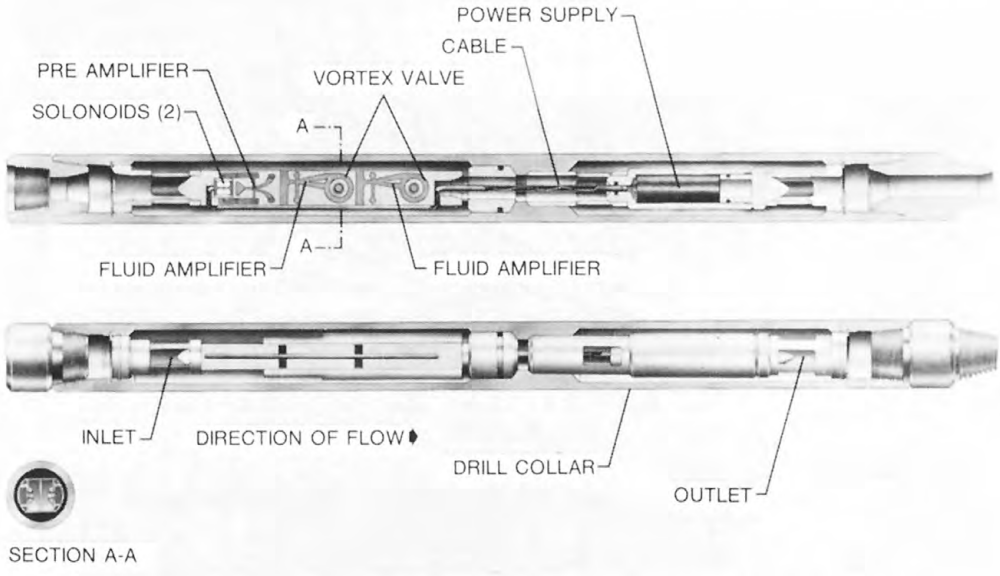

FIGURE 54.—Artistic representation of a four-stage A-type fluidic pulser in a drill pipe

When a fluidic valve is designed for use as a mud pulser, practical consideration (limited space available in a drill pipe, large flow area requirements, and response times) usually dictate the use of several circuit stages arranged to discharge in parallel along the central axis of the drill pipe. Figure 54 shows a sample circuit arrangement. The number of flow area per stage determines the effective flow area of a multistage circuit. The volume of an individual stage establishes the response of a multistage circuit, and the use of multiple stages makes it possible to design valves with large flow areas to reduce operating drop without sacrificing response.

When any valve is designed to produce pressure pulses in a drill pipe, the effective port areas and response of the valve determine the amplitude of the pulse and the average operating pressure drop across the valve. If, for example, a valve can open or close fast enough to produce a pulse which does not have time to travel the distance between the pump and back at the local speed of sound in

the drilling fluid before the next pulse is produced, the amplitude of the pulse can be calculated using the standard equation for water hammer pressures

$$Q_1 - Q_2 = \text{l-K}\ (P_1 - P_2) \qquad (2)$$

where P_1 and Q_1 are the high resistance pressure and flow rate, P_2 and Q_2 are the low resistance pressure and flow rate, and K is a proportional constant given by $K_1 = A/c$, where A is the drill string cross-sectional area and c the speed of sound in the drilling fluid (approximately 4,800 ft/sec).

If the time the value is shut equals the time open, the average flow rate through the valve will equal $\frac{(Q_1 + Q_2)}{2}$ and the average pressure drop will simply be equal to one half the sum of the pressure drop across the valve while shut and open, as given by

$$P = \tfrac{1}{2}\, Q_1/K_1 - Q_2/K_2 \qquad (3)$$

where P = average pressure drop, $K_1 = A_H\sqrt{2/\sigma}$, $K_2 = A_E\sqrt{2/\sigma}$, where σ is the drilling fluid density, and Q_1 and Q_2 = the circulation rate during operation in the vortex and non-vortex mode.

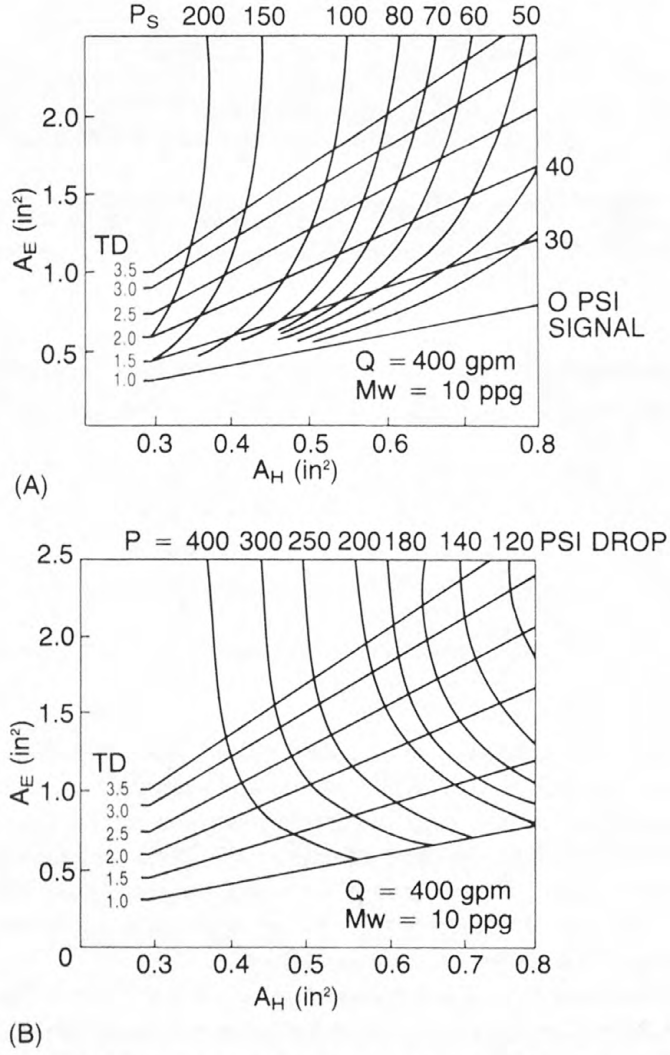

FIGURE 55.—Theoretical curves showing the relationship between effective valve part areas A_E, A_H, and (a) signal pressure P_s, (b) average pressure drag P, and (c) efficiency P_s/P

The flow equations describing the relationship between pulser flow area, drill bit nozzle area, and drill pipe cross-sectional area are developed in equation (1). The results of the analysis are presented in graphical form in figure 55. The curves describe the operation of a valve mounted in a 3.75 ID drill pipe in series with a 0.36 square inch drill-bit nozzle operating at a circulation rate equal to 400 gal/min with a 10 lb/gal mud. An operating duty cycle time on plus time off/time on equal to 0.5 was assumed. For the stated conditions, the curves show that a valve would have to be designed with an effective valve port area of 1 square inch or greater to produce a 100 psi signal pressure with a reasonable pressure drop. The curve shown in figure 56 describes the ratio of the signal pressure to the average pressure drop required to produce the signal as a function of area change. The changing slope of the curve indicates that very little is to be gained by designing a valve to produce an area change greater than 3/1. These curves a, b, and c on figure 55 form the basis for selecting the port areas required to produce a given signal at a specified pressure, circulation rate, and mud weight.

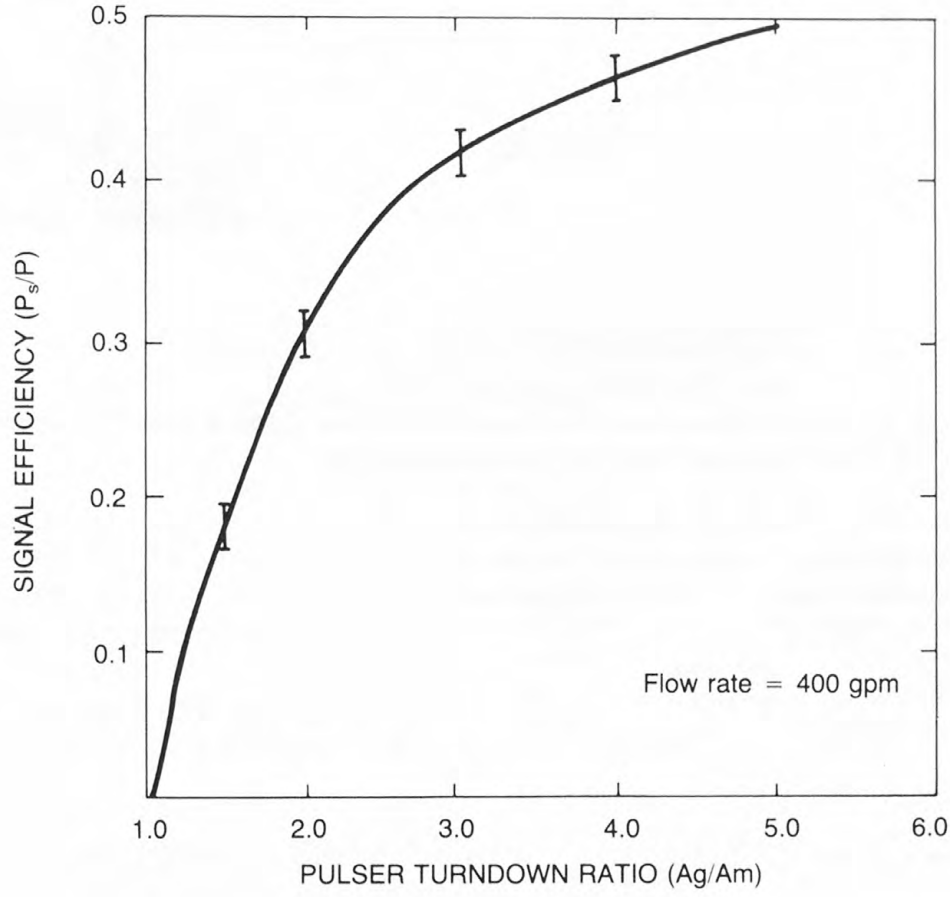

FIGURE 56.—Signal efficiency versus turn down ratio

Flow models representing circuits A and B (fig. 53) were constructed. Photographs of circuit A flow model are shown in figure 57. Extensive laboratory tests were conducted on the flow models in an effort to establish optimum flow geometry for maximizing effective flow area and reducing res ponse time. The models were tested on a horizontal flow loop at the Drilling Research Laboratory (DRL) in Utah. Measurements were made of pressure, flow rate, fluid density, and response time at circulation rates between 25 and 130 gallons per minute per circuit stage. Water and drilling fluids were used as test fluids. The measurements were used to calculate equivalent flow areas per stage using equation (1).

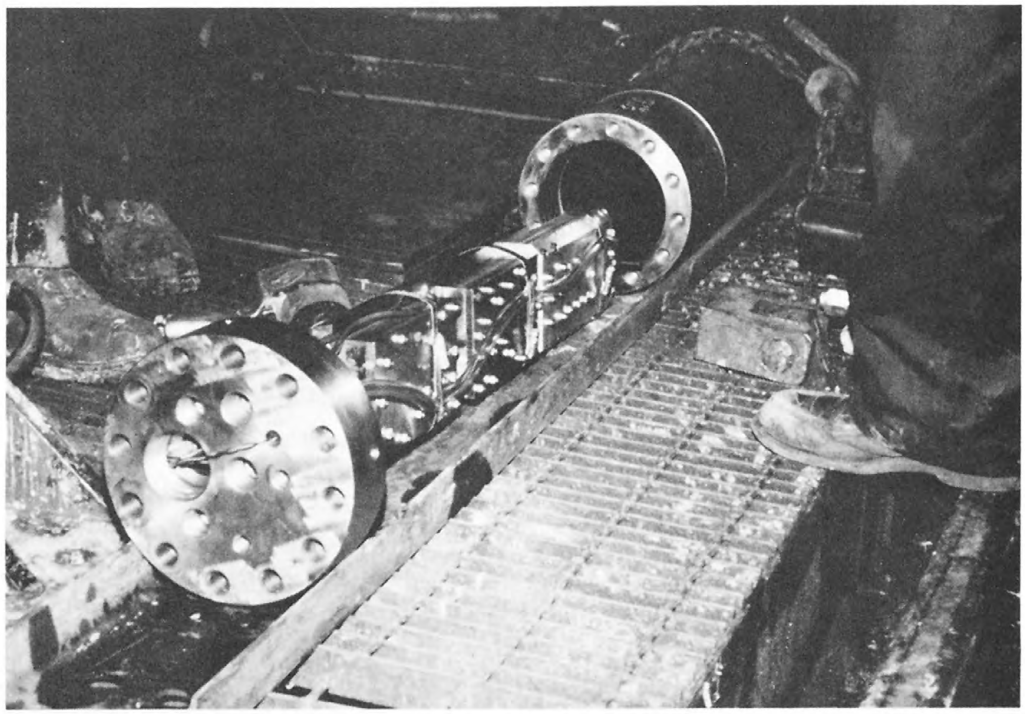

FIGURE 57.—Circuit A test assembly

Results of the tests are summarized below and clearly show circuit B to exhibit superior operating characteristics from the standpoint of flow area and response.

	Circuit A	Circuit B
Actual Nozzle Area	0.385 in^2	0.385 in^2
Effective Nozzle Area	0.30 in^2	0.04 in^2
Turndown ratio	3.8	2.5
Turndown time	0.04 sec	0.02 sec
Turnup time	0.18 sec	0.04 sec
Maximum pulse rate	1.24 Hz	8.0 Hz*

*Limited by actuator response

The slower response exhibited by circuit A is caused by a complex flow interaction which occurs in the amplifier and which lengthens the time required to divert the amplified stream from the tangential to the radial inlets and to the vortex valve. The reduction in maximum effective flow area is attributed to additional frictional pressure drop created in the amplifier.

Circuit B exhibited a maximum effective port area equal to 0.4 square inches, 0.15 square inches per stage. The time required to produce the vortex was 0.015 seconds, and to designate the vortex was 0.35 seconds, as indicated by the rise and decay time of the measured pulses. A comparison between vortex data and mud data showed no specific differences in operation.

Although response characteristics of circuit A might be improved by using a different type amplifier, test conclusions showed that the superior response and inherent simplicity of circuit B makes that design approach more suitable for further mud pulser development.

A three-stage B-type valve was designed and constructed for use with standard (4.5 inches OD × 3.75 inches OD) drill pipe. A photograph of the valve is shown in figure 58.

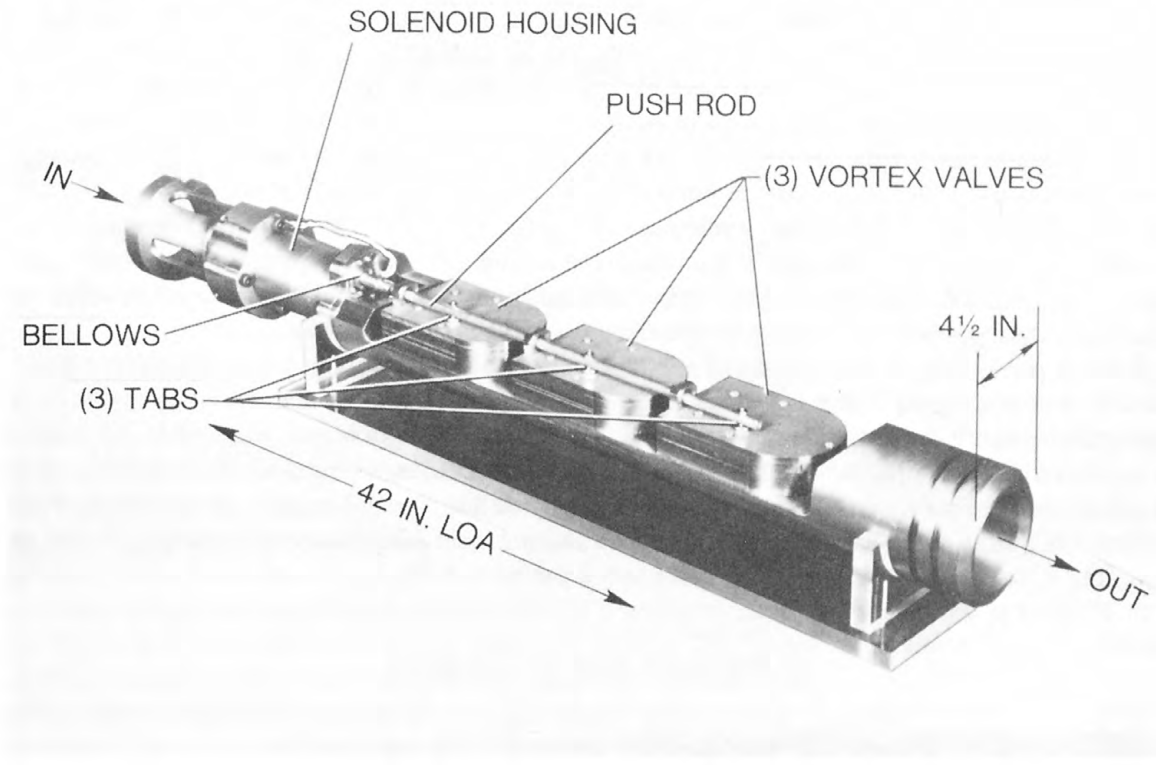

FIGURE 58.—Photograph of a three-stage fluidic mud pulser

The valve has a maximum effective flow area equal to 1.2 square inches and operates at a turndown ratio of 2.5. The response of the valve at 400 gallons per minute is 0.015 seconds for turndown and 0.035 seconds for turnup. The valve is designed to produce 0.4 psi signal per psi pressure change when operated on a 50 percent duty cycle ($\frac{\text{time open} \times \text{time closed}}{\text{time open}} = 0.5$). This arrangement converts to a pulse amplitude equal to 130 psi at 400 gallons per minute using 10 lb/gal mud (see fig. 54). The minimum duration of a pulse which can be produced is 0.05 seconds at 400 gal/min.

The valve is actuated by a 24-volt solenoid housed in a sealed pressure-balanced container. Motion of the solenoid armature is transmitted through the wall of the container by a flexible bellows which has a shaft attached to its outer end and which in turn moves three tabs simultaneously into and out of the vortex chamber to produce valving action.

Power to actuate the valve during the planned flow tests will be provided by a separate 24-volt battery-operated power supply. The power supply, flow switch, and programing circuit are housed in a sealed container. The assembly is positioned in a separate drill pipe section located upstream of the valve.

Conclusions

Results from tests were used to develop a design for a prototype valve. Emphasis on valve design was placed on maximizing response and minimizing pressure drop through the use of large port areas. Note, however, that the rate at which data can be transmitted by any valve as well as the average pressure drop produced by a valve also depends upon the type of pulse coding (i.e., binary, pulse position, modulation, FM, etc.) scheme selected because of duty cycle considerations.

The 50 percent duty cycle described above represents a worst case condition (from the average pressure drop and power consumption point of view) because the valve is actually in use one half of the time. Operating at a lower duty cycle reduces average pressure drop and power requirements because the valve can be full open and unenergized during a major portion of an operating cycle. At lower duty cycles the average pressure drop produced by the valve would approach that which is calculated with the maximum effective flow area (A_E) as given by equation (1).

Work is proceeding at this writing on the fabrication of the three-stage pulser which will have associated power supply and programing circuits. Drilling Research Laboratories will conduct a test series to measure valve response and reliability. In addition, tests in a well bore are being planned to conduct a full-scale pulser test in a well bore. The full-scale experiment is envisioned to consist of (a) running the pulser and associated hardware in a well to various depths, (b) circulating flow through the pulser while the valve is actuated by series of variable frequency input signals and, (c) recording the pressure signals as they arrive at the surface.

Reports and References

Holmes, A. B., 1980, Fluidic mud pulse telemetry technology investigations for measurement while drilling applications: Harry Diamond Laboratories, Silver Spring, MD. [in press].

Holmes, A. B. and Gehman, S. E., 1979, Fluidic approach to the design of a mud pulser for borehole telemetry applications during drilling: Harry Diamond Laboratories, HDL-TM-79-21, Harry Diamond Laboratories, Silver Spring, Md.

Suppression of Blowout Fires

Principal Investigator: John G. O'Neill
Center for Fire Research
National Bureau of Standards
Washington, DC 20234

Objective: To develop blowout fire suppression technologies for offshore oil and gas drilling and production.

Perhaps the most serious of all accidents which can occur in offshore oil and gas operations is a blowout. Fires resulting from blowouts (the ignition of methane gases and other flammable formation fluids) can destroy a platform or rig.

A potential blowout situation arises when the hydrostatic pressure exerted by a column of drilling fluid, or mud as it is sometimes called, falls below the pressure of the formation fluids entering the well. The occurrence of an influx, referred to as a kick, is common during drilling, and much technology has been developed to mitigate the problem. The procedures used to control kicks are described in "Development of Improved Blowout Prevention Procedures for Deepwater Drilling Operations" where the report explains that in deepwater drilling the procedure of carefully maintaining proper well pressure is complicated by fracture pressures which are less than those observed on land or in shallow water at equivalent depths. The fracture pressure is when an exposed subsurface formation will rupture and accept fluids from the well bore.

Offshore drilling usually sustains kicks which result in pressures exceeding 6,000 psi measured at the surface. These high pressures present stress upon components of the blowout preventer (BOP) stack, choke assemblies, valves, and other equipment installed to prevent blowouts. Although the equipment is designed to contain such pressures, the harsh marine environment in which it must function, together with human error, seems to allow blowouts to continue. For example, the internal surfaces of the choke assembly are exposed to kick fluids including pieces of rock or shale moving at very high velocities. Because the choke assembly is used to resist flow in order to permit safe venting of kick fluids, its orifices, valves, and elbows are subjected to high internal reaction pressures. Failures of critical components on a platform exposed to hydrocarbons at such high pressures present a significant hazard in the wellhead area. Resulting fires are of such intensity that structure steel can weaken and collapse within minutes. The risk of damage is not only high when measured in terms of potential life and property loss, but also regaining well control may be impossible because of critical equipment failure and the inability to gain access to the well.

An analysis of available data indicates that between 1973 and 1980, 10 blowout fires or major explosions occurred on the OCS, 5 of which occurred in 1979 and 1980. In the incidents where blowouts occurred on a platform, the actual location of operational failure varied—choke assembly, end of the drill pipe on the drilling deck, top of the well annulus just below the rotary table, and flange connections in the BOP stack located in the substructure below the derrick.

The Center for Fire Research of the National Bureau of Standards is using two approaches to develop fire suppression technologies for blowout fires originating at these locations. One approach is to extinguish blowout fires originating from influxes which rise in a well annulus. The location of blowout fire can vary from this type of influx, and an efficient suppression system is very complex. The tremendous fuel rate typically resulting from a blowout suggests that a suppression system should concentrate the extinguishing agent at the source of the fire. Therefore, studies are being conducted to inject the agent into a conduit upstream of an orifice supplying methane gas to a diffusion flame.

This concept envisions in full scale a system which injects an extinguishing agent into the marine riser below the platform and the flow point which feeds the blowout fire. The major problem is to

deliver the agent at a sufficient rate so as to mix it with the flowing hydrocarbons and extinguish the fire.

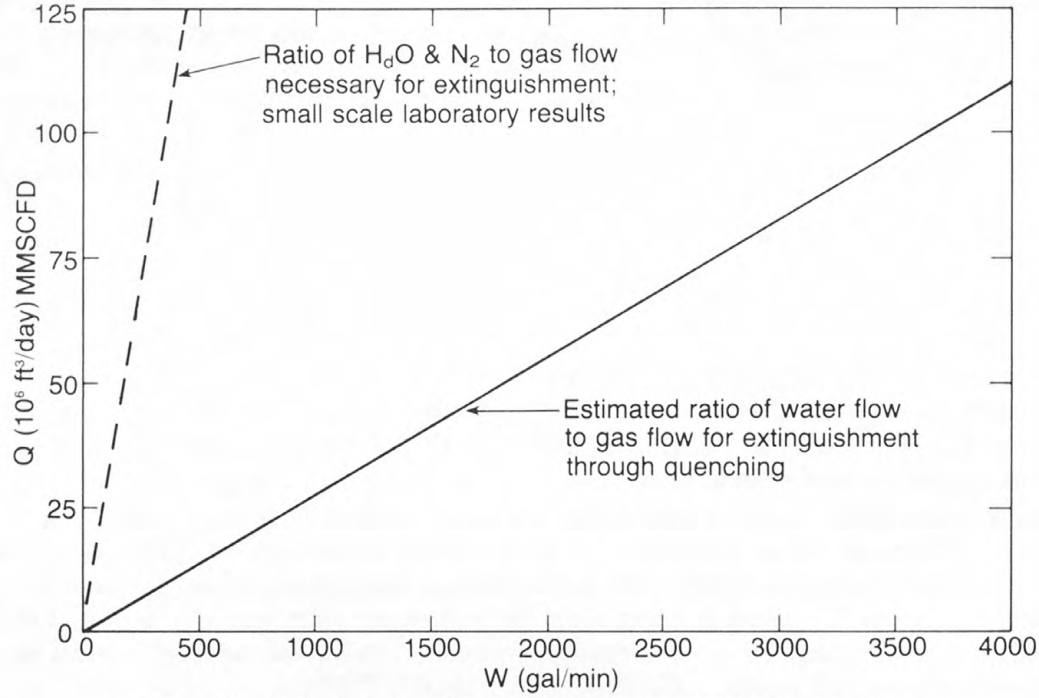

FIGURE 59.—Estimated ratios of water-to-gas necessary for extinguishment

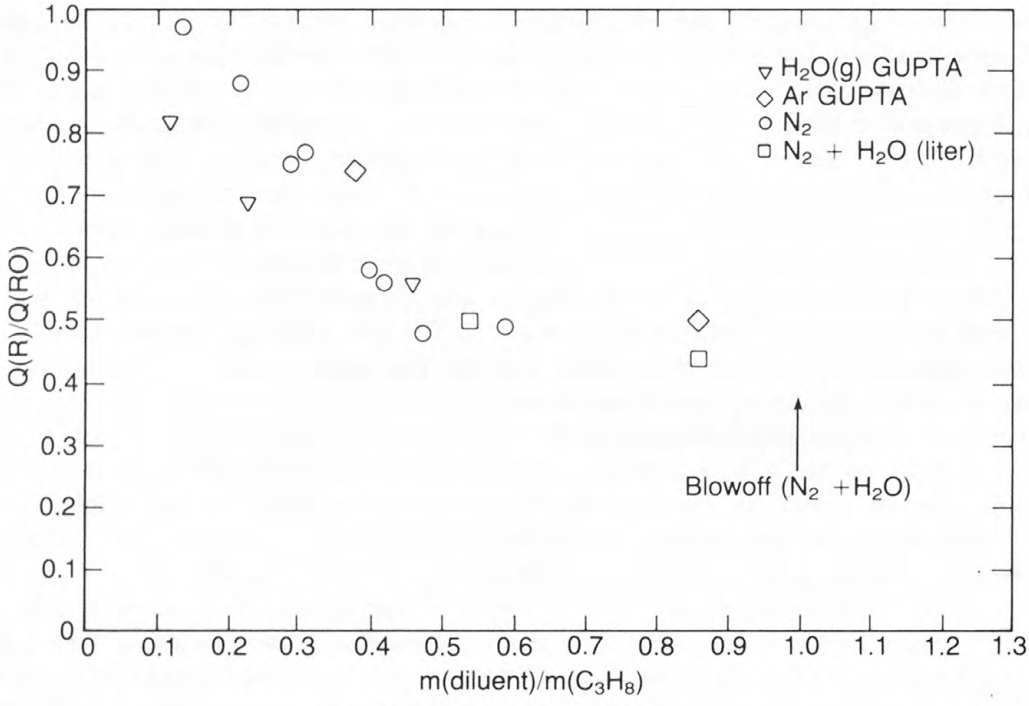

FIGURE 60.—Reduction in radiation

Currently, the project is investigating the ratio of water to methane gas necessary to extinguish the fire. Figure 59 indicates the estimated ratios necessary to extinguish a methane gas fire through quenching. The gas flow rates shown include a range of flows estimated for full-scale blowout situations. In small-scale experiments, as shown in figure 60, a methane gas flame was extinguished at a more favorable ratio than estimated. Results of these tests indicate a reduction in heat transfer through radiation as the flow of the extinguishing agent was increased. Finally, the fire was

extinguished when the ratio of mass flow of water and nitrogen to methane gas approached unity. The data correlate well with previous tests (Gupta, 1976) using steam and argon to reduce the radiation from flames. The improved ratio, extrapolated to full scale, is shown in figure 59. Experimental work will progress toward larger scale tests to determine if the efficiency demonstrated at small scale can be maintained.

Although other suppression agents are also being examined for use in this type of system, water is considered the most practical for use of offshore platforms. Future tests will include injection of suppression agents into more complicated, although realistic, flow streams such as gas and drilling mud mixtures resembling upward migration of gas in a well bore containing drilling mud.

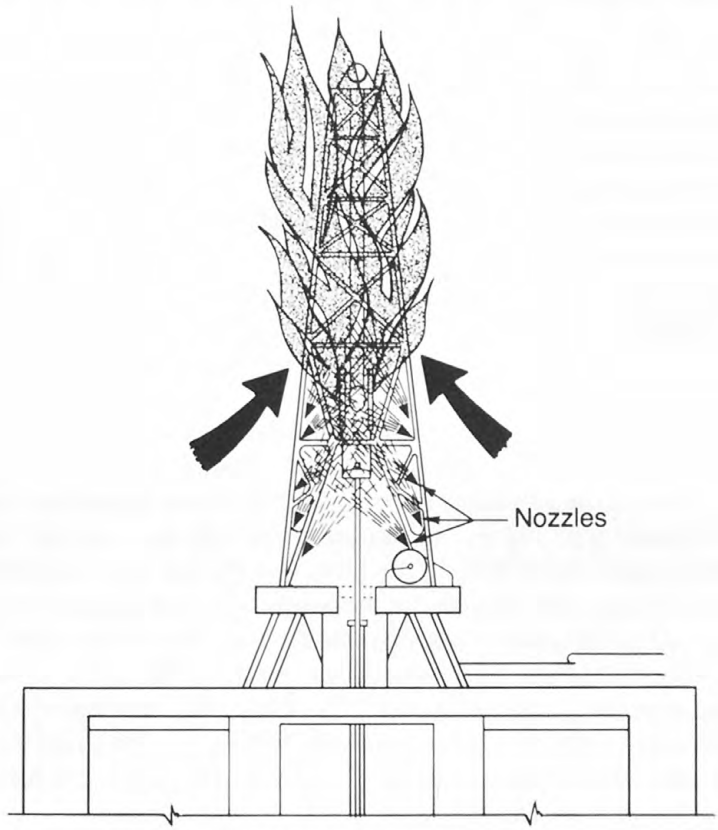

FIGURE 61.—Air entrained fire extinguishing system

The second fire suppression system technology being developed in this program is directed at a fire resulting from a blowout through a drill string. This type of blowout fire precipitated the IXTOC disaster in Campeche Bay, Mexico, in 1979. Figure 61 depicts such a blowout fire. In this case, the end of the drill string acts as a hug diffusion burner which entrains a tremendous amount of air for combustion. Since the injection system previously described is not feasible for this type of fire, the suppression agent must be applied from the exterior. The concept under study takes advantage of the entrained air to help deliver the extinguishing agent into the flame. Here again, water in the form of fog sprays is the primary agent for consideration on offshore platforms. Experimental efforts at NBS are concentrated on quantifying the ratio of water to gas necessary to accomplish extinguishment. In addition, information is being developed to determine optimum position and direction of spray nozzles for this application.

Reference

Gupta, M., 1976, Experimental investigation of the radiation from turbulant hydrocarbon diffusion flames: Unpublished thesis, University of Waterloo, March 1976.

Overpressured Marine Sediments

Principal Investigator: Dr. Louis J. Thompson
Civil Engineering Department
Texas A&M University
College Station, TX 77843

Objective: To develop a consolidation theory which is applicable to the progressive burial of ocean-bottom sediment and describes porosity as a function of depth and time at various rates of deposition.

In the uncased portion of the well, the borehole fluid pressure at each formation must be kept between two critical pressures if the well is to be drilled safely. The lower critical pressure develops when the borehole fluid pressure is lower than the formation fluid pressure so that the flow is into the well; if uncontrolled, this condition may cause a blowout. The upper critical pressure develops when the borehole fluid pressure is high enough to cause expansion of the borehole and fracturing of the formation so that flow from the well, if uncontrolled, may cause either a stuck drill stem or loss of fluid circulation in the borehole. The upper critical pressure is as dangerous as the lower pressure. When circulation is lost at a lower formation, the dropping column of borehole fluid can cause its pressure to drop below the lower critical pressure in a higher formation and cause a blowout.

Blowouts occur from porous formations where significant flow into the well can develop. If the formation fluid contains sufficient gas either in the dissolved or free state, it expands into the borehole; and if the flow is uncontrolled, the blowout can persist for a long time. The lower critical borehole pressure depends primarily on the formation fluid pressure and the formation permeability. The formation fluid pressure depends upon the history of the site and can be either lower or higher than geostatic water pressure even though the deposition occurred millions of years ago.

Fracturing is more likely to occur in the more brittle formations. The upper critical pressure depends on the formation fluid pressure, overburden stress, coefficient of earth stress at rest (K_0), cohesive strength, and angle of internal friction. The higher the principal mean free field stress supported by the mineral fabric, the more ductile the formation. The strain history of the site also influences both the strength and stiffness of the formation. The higher the formation fluid pressure, the lower the strength of the formation.

The maximum formation fluid pressure is probably limited by natural fracturing. Manifestations of natural fracturing are mud volcanoes, salt domes, diapirs and faults in sedimentary deposits. They can develop when the mineral fabric has little or no shear strength or when the force in the water is greater than or equal to the overburden force, the force in the mineral fabric being either zero or tensile.

In progressive burial of sediment on the ocean floor, the deposited mass both loads and insulates the previously deposited sediment. The load tends to densify the sediment and increase both the temperature and pressure in the interstitial water. Its bulk also retards the upward flow of water necessary for dewatering the sediment. In fact, as shown by the experiments conducted by the principal investigator, the effect of the retardation of water flow is orders of magnitude greater than the effect of the loading. Also the bulk of deposited sediment slows the earth cooling and this tends to raise both the temperature and pressure in the interstitial water.

By applying the field equations of mechanics to both the water and the mineral fabric, together with the experimentally determined power laws that relate both the force in the sediment and the permeability to the porosity, equations have been derived that give the porosity and temperature as a function of depth and time. The equations also require, as input, the area of contact between the mineral particles. Four different sets of experiments show that this is about 20 percent of the total

area for a clay. Numerical solution of the equations allows the porosity, settlement, temperature, and interstitial water pressure to be calculated as a function of depth and time. When the calculated settlement is compared to actual settlement, as measured in an unaxial consolidation laboratory test, results indicate (fig. 62) that the computed values closely approximate the measured values for all times.

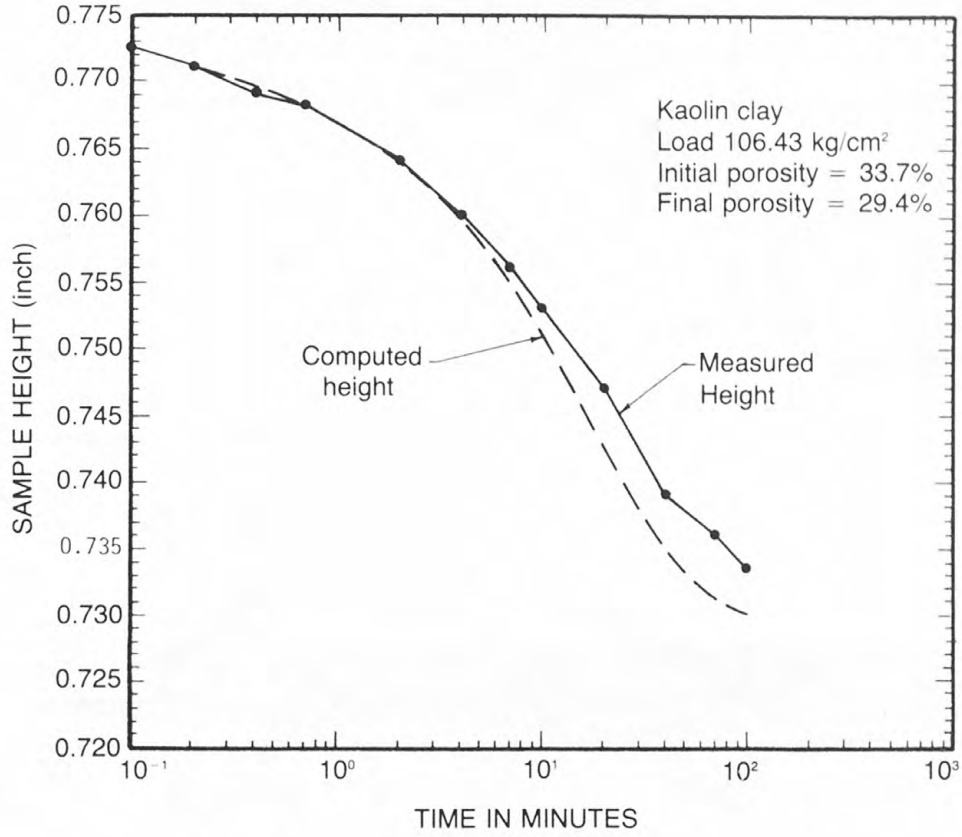

FIGURE 62.—Height as a function of time for uniaxial compression of clay

Since the theory and numerical solutions are realistic, prediction should be possible for the formation water pressure in a sandstone adjacent to a shale if the type of clay mineral can be determined and if its material properties have been previously cataloged. The shale porosity in the unloaded state and in situ state must also be known. No simple test such as the Atterberg limits has been found to correlate indirectly with the material properties. So far, the pertinent material properties have been determined for quartz sand and kaoline, illite, and smektite clays compressed to 10,000 psi. The clays have been identified by X-ray diffraction. This calculation scheme is shown in figure 63.

The theory has not been checked in the field because of the difficulty of getting wet samples of shale from depths where the temperature, formation water pressure, and shale density were measured.

The experiments have shown that the temperature (20° to 100°C) does not have much influence upon the compressibility, absolute permeability, and heat conductivity of sand and the three clays tested. Experiments show that both the porosity and type of clay mineral have little influence on vertical heat conductivity, which is about 3×10^{-3} cal/cm-sec-C°. In addition, experiments show that horizontal conductivity could be as much as two times the vertical conductivity. As the porosity

of the clays were changed in range of 55 to 25 percent, vertical thermal conductivity changed slightly; vertical electrical resistivity changed appreciably and permeability varied by more than two orders of magnitude.

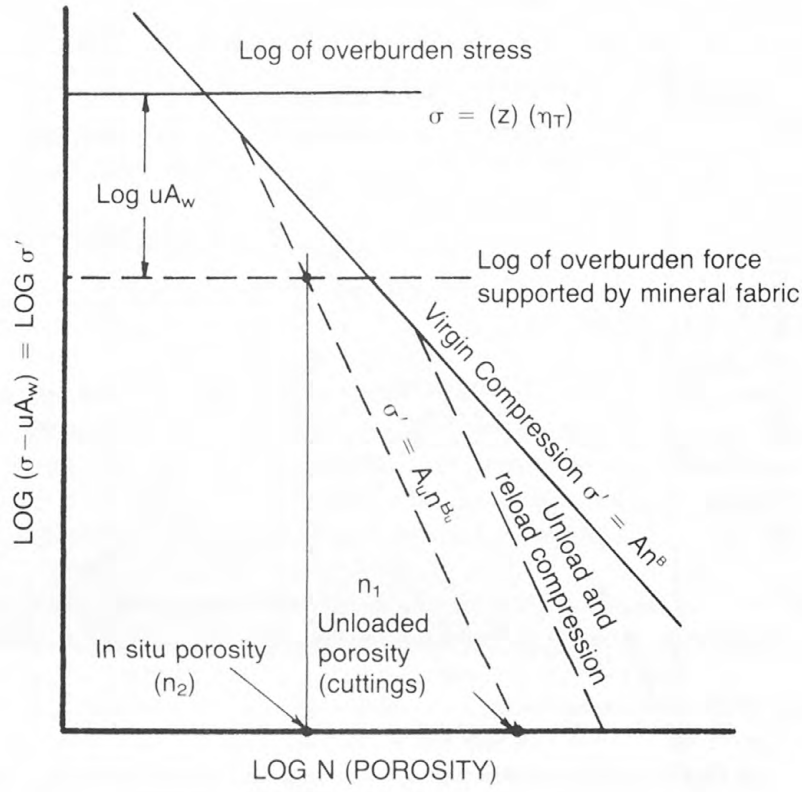

A_w = water to total area ratio
u = formation water pressure
n = porosity (ratio)
σ = overburden total stress
$\sigma' = \sigma - uA_w$ = stress supported by mineral fabric

FIGURE 63.—Use of uniaxial compression data to compute clay pore water pressure

Reports and References

Chen, R. H. N., 1976, Empirical relationships between consolidation pressure, porosity and permeability for marine sediments: Thesis, Texas A&M University, College Station, Tex.

Enderby, J. K., 1981, Thermal conductivity, electrical resistivity and permeability of saturated soils at various porosities: Thesis, Texas A&M University, College Station, Tex.

Miller, J. W., 1979, Thermal conductivity of sediments as a function of porosity: Thesis, Texas A&M University, College Station, Tex.

Thompson, L. J., 1979, Overpressured marine sediments: The thermomechanics of progressive burial: Texas A&M University, College Station, Tex.

Thompson, L. J., and Callanan, M. J., 1981, Overpressured marine sediments: Vol. 1: The prediction of hydrofractures and K_0 during drilling: Texas A&M University, College Station, Tex.

Thompson, L. J., Chen, R. H., and Bryant, W. R., 1977, Overpressured marine sediments: Texas A&M University, College Station, Tex.

Thompson, L. J., and Lee, H. T., 1981, Overpressured marine sediments: Vol. II: Compressibility and permeability of clays at high pressure: Texas A&M University, College Station, Tex.

Subsea Collection of Oil From a Blowing Well

Principal Investigator: Dr. Jerome Milgram
Department of Ocean Engineering
Massachusetts Institute of Technology
Cambridge, MA 02139

Objective: To quantify the parameters within which oil may be collected as it emanates from a blowing well.

The concept of installing an oil collector immediately above a subsea blowout has been considered for a long time. The most ambitious implementation of such a collection device was carried out at the IXTOC 1 blowout, Campeche Bay, Mexico, during the autumn of 1979. Figure 64 shows a photograph of the collection device or "Steel Sombrero," as it was called. The triangular steel truss was supported from a platform 200 feet from the well. Oil, gas, and water entered the conical collector above the wellhead and was carried by gas-lift up the sloping riser to separation equipment on a specially erected platform to which the truss was clamped.

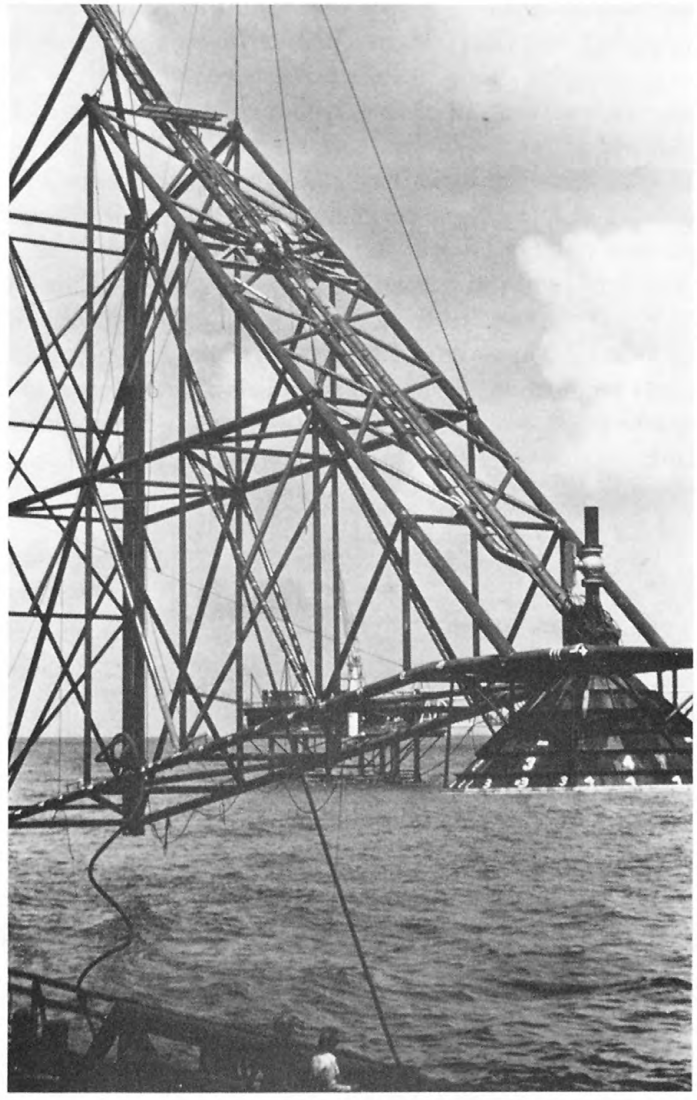

FIGURE 64.—Steel Sombrero open bottom collector used on the IXTOC 1 blowout Campeche Bay, 1979

Sending a collector to the ocean floor would be the most efficient collection scheme, but once a blowout has occurred, seating the collector in place is not feasible for several reasons, including difficulty of sealing and problems of coping with debris which probably has fallen around the wellhead. Therefore, plans for emergency response to a blowout generally would have to be based on positioning a collector at some height above the seabed.

In particularly vulnerable areas, installing a bottom-mounted collector in advance might be justified so that drilling operations would take place through its top. This configuration, though evaluated by the principal investigator, is not discussed herein. For collectors which could be placed over conventional wellheads after a blowout, some kind of open-bottom arrangement probably is necessary; open-bottom collector technology is the subject of this summary.

Having flow data collected during the IXTOC 1 operation, MIT established an experimental laboratory to determine efficient collector configurations and operating parameters. From these experiments and under most circumstances, the amount of gas spewing from a well is more than that required for most efficient collector operation. The amount of blowing oil which is collected decreases as gas flow increases beyond optimum flow. To overcome this dificulty, Dr. Milgram devised a collector which separates the gas from the liquid so that performance is not degraded by increased gas flow. Although only preliminary tests have been run on this separating collector, sufficient data have been obtained to demonstrate feasibility of the device. Results of these preliminary tests are described below, together with results for simple non-separating collectors. Experiments with separating collectors continue in order to gain additional insight into this technology.

Laboratory experiments were performed in a cylindrical, open-topped, 13-feet-high tank having a diameter of 6 feet. Air and oil were delivered to a short nozzle in the bottom of the tank, which simulated a wellhead. The ranges of experimental flow rates were from 2.5 to 20 standard cubic feet (SCF) for gas and 0.5 to 3.0 gallons per minute (GPM) for oil. The physical sizes of the experimental devices were roughly 1/15th of full scale. Correct dimensional scaling, as will be described, requires that flows scale in proportion to the 5/2's power of the length (collector diameter, for example) so as to correspond to full-scale flow rates of approximately 3 to 25 million SCF of gas per day and 15,000 to 90,000 barrels of oil per day. These large-scale values of oil flow were used because the results for fraction of blowout oil collected were found to be insensitive to variations in oil flow (the oil is essentially a "tracer" in the gas-liquid plume) and larger oil volumes were easier to measure.

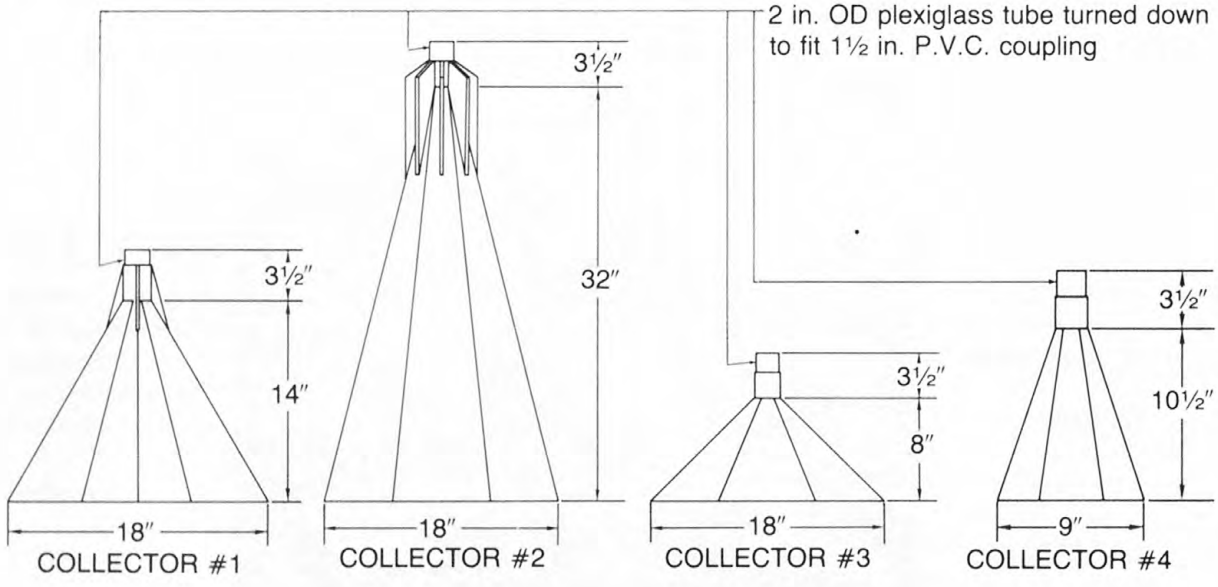

FIGURE 65.—Model collectors used in MIT laboratory experiments

Inverted cone shaped collectors shown in figure 65 were tested. The flow was driven up the riser by gas-lift as in the case of the full-scale Sombrero. For a specific situation, the flow was varied by changing the riser resistance with a valve located near its top. In each experiment, wellhead gas and oil flows were known and collected oil and water flows were determined by sampling the liquid emanating from the riser. The experimental arrangement used is sketched in figure 66.

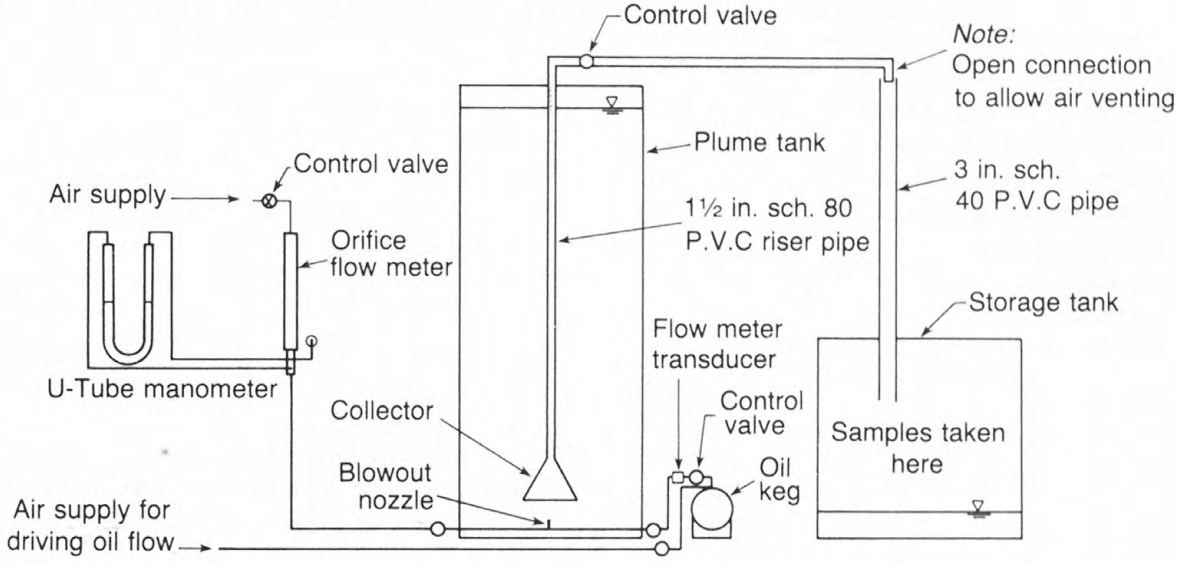

FIGURE 66.—Schematic arrangement of experimental apparatus

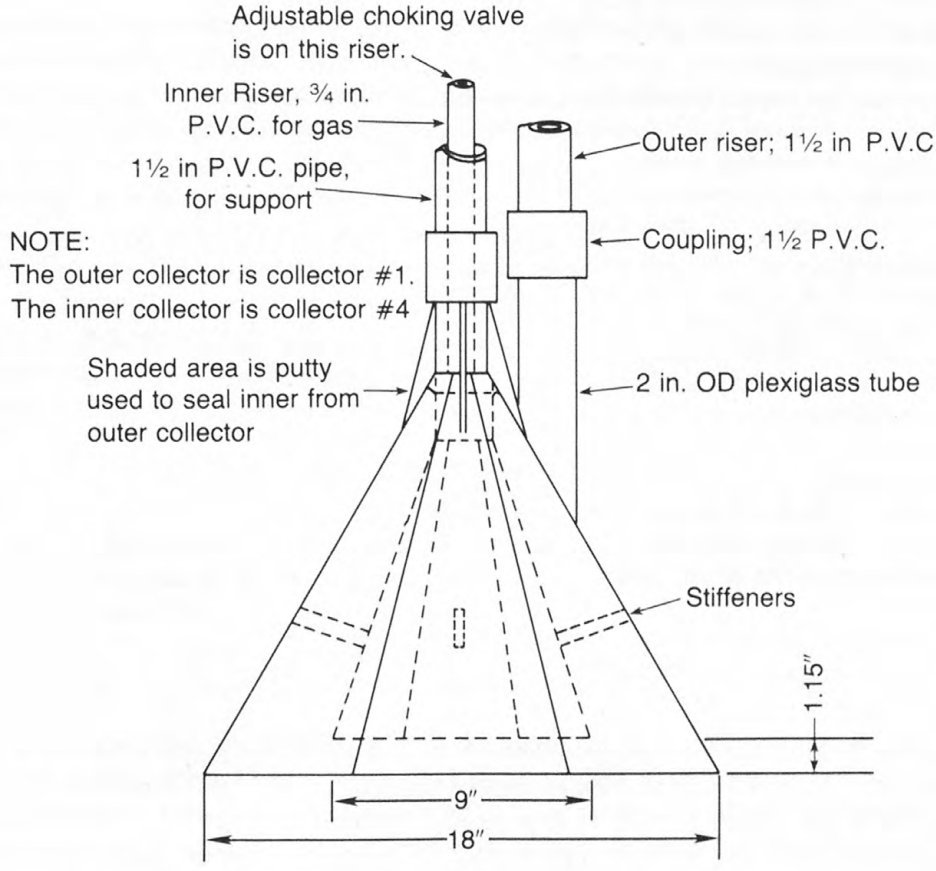

FIGURE 67.—Gas separating collector

Excessive gas flows (which occur with most well blowouts) degraded the performance or the fraction of blowout oil collected by the system. To overcome this problem, the collector shown in figure 67 was devised, which separates most of the gas from the remainder of the flow. This collector contains an inner and outer cone. Nearly all of the gas initially enters the inner cone whose riser resistance can be adjusted to allow the passage of nearly all of the gas, but essentially none of the liquid. A small amount of gas spills across the bottom edge of the inner cone into the outer cone. This small amount is sufficient for driving the maximum possible gas-lifted liquid flow through the riser attached near the top of the outer cone.

One of the most obvious features of the data obtained for the various collectors (using a variety of flows and riser resistances) is that the fraction of blowout oil collected is independent of oil flow when all other quantities are held constant. Essentially, the oil is only a tracer in the main water flow, permitting averaging of the results for a variety of oil flows in which the other variables were held fixed. Thus, the number of conditions needing evaluation were greatly reduced. Furthermore, oil flows may be eliminated from a list of important independent variables which affect the fraction of oil collected.

Further preliminary observations of averaged data reveal that the most important independent variables for influencing collection performance are air flow rate and total liquid flow rate into a collector.

From the standpoint of dimensional analysis, 19 relevant independent physical variables need to be considered. The important dependent variable, both for an actual blowout collection operation and for the MIT experiments, is the fraction of blowing oil collected. These variables are listed below.

Independent Variables:

- d—diameter of outlet nozzle (well bore)
- D—diameter of base of collector
- g—acceleration of gravity
- h—vertical distance from nozzle (blowout) outlet to base of collector
- g_g—gas volume flow rate at nozzle (blowout)
- Q_o—oil volume flow rate at nozzle
- Q_c—volume flow rate of collected oil
- Q_w—volume flow rate of collected water
- Q_T—total collected liquid flow rate ($=Q_c+Q_w$)
- s—vertical height of collector (base to riser connection)
- T_{og}—oil-gas interfacial tension
- T_{ow}—oil-water interfacial tension
- T_{wg}—water-gas interfacial tension
- P_g—gas (mass) density
- P_o—oil density
- P_w—water density
- ν_g – kinematic viscosity of the gas
- ν_o – kinematic viscosity of the oil
- ν_w – kinematic viscosity of the water

Dependent Variable:

- P – fraction of escaping oil collected

These 19 independent variables can be combined into 16 independent dimensionless groups which are obviously too many for efficient analysis of an experiment of the type described. Hence, all but the most influential independent variables need to be eliminated from further consideration. Because the volume flow of escaping oil has no significant influence on the fraction collected it can be eliminated. Further simplification results from the elimination of all Reynolds and Weber numbers

from a list of influential dimensionless variables, which can be justified by an analysis of the possible effects of viscosity and surface tensions. Under these conditions, the list of important dimensionless independent variables is reduced to the four dimensionless groups shown below.
Important Independent Dimensionless Groups:

$F = \frac{Q_T}{\sqrt{gh^5}}$, Froude Number

$R = \frac{Q_T}{g_g}$, Phase Ratio

$E = \frac{D}{h}$, Enclosure Ratio

$S = \frac{s}{D}$, Shape Factor

Preliminary data analysis shows that the results are highly dependent on total liquid and gas flow, which indicates that both the Froude number and the phase ratio (listed above) are of major importance if nearly all the gas is collected. When some gas escapes outside the collector, performance generally is markedly improved as a result of the higher phase ratio, the increase of which has been found to improve performance for all realistic conditions. But generally, anticipating oil collection operations is not feasible where a significant amount of gas is permitted to escape from the collector because of the resulting dangerous surface operations. Therefore, further analysis includes only those conditions for which nearly all of the gas is collected. Under these circumstances, the effect of enclosure ratio is relatively minor, so it will be omitted from the list of influential variables, thereby leaving only the Froude number and the phase ratio as important influential dimensionless variables. The results obtained in this way need to be viewed as "averages" over the practical range of enclosure ratios. In particular, collection efficiency variations of 10 percent can be expected from the use of various enclosure ratios.

In consideration of the fraction collected, P, as influenced mainly by the Froude number, F, and the phase ratio, R, we can write

$$P \sim f(F,R) \qquad (1)$$

Maximum engineering utility of the experimental measurement is provided by determining an approximate functional form for the relationship described symbolically in equation (1). Inasmuch as the equation is meaningful only when nearly all of the gas is collected, a functional form needs to be determined when there is a significant escape of air, which occurred from 15-20 SCF. By examining the data, and by several numerical tests, a suitable functional form for equation (1) was determined:

$$P = [1-\exp(\frac{-AxRxF}{B+R})]^c \qquad (2)$$

where A,B, and C are constants to be determined. Evaluation of these constants was accomplished by means of a computer-based nonlinear optimization process for fitting the functional form to the data. The values obtained are:

$$A = 77.0311, \qquad B = 1.41879, \qquad C = 0.42753 \qquad (3a, b, c)$$

The resulting estimates from equation (2), as compared to the data, have a standard deviation of 0.087.

Equation (2) is intended as a smoothing and interpolating function. It is used to generate smoothed curves of fraction collected vs Froude number for various phase ratios. These curves, shown in figure 68, represent a fairly complete summary of results for single cone open-bottom collectors for which all of the gas is collected. It shows, very specifically, the approximate fraction of blowout oil that can be collected for any set of circumstances.

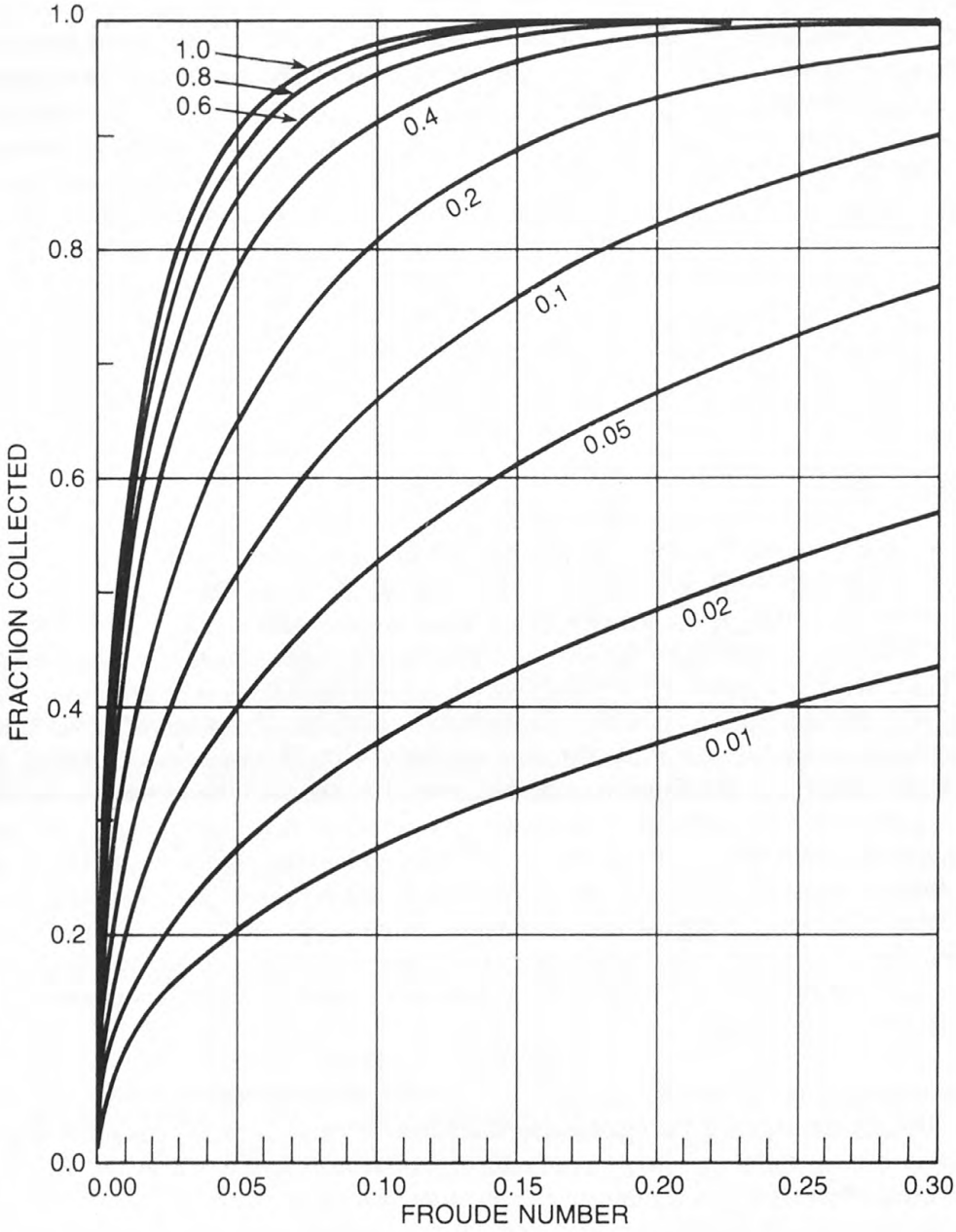

FIGURE 68.—Fraction of blowout oil collected versus Froude number obtained from equations (2) and (3)

The results of the tests of oil collection performance for open-bottom collectors reveal that, for a given Froude number, performance is degraded as the phase ratio is decreased. The separating collector, described herein and shown in figure 67, was designed to reduce this detrimental effect. Control of the separation is achieved by means of the valve on the gas riser. When gas riser resistance is low, nearly all of the gas and some of the liquid flows through it. As the gas riser resistance is increased by partially closing the gas riser valve, the liquid flow in the gas riser can be eliminated. Still further increases in gas riser resistance results in a small amount of gas spilling from the inner collector into the outer collector. This escaping gas provides the gas lift in the liquid riser and drives the liquid collection process.

A limited number of experiments on this gas separating collector were conducted. For these tests, the liquid riser used was the same one for the tests on the open-bottom collectors. The valve on this

riser was fully opened which is the condition for the highest liquid collection rates in the open-bottom collector tests. The model gas riser was a ¾ inch pipe extending through the height of the test tank. The flow resistance of this pipe itself was sufficient to prevent liquid from flowing through it. Nearly all of the gas flowed through the gas riser with a small amount escaping into the outer collector.

The initial tests on the separating collector, reported here, were performed to determine its feasibility. The resistance was not varied in the gas riser to optimize conditions for each gas flow. Test conditions and results are shown below.

Collector diameter = 18 inches		Collector Height = 7 feet	
AIR FLOW RATE (SCFM)	FROUDE NUMBER (F)	PHASE RATIO (R)	% OF BLOWOUT OIL COLLECTED
10	0.036	0.31	49
10	0.040	0.36	57
10	0.035	0.30	46
15	0.333	0.19	48
15	0.030	0.18	45
15	0.034	0.20	49
20	0.029	0.13	44
20	0.030	0.13	47
20	0.040	0.18	62

Even though no special steps were taken to optimize the resistance in the gas riser, the total collected liquid flow was greater for every test in which the separating collector was used than for any of the tests using single cone collectors. Although collected liquid flows diminished with increasing gas flows, this diminution was small and the total flow rate always remained greater than for cases employing a single collector. The most important result is that the fraction of the escaping oil collected does not diminish as the gas flow rate is increased. The detrimental effect of decreasing phase ratio for single cone collectors is eliminated by using separating collectors. All of

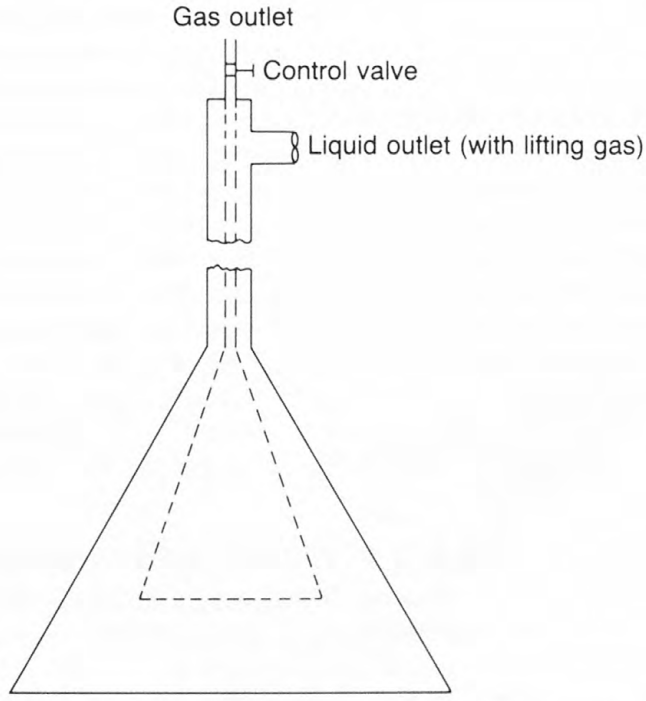

FIGURE 69.—Concept for separating collector having concentric risers

the tests upon the separating collector had nearly the same Froude number. The fraction of escaping oil collected was comparable to that for a single cone collector operating at the same Froude number but having a favorable phase ratio. The separating collector eliminated this necessity for a favorable phase ratio.

The separating collector probably is a very important development. The few tests performed thus far have demonstrated its feasibility and its desirable feature of being insensitive to phase ratios. To fully determine the anticipated performance of separating collectors under a wide range of conditions, more extensive tests will be performed to determine the effects of various resistances in both the gas and liquid risers. Further, variations in separating collector geometry need to be evaluated as well. In an actual accident response device, the two risers, gas and liquid, can be separate as shown in figure 67 or concentric as shown in figure 69. Although concentric risers can be expected to yield the best performance, outstanding performance of a separating collector probably can be achieved with separate risers, which is a system that may be much easier to construct.

Subsea collection of the oil from blownout offshore wells is feasible. Collecting a high percentage of the blownout oil requires adequately large Froude numbers and phase ratios. The general relationship between the fraction of the blownout oil collected, the Froude number, and the phase ratio is shown in figure 68. Achieving a high Froude number requires a high liquid flow rate and a small distance between the wellhead and the bottom of the collector. To achieve a specific Froude number, the closer a collector is to the wellhead, the smaller can be the collected liquid flow. Generally speaking, the collection of large liquid flows requires a large diameter riser having a relatively small total lift above the sea surface.

For all except the highest Froude numbers, the performance of single cone collectors is degraded by the excessive gas that will almost always be present. This difficulty can be overcome by use of a separating collector of the type described herein.

Toxicity of Drilling Fluids on Corals

Principal Investigator: Eugene A. Shinn
U.S. Geological Survey
Fisher Island Station
Miami Beach, FL 33139

Objective: To determine potential effects of offshore drilling upon coral reefs

During oil- or gas-well drilling, a mixture of water and clays called drilling mud is circulated downhole through the drill bit and back to the surface for several operational purposes: (1) lubricating and cooling the bit, (2) circulating cuttings to the surface for geological examination, (3) forming a supportive wall or mud casing to the wall (generally called a mud cake), and (4) preventing blowouts.

In recent years, the possible effects of drilling mud discharges during offshore operations have become an environmental concern. The deposition of drilling mud on corals first became an issue in the early 1970's when tracts were leased near a coral-capped salt dome known as the Texas Flower Gardens. Concern deepened in 1973 when tracts were leased and drilled on and near the Florida Middlegrounds, a coral-encrusted bedrock feature west of Tampa, Fla. The recent move to establish the Texas Flower Gardens as a national marine sanctuary has further stimulated environmental interest in the possible consequence of using drilling mud near corals.

Over the last few years, the environmental concerns have been the subject of research conducted by personnel of the Fisher Island Station, and the findings are presented below.

Toxicity of Drill Mud on Corals

Three years ago, Dr. Jack Thompson, then a Ph.D. candidate at Texas A&M University, performed experimental studies under the principal investigator to develop quantitative information on mud-coral interaction: Thompson (1979), Thompson and Bright (1980), and Thompson and others (1980). These experiments were conducted in the Fisher Island Station laboratories of USGS as well as offshore areas where numerous thriving coral reefs are found.

Seven species of corals were tested employing whole, used drilling mud (mud and cuttings) to determine the degree of exposure that corals can tolerate. The species chosen represent typical reef-building corals, some of which are also found at the Texas Flower Gardens.

The study concluded that of the seven species tested, concentrations of 476 mg/l suspended solids were required to kill three of the species during the 96-hr bioassay. Although behavioral effects were observed (such as polyp retraction), none of the seven species was killed at lower dosages of 150 and 11 mg/l. These findings raised the question, "At what distance from a drilling platform would these concentrations of suspended solids be found?" In addition, the question was posed, "Has drilling near a coral reef, such as at the Texas Flower Gardens, caused any negative effects on coral growth?" To answer the above questions, the principal investigator studied drill mud plumes from seven offshore platforms in the Gulf of Mexico and investigated past growth rates at the Flower Gardens Reef using a coral banding technique developed by Hudson and others in 1976.

Coral Banding in Florida and the Texas Flower Gardens

Hudson and Robbin (1980) conducted a two-part study to determine effects of drilling mud on the massive coral *Montastrea annularis*. The study involved determination of long-term effects on growth of this coral following short-term massive doses, and effects on the growth rate of the same species living at the Texas Flower Gardens Reef 200 km off the Texas coast, where drilling commenced nearby in 1975 (fig. 70).

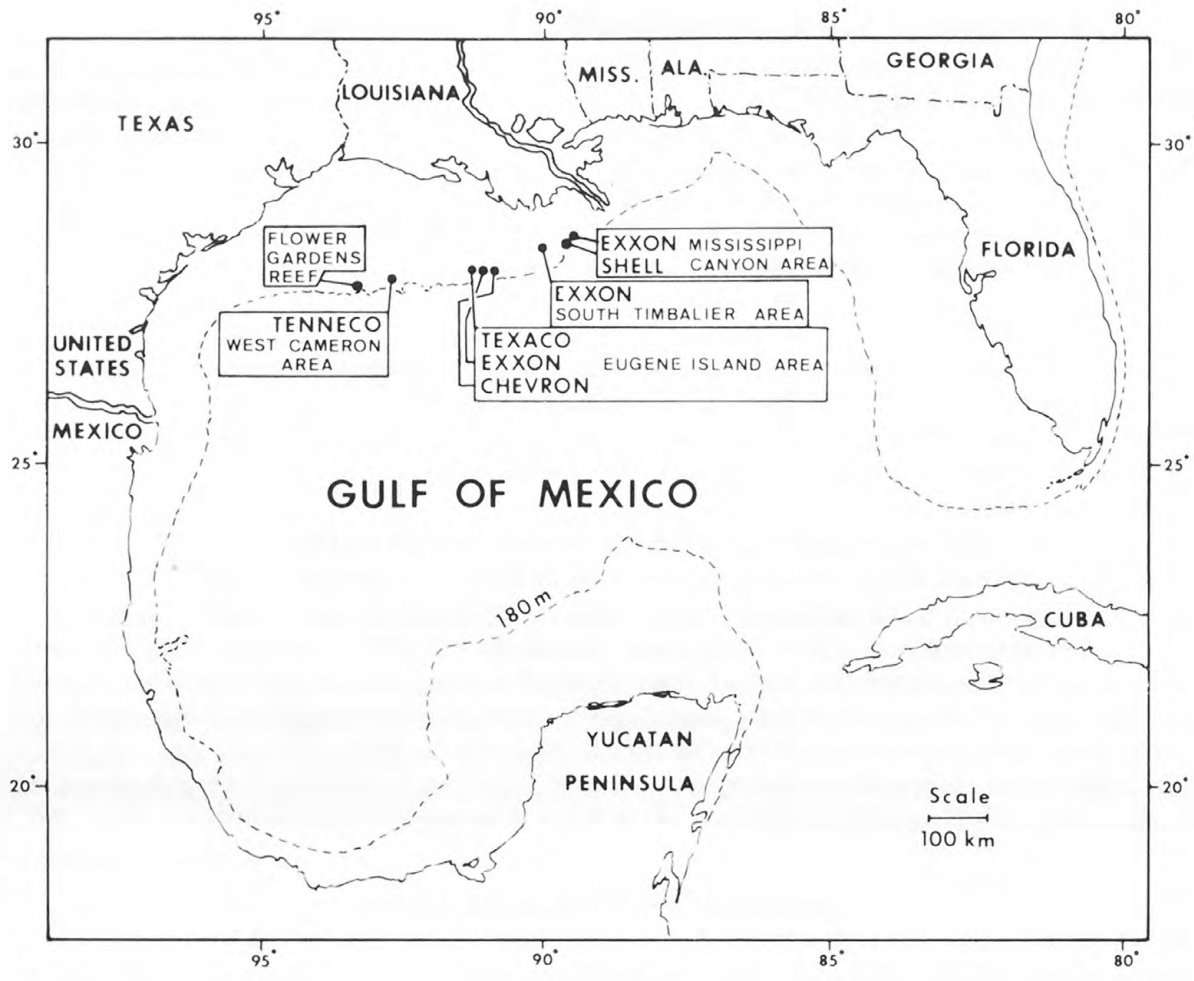

FIGURE 70.—Map of Gulf of Mexico showing location of Flower Gardens Reef and offshore

In the Florida study, performed in cooperation with a team of graduate students headed by Thomas Bright, live corals were dosed by divers four times every 2.5 hours. Drill mud was applied from a plastic bag in sufficient quantity to form a 2- to 4-mm-thick layer of mud over the living coral. Effects were monitored on a 24-hour basis using closed circuit underwater television and photography. All the corals removed the drill mud within 1 hour with the aid of normal wave surge. All specimens tested survived and were allowed to live on the reef for 6 months, at which time they were collected and examined in the laboratory. X-ray photographs of the coral, which contains tree-ringlike bands, showed that the growth rate associated with the period of heavy dosage was slightly reduced, even though barite (a common ingredient of drilling mud) was incorporated within the skeleton to levels as high as 1,200 ppm. Normal barite content is approximately 12 ppm.

The second phase of this study was conducted at the Texas Flower Gardens (fig. 71), where 12 large heads of *Montastrea annularis* in 20 m of water were core drilled. The cores were sliced and X-radiographs made to examine annual growth bands. Using this technique, measurements could be made of annual growth rates since 1900, as well as growth since 1975 when drilling commenced nearby. The location of wells drilled between 1974 and 1979 is shown in figure 71. In addition, sampling was possible of coral skeleton laid down during the period of drilling to analyze this material for barite and chromium. These analyses showed that (1) no change occurred in growth rate during the year drilling occurred, and (2) barite and chromium levels were no greater than those found in pre- and post-oil drilling coral bands.

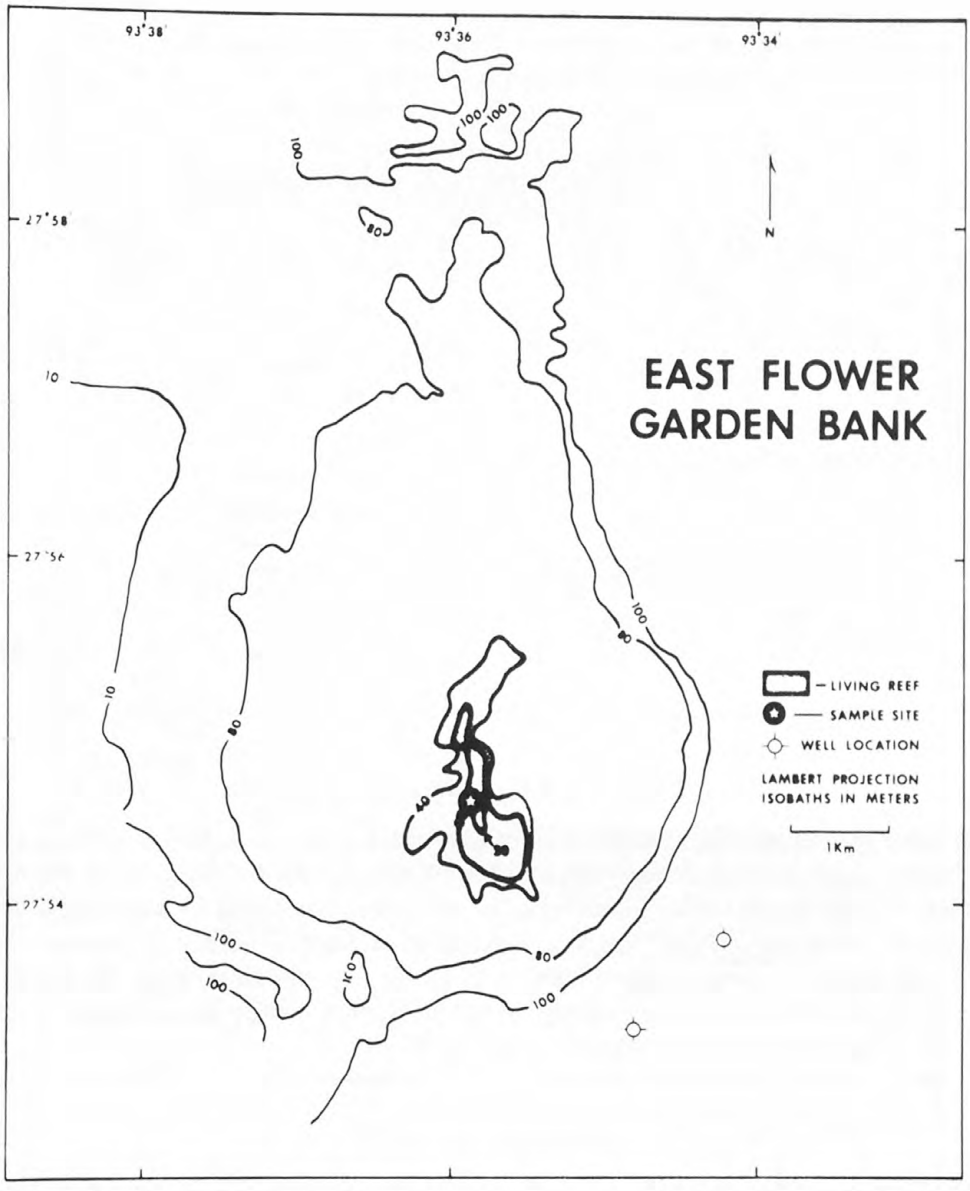

FIGURE 71.—Map of East Flower Garden Bank showing locations of living coral, sampling area, and nearby exploratory wells drilled between 1974 and 1979

Analysis of the growth bands did show, however, that a sudden reduction in growth rate had occurred in 1957, the reason for which is unknown. But Richard Rezak of Texas A&M University, who has been studying the reef under Bureau of Land Management (BLM) funding, suggested salt dome collapse. Rezak, in a personal communication to the principal investigator, pointed out that nearly all other salt domes in the areas contain grabens or down-faulted blocks on their crests, a phenomenon related to salt movement or dissolution. Further, an extensive brine seep near the base of East Flower Gardens Reef has been reported (Bright and others, 1980). Workers on a nearby Pennzoil platform have reported earth tremors that occassionally shake the platform (Rezak, personal communications to the principal investigator). The tremors are thought to be caused by minor faulting related to loss of salt from the dome beneath the coral reef. The reef possibly may have collapsed several meters in 1957 which lowered the corals to areas of lower light levels, thereby reducing the rate of growth. This hypothesis is supported by the observation that growth rates have never returned to pre-1957 levels (see fig. 72).

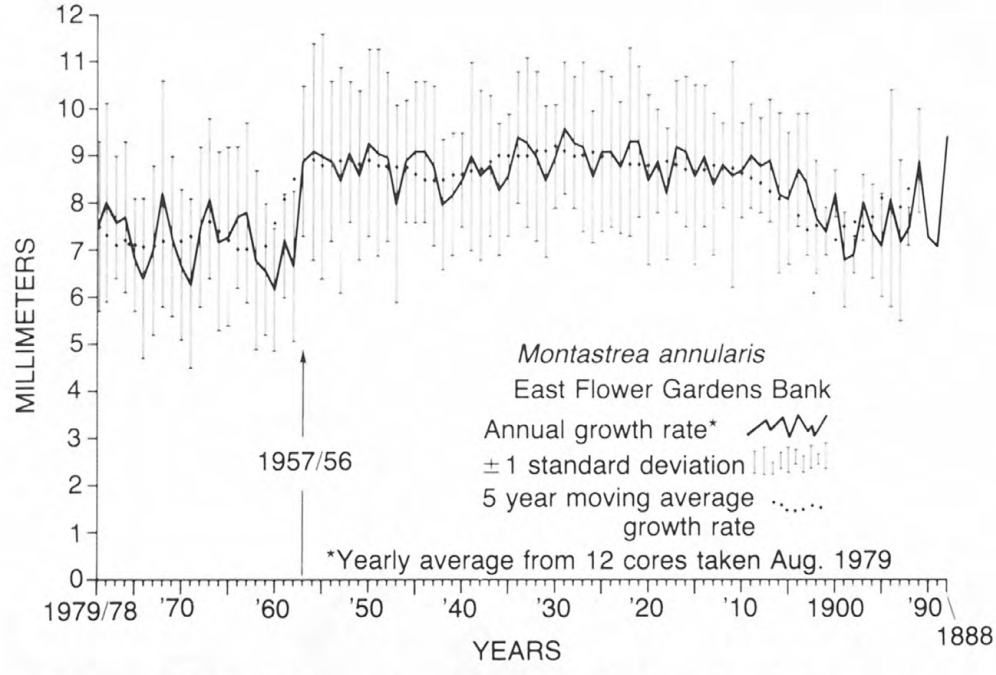

FIGURE 72.—Graph of average growth rate obtained from cases from 12 living corals

Drilling Mud Plume Study

To gain more insight into the concentration of suspended solids contained in drilling mud plumes, the principal investigator made a study of plumes from seven different platforms in the northern Gulf of Mexico. (See figure 70 for locations.) The study was conducted by attaching a line to or near the point of discharge. Water from the densest part of the near-horizontal plumes was collected in 10-liter bottles almost simultaneously from 1, 6, 12, 24, 48, and 96 m from the source. The collection operation, shown diagrammatically in figure 73, was usually accomplished in 30 minutes or less, often without attracting the operators' attention.

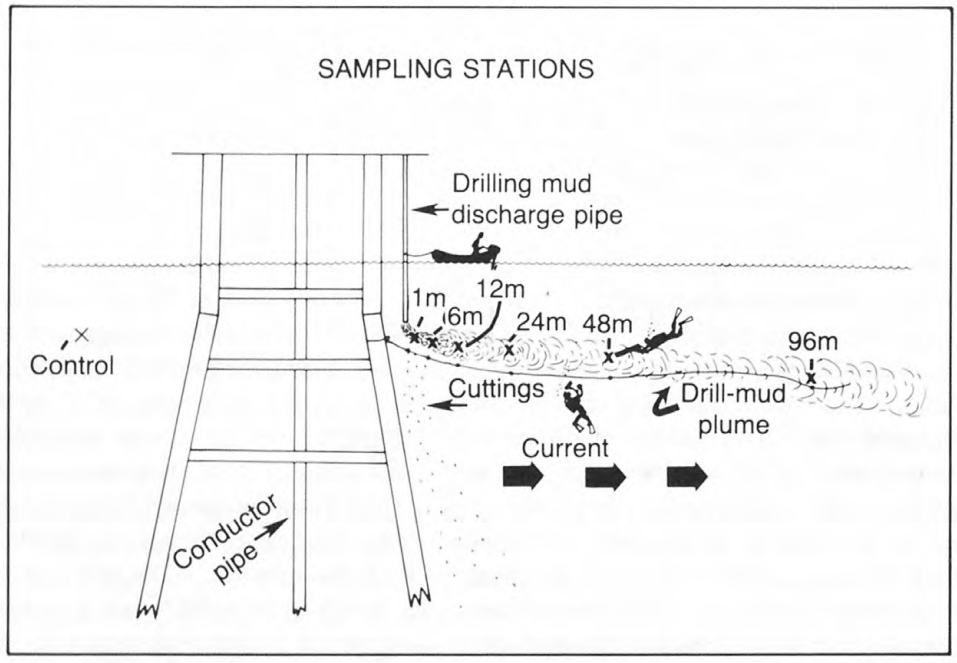

FIGURE 73.—Schematic drawing of plume sampling technique

Using air pressure, water samples were passed through a 0.4 mm pore size polycarbonate filter disk. The material filtered on the disk was later dried in the laboratory, weighed, and the amount expressed as mg/liter. The average concentration of suspended solids for six plumes is indicated by the bold line in figure 74. The dashed line shows concentration from the seventh platform, where the sampling intervals were slightly different.

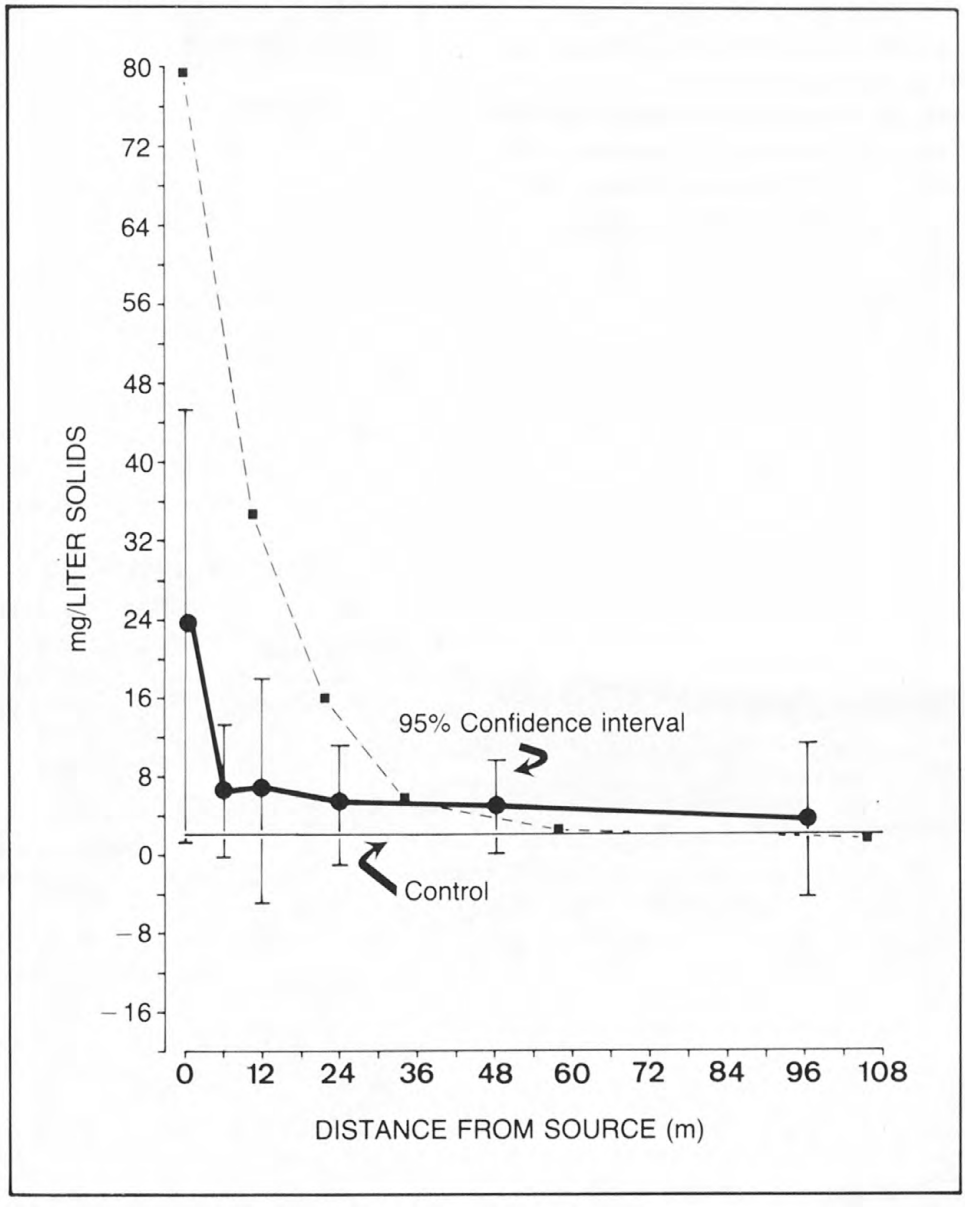

FIGURE 74.—Average of data from six separate plumes

The plumes examined were those that normally occur during exploratory drilling and such plumes may persist for several months, depending upon the time required to drill a well. Larger plumes occur several times during the drilling of a well when bulk discharges are necessary to remove sand from the mud pits or for other reasons. Such "dumps," which may involve more than 1,000 barrels, usually last 1 to 6 hours. Thus, the values reported in our study relate only to the chronic pollution resulting from exploratory drilling rather than from the more sudden, short-lived, high concentration bulk discharges.

The values shown in figure 74 should be compared with the concentrations used by Thompson, as well as those employed by others in bioassay studies. Apparently, most published studies have employed unrealistically high concentrations, and their results, therefore, may say little about effects in the real world. For example, note that the concentration found just 1 m from the discharge pipe was 80 mg/l and that the average was around 24 mg/l. Just 6 m from the source, the average value for six of the plumes was less than 8 mg/l. Between 48 and 96 m from the source, all seven plumes had been diluted to near background levels, even though the plumes could be seen to be continuing beyond for as much as 1,000 m.

Therefore, the average concentration just 1 m from the discharge pipe was approximately 14 times less than the concentration required to kill three of the seven species tested by Thompson and Bright (1980) and Thompson and others (1980). At 96 m from the source, the concentration was 132 times less than that required to cause coral mortality. Apparently, the plumes resulting from normal exploratory drilling should have a minor effect on coral growth, even within 100 m of source. Bulk discharging, however, might have a greater effect, but note that such dumps last only a few hours, and concentrations within 100 m of the source rarely approach the values that have been determined to kill corals in a 4-day test. Thus, even with high-concentration, short-lived dumps, the duration of impact may be too short to result in mortality, although growth rates might be temporarily reduced below normal. Corals 100 m from the source would unlikely experience the kind of extreme dosage that was experimentally applied in the study described by Hudson and Robbin (1980a). In addition, remember that coral reefs rarely grow in low-energy areas, where fine-grained drilling mud carbonate sand between coral heads is coarse due to frequent high energy, and drilling mud has not been able to accumulate there (Meyer and others, 1981).

A reasonable approach to more conclusive assessment to the effects of drilling on coral reefs would be to study areas where drilling has occurred directly on top of living coral reefs. Such areas exist in the Far East, such as the Samarang Field off Sarawak (Borneo) and the Nido and the Matinloc Fields near Palowan Island in the Philippines. Further studies will be made in such areas.

Reports and References

Bright, T. J., Powell, E. N., and Rezak, R., 1980, Environmental effects of a natural brine seep at the East Flower Garden Bank, northwestern Gulf of Mexico, *in* Geyer, R. A., ed., Marine Environmental Pollution, Hydrocarbons, v. 1, p. 292-316, Elsevier Scientific Pub. Co., Amsterdam.

Hudson, J. H., and Robbin, D. M., 1980a, Effects of drilling mud on the growth rate of the reef-building coral, Montastrea annularis, *in* Geyer, R. A., ed., Marine Environmental Pollution, Hydrocarbons, v. 1, p. 455-470, Elsevier Scientific Pub. Co., Amsterdam.

_____, 1980b, effects of drilling mud on the growth rate of the reef-building coral, Montastrea annularis: Research on Environmental Fate and Effects of Drilling Fluids, Lake Buena Vista, Fla., Proceedings, v. II, p. 1101-1119.

Meyer, D. B., Trefry, J. H., and Trocine, R. P., 1981, Geochemical assessment of the environmental impact of offshore drilling operations on the Texas Flower Gardens: Annual Mtg. of Florida Acad. of Sci., Abs., v. 44, suppl. 1, p. 44.

Shinn, E. A., Hudson, J. H., Robbin, D. M., and Lee, C. K., 1980, Drilling mud plumes from offshore drilling operations—implications for coral survival, *in* Geyer, R. A., ed., Marine Environmental Pollution, Hydrocarbons, V. 1, p. 471-496, Elsevier Scientific Pub. Co., Amsterdam.

Thompson, J. H., Jr., 1979, Effects of drilling mud on seven species of reef-building corals as measured in field and laboratory: Thesis, Texas A&M University, Department of Oceanography, College Station, Tex.

Thompson, J. H., and Bright, T. J., 1980, Effects of an offshore drilling fluid on selected corals: Research on Environmental Fate and Effects of Drilling Fluids and Cuttings, Lake Buena Vista, Fla., Proceedings, v. II, p. 1044-1076.

Thompson, J. H., Shinn, E. A., and P ght, T. J., 1980, Effects of drilling mud on seven species of reef-building corals as measured in the field and laboratory, *in* Geyer, R. A., ed., Marine Environmental Pollution, Hydrocarbons, v. 1, p. 443-453, Elsevier Scientific Pub. Co., Amsterdam.

Environmental Effects of Wellhead Removal by Explosives

Principal Investigator: Dr. Earle Hays
Department of Ocean Engineering
Woods Hole Oceanographic Institution
Woods Hole, MA 12543

Objective: To determine the probabilities of killing fish from removing wellheads by means of explosives.

International and Federal laws prescribe the removal of structures from the ocean upon their abandonment so that they cannot become hazardous to navigation and to fishing operations. On the OCS, after exploratory drilling operations are completed, the wellheads must be removed at least 15 feet below the mud line. The severed wellhead and attached casings are thereupon lifted to the surface. Wellheads may be severed mechanically, or as most operators prefer, by means of special explosive charges placed inside the wellhead beneath the seafloor. These charges can completely sever the concentric casings and cement grouting used to ensure that pressurized formation fluids do not blowout around the casing. Figure 75 pictures a casing string severed mechanically in 600 feet of water in the Gulf of Alaska. The conductor casing (outer casing) is 30 inches OD.

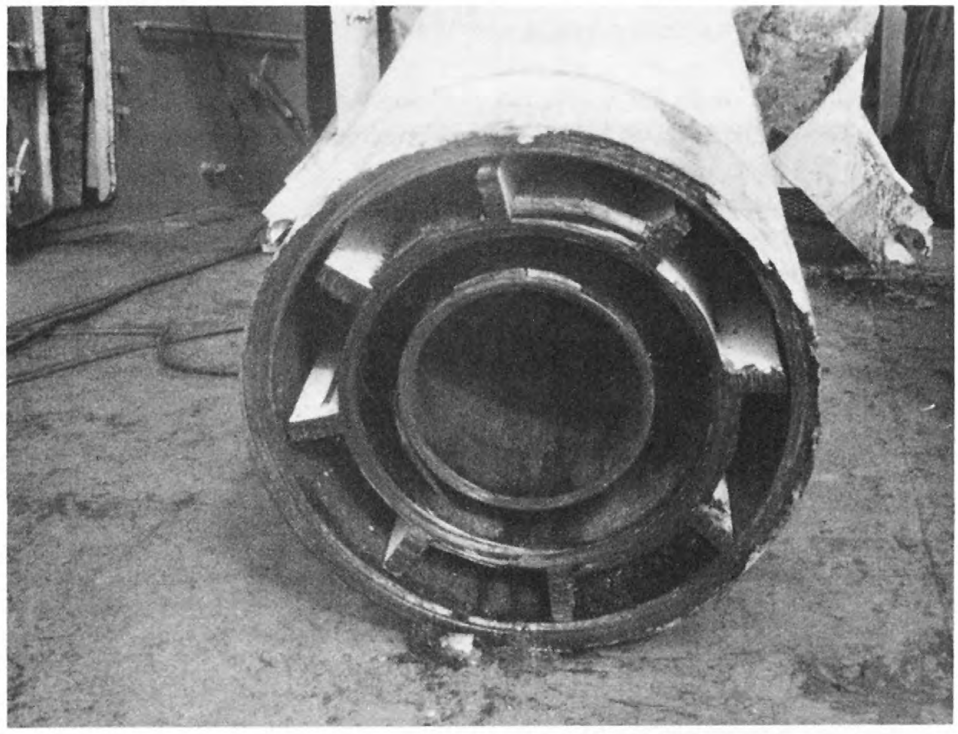

FIGURE 75.—Casing string severed mechanically in 600 feet of water

The more important considerations involved in determining whether to cut or blast are the number of strings to be severed, cement around casing, size of conductor hole, type of sediments in the wellbore, depth of water, and compressive strength of cement in the annuli. The ribbed part of the wellhead housing is usually above the cut except in special cases when the casing cannot be retrieved from depths greater than 15 feet. The cut will then have to be made at a shallower depth, possibly encountering the ribbed area, as has occurred in the wellhead shown in figure 75.

The drive or structural casing (middle casing) and the conductor casing are cemented to the ocean floor but the annulus between the surface casing (inner casing) and the drive casing is not cemented.

In some regulatory areas, there is a moratorium on blasting and in others permissible explosive charges are stipulated. For example, in the Gulf of Alaska, stipulations require the USGS Area Supervisor to assure that blasting is used only when necessary to protect human safety, fishing equipment, or navigation; that failure to permit blasting will result in greater environmental harm and economic costs than the blasting itself; or that blasting will not pose a risk of significant damage to marine life. Blasting refers to high velocity explosives which are defined as those with burning rates greater than 5,000 fps or creating a pressure curve having a rise time of less than 0.18 milliseconds.

The question of explosives has been addressed by various investigators over the years, and in the context of wellhead removal, the Naval Surface Weapons Center (NSWC) has recently performed a series of experiments at half scale to define pressure signatures which result from use of certain explosive configurations.

Prior to designing the experiments, NSWC conducted a literature search of industry practice. They determined that nitromethane is the basic explosive component used for most wellhead removals, and in certain cases, other explosives are used, including dynamite. A cylindrical canister of explosives, positioned inside the innermost casing 15 to 20 feet below the mudline, is the usual blasting configuration. Depending on the number, diameter, wall thickness, and material of the casing strings, the quantity of explosive material is determined. Usually, somewhere between 26 to 180 pounds are used. Double end initiation (two explosive loads which generate a reinforced pressure signal midway), exploding bridge wire (EBW), and to a lesser extent, single point initiation are employed.

In the half-scale experiments, explosive charges were sized by means of cube root scaling. Explosives selected for the severing charges were a mixture of nitromethane (NM) and an amine sensitizer, Comp C-4, and TNT.

Steel pipe, having inside diameters of 15, 8, and 5 inches, were used to simulate the wellhead casing. The annuli between the casings were filled with class "G" cement, a type commonly used in underwater structures.

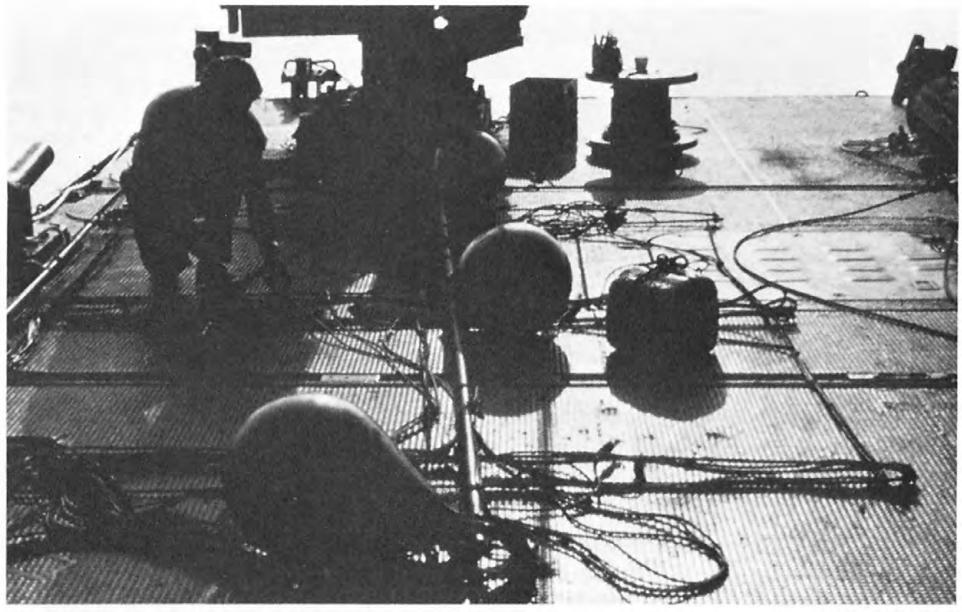

FIGURE 76.—Pressure field measurement array under test on deck of experiment barge

Nine tests were conducted. One charge of each of the three compositions was fired in free water, using only the explosive canister. A second series, wherein the charges were placed inside the simulated wellhead casings, also was run in free water. For the third series, the wellheads were driven into the mud bottom of the lower Potomac River, where all testing was accomplished. In this latter case, the explosives were detonated 7.5 feet below bottom.

Shock wave recording gages were positioned in an array, figure 76, to map the pressure field adjacent to the blast. Data from the two free water series and from the below bottom experiment were compared. Peak pressures, impulse, and energy values were found to decrease dramatically, about 90 percent, for the below bottom detonation.

Results extrapolated for multistring casings as shown in figure 75 indicate that, with any of the explosive configurations tested, complete severings can be accomplished with 25 to 43 pounds of explosive. A complete analysis and report of the explosives program is in preparation.

In order to relate blast effects upon different species and sizes of fish, Woods Hole Oceanographic Institution is beginning to assemble what information exists in the open literature. In addition, further experimentation, especially on blast effects, will have to be planned.

Other factors, such as time of year, water depth, and location are very important to a probabilistic determination of kill rates.

☆ U.S. GOVERNMENT PRINTING OFFICE: 1981 - 155 - 101